

Technology and Energy Inventory of Ice Rinks

PAVEL MAKHNATCH



**KTH Industrial Engineering
and Management**

Master of Science Thesis
Stockholm, Sweden 2011



**KTH Industrial Engineering
and Management**

Technology and Energy Inventory of Ice Rinks

Pavel Makhnatch

Master of Science Thesis Energy Technology EGI-2011-075MSC
KTH School of Industrial Engineering and Management
Division of Applied Thermodynamics and Refrigeration
SE-100 44 STOCKHOLM



**KTH Industrial Engineering
and Management**

Master of Science Thesis EGI-2011-075MSC

Technology and Energy Inventory of Ice Rinks

Pavel Makhnatch

Approved 10-June-2011	Examiner Björn Palm	Supervisor Jan-Erik Nowacki
	Commissioner	Contact person

Master student: Pavel Makhnatch
Armegatan 32 Läg 1512
17171 Solna

Registration Number: 850122-0696

Department Energy Technology

Degree program Sustainable Energy Engineering

Examiner at EGI: Prof. Dr. Björn Palm

Supervisor at EGI: Jan-Erik Nowacki

Abstract

Currently 341 ice rinks are in operation in Sweden with an estimated total energy consumption of 384 GWh/year. As it has been revealed in previous studies, most of the ice arenas are constructed and/or not operated efficiently. Thus it is considerable energy saving potential, which could be achieved in this area. The potential is even more significant if one can consider the savings in the ice rinks all over the world.

This report is an in-depth study, which aims at analysing the Swedish ice rinks energy consumption and estimation of the corresponding energy saving potential. The report analyses the energy statistics obtained through the Stoppsladd study, which includes the ice rinks inventory, data collection and compilation of energy relevant data for 100 ice rinks located in Sweden. The inventory has revealed a number of important statistical figures, such as total energy consumption average in total (estimated to be 1,137 MWh/year) and for different ice arenas categories in particular. Relevant specific energy consumption values as well as a number of other important figures are also provided in the paper, thus giving an idea on the way to minimise energy consumption at each specific ice rink. The results are additionally supported by statistical multifactor regression analysis, which resulted in a relation between the ice rink's total energy consumption and some known factors values affecting it.

Two in-depth studies fulfil the Stoppsladd project by analysing water quality and ice quality effect on the ice rink's energy consumption and investigation of the static and dynamic heat flow distribution in ice rink slab.

A static heat flow distribution model of an ice rink evaluated the effect of concrete with different properties on temperature and heat flow distribution within an ice rink floor slab. The study proves that the ice rink refrigeration system COP₂ could be increased with 3.5 % just implementing new high thermal conductivity concrete layer into the conventional concrete ice rink floor.

The static analysis results were further completed with dynamic analysis, which adequately reflects the thermodynamic response of the concrete ice rink floor to a varying heat load.

As a result, the thesis represents a holistic approach to the ice rink energy efficiency increase problem and provides a good basis for further studies in relevant areas. It is proved that modified concrete allowing higher (efficient) secondary refrigerant temperatures and also provides better response to change in heat load to the system.

Key words: energy efficiency, ice rink, ice arena, Stoppsladd, prediction, ice quality, CFD.

ACKNOWLEDGMENT

This thesis work is a part of the “Stoppsladd” project. The ‘Stoppsladd’ project was initiated by Sveriges Energi- & Kylcentrum (SEK) and performed in collaboration with the Swedish Ice Hockey Association (SIF). This project is co-financed by the Swedish Energy Agency (Energimyndigheten).

First of all, I would like to express sincere gratitude to Jörgen Rogstam for his continuous support in performing this thesis work, for his valuable advices and for being indulgent towards me and helpful when some things were wrong.

Additionally I would like to thank my master thesis supervisor JanErik Nowacki for his help in organising of work and for the valuable advices. Furthermore, I would like to thank Professor Björn Palm and the Sustainable Energy Engineer program supervisor Andrew Martin for giving me the opportunity to achieve my Master Degree in the Royal Institute of Technology at Division of Applied Thermodynamics and Refrigeration.

I would like also thank Samer Sawahla for his help in performing the simulations and establishing working and studying processes; Ehsan Bitaraf Haghighi for his goodwill to requests and for performing a number of measurements and Aleh Kliatsko for his constant support and help in the laboratory.

Table of contents

Abstract	7
List of Figures.....	11
List of Tables	12
Nomenclature	13
1 Introduction.....	16
1.1. Aim and objectives	16
1.2. Methodology.....	16
1.3. Scope and limitations	17
2. Ice rink's energy system and energy saving potential	18
2.1. Ice rink classification	18
2.2. Ice rink energy system	19
2.3. Energy saving potential	21
2.2.1 Low Emissivity Ceilings.....	21
2.2.2 Ice surface temperature controls	22
2.2.3 Capacity controlled brine pumps.....	23
2.2.4 Waste Heat Recovery	24
2.2.5 Air Handling and dehumidification	25
2.2.6 CO ₂ as a secondary refrigerant	25
2.2.7 Water treatment and ice maintenance	26
3. Energy saving potential of the Swedish ice rinks: Stoppsladd study.	28
3.1. StoppSladd general information	28
3.2. Main results	28
3.3. Statistical prediction of energy load.....	36
3.4. Discussion	40
4. Water treatment and Ice quality	43
4.1. Introduction to the problem.....	43
4.2. Water properties tests	45
4.2.1 Electrical conductivity measurement	45
4.2.2 PH level measurement	45
4.2.3 Freeze rate tests	46
4.2.4 Ice visibility test	47

4.2.5 Viscosity test	48
4.3. Discussion	49
5. Ice rink floor material influence on system performance (simulation/experiment)	50
5.1. Introduction to the problem.....	50
5.2. Thermal conductivity measurement of a number of samples	51
5.2.1 Principle.....	51
5.2.2 Results.....	53
5.3. Static simulation of temperature distribution within the ice rink slab with different concrete samples.....	54
5.4. Energy saving potential estimation.....	61
5.5. Dynamic simulation of temperature distribution within the ice rink slab using different concrete samples.....	62
5.6. Discussion.....	69
6. Conclusion	71
References.....	73
Appendix A: Water electrical conductivity test.....	76
Appendix B: pH level test	79
Appendix C: Water freeze rate test	81
Appendix D: Ice visibility test	85
Appendix E: Viscosity test (measurement report summary).....	86
Appendix F: The COP ₂ increase estimation, analytical approach.	95
Appendix G: thermal conductivity measurement	97

List of Figures

Figure 2.1: Medium-sized spectator arena (Svenska Ishockeyförbundet 2009)	19
Figure 2.2: Ericsson Globe, Event arena B (photo by Fredrik Persson)	19
Figure 2.3: Ice rink energy system main components (IIHF 2010)	20
Figure 2.4: Indirect (left) and direct (right) energy system (Månberg 2010)	20
Figure 2.5: Ice rink energy consumption drop, July 2008 – Nov 2009 (J. Rogstam 2010)	21
Figure 2.6: Radiant heat transfer mechanism, redrawn from (Manitoba Hydro 1991)	22
Figure 2.7: Applications for recovered waste heat (CETC 2005)	24
Figure 2.8: CO ₂ as a secondary refrigerant at Woodyhallen ice rink, Katrineholm Sweden	26
Figure 2.9: Percentage increase in compressor work compared to ice that is 19 mm thick, redrawn from (Manitoba Hydro 1991)	27
Figure 3.1: The Stoppladd database main window	29
Figure 3.2: The arena type distribution within the analysed data	29
Figure 3.3: Ice rinks by age	30
Figure 3.4: Total amount of bought energy, averaged by arena category, MWh/year	31
Figure 3.5: Total amount of bought energy by arena, MWh/year	31
Figure 3.6: Resurfacing water temperature, °C	32
Figure 3.7: Lighting type and lighting time effect on the efficiency	33
Figure 3.8: Refrigeration system type	33
Figure 3.9: Refrigerant type used in Swedish ice rinks refrigeration systems	34
Figure 3.10: Secondary refrigerant types	34
Figure 3.11: Coolant solutions	35
Figure 3.12: Ventilation heat source	36
Figure 3.13: Total energy consumption observed over predicted data comparison	40
Figure 4.1: Dissolved Oxygen in Fresh Water (at atmospheric pressure) (The engineering toolbox n.d.)	44
Figure 4.2: RealIce Base product (Watreco 2010)	44
Figure 4.3: Realice system with the 3 vortex generators inside it (Realice System - Improved Ice Quality 2010)	44
Figure 4.4: Water properties measurements	46
Figure 4.5: Freeze rate test	46
Figure 4.6: Ice visibility test 1 (1 – preheated to boiling temperature; 2 – reference untreated sample; 3 – Realice vortex-treated water)	47
Figure 4.7: Ice visibility test 2	48
Figure 4.8: Falling ball viscometer (a) and its working principle (b)	48
Figure 5.1: Typical ice rink floor design (ASHRAE 2002)	50
Figure 5.2: A typical TPS sensor (Bitaraf H. 2010)	52
Figure 5.3: The samples and the assembling procedure	53
Figure 5.4: Concrete samples properties	54
Figure 5.5: The simulation model design	55
Figure 5.6: COMSOL model of ice slab: constant Ice temperature simulation	56
Figure 5.7: COMSOL model of ice slab: constant inner tube temperature simulation	57
Figure 5.8: Horizontal cross section for temperature distribution at ice surface, line 1 in Figure 5.7	58

Figure 5.9: Vertical cross section for temperature distribution in COMSOL model, lines 2 and 3 in Figure 5.7	59
Figure 5.10: COMSOL model of the ice slab	60
Figure 5.11: Vertical cross section for temperature distribution in COMSOL model	60
Figure 5.12: CoolPack refrigeration cycle analysis	62
Figure 5.13: Predicted heat flux to the ice surface	65
Figure 5.14: The measured cooling load maintained by refrigeration equipment. (1 day , 1400 min)	66
Figure 5.15: Predicted heat flux and respective measured cooling load	66
Figure 5.16: Function cool(t) plot, 24 hours operation period	67
Figure 5.17: The required second refrigerant temperature distribution over the time, Model1 (conventional concrete, blue line) and Model2 (improved concrete, red line). Simulation 1: 5 days operation.....	68
Figure 5.18: The required secondary refrigerant temperature distribution over time period, Simulation 2: 24 h operation, steady conditions.	69
Figure A.1: Water electrical conductivity measurement.....	77
Figure B.1: Water pH measurement	80
Figure C.1: Water freeze rate test 1	82
Figure C.2: Water freeze rate test 2	83
Figure F.1: Approximate values for the Carnot efficiency of practical vapour compression systems (Eric Granryd 2005).....	96

List of Tables

Table 2.1: Ice arenas characteristics, by type (Svenska Ishockeyförbundet 2009)	18
Table 3.2: Correlation analysis of Stoppsladd data	37
Table 3.3: Regression function coefficients	38
Table 3.4: t-statistics for independent values	38
Table 5.1: specifications for TPS 2500 (Bitaraf H. 2010).....	52

Nomenclature

Roman

A	Area [m ²]
c _p	Specific heat [kJ/kg.K]
E	Electric field strength [kg·m s ⁻³ ·A ⁻¹]
f	Grey body configuration factor [-]
h	Heat transfer coefficient [W/m ² K]
J	Current density [A/m ²]
k	thermal conductivity coefficient [W/(m·K)]
L	Distance [m]
Q	Heat gain, heat (cool) load [W]
T _{90,43}	Critical Student's t value (90-percent confidence, 43° freedom)
v	Air velocity [m/s]

Greek

α	Angle factor [-]
ε	Emissivity [-]
μ	Dynamic viscosity [cP]
ρ	Density [kg/m ³]
σ	Stefan-Boltzmann constant [W/m ² K ⁴]
σ _(n)	Electrical conductivity [μS/sm]

Subscript

air	Air
c	Concrete
ceil	Ceiling
cool	Cooling
cv	Convection
f	Flood
gr	Ground
ice	Ice
light	Lighting
lum	Luminary
r	Radiation
ref	Reference sample
res	Resurfacing
Ri	Vortex-generator treated water
rink	Rink
Sr	Secondary refrigerant
surf	Surface

1 Introduction

A path towards sustainable society requires continuous development in the energy sector: both production of energy and its consumption. While the production is constantly developing towards more energy efficient and less-carbon emissive technologies, the consumption of energy resources tends to increase.

Ice rinks operation demands on significant amount of energy. As it is estimated, the typical ice arena consumes averagely 1,138 MWh/year. Moreover, a number of skate rinks in Sweden, that were built sometimes more than 30 years ago, most probably now operate inefficiently. The total amount of consumed energy by ice rinks in Sweden is roughly estimated to be 380 000 MWh. Hence, there is a considerable potential to for energy saving measures.

There are a number of promising technologies to minimize energy consumption of ice rinks. However, the exact technical and energy related data should be collected to estimate real saving potential and justify the choice of effective technologies to implement.

1.1. Aim and objectives

The aim of this thesis work is to evaluate the energy usage and saving potential in Swedish ice rinks.

In order to fulfil the aim of the study – the following objectives were set:

- Make a comprehensive literature review of energy issues in ice rinks and energy savings methods;
- Collect, structure and analyse as much as 100 unique ice rinks in order to identify possible energy saving potential;
- Develop, calculate and compare the key figures for proper ice rink analysis and comparison;
- Collect energy data for some ice rinks which can serve as a “good energy saving examples” for other ice rinks with large energy consumption;
- Create a basis for future research and energy saving potential analysis;
- Identify saving measures to improve ice rinks’ efficiency and reduce energy consumption.
- Identify the energy saving potential of ice rink floor modification.

1.2. Methodology

The thesis work will start with literature review of ice rink design technique and existing energy saving technologies used in this area. The obtained theoretical information will be complemented with the Swedish ice rinks’ inventory results, obtained during the realization of “Stoppsladd” project. All the acquired information will be analysed using qualitative and quantitative methods. The analysis results will be supplemented with the experimental studies in order to define the most promising energy saving methods. Finally both the data, obtained from laboratory experiments, and analysis results will be used to identify the energy saving actions and potential.

1.3. Scope and limitations

In this study the focus is limited to the number of ice rinks located in Sweden. Therefore Swedish weather conditions, construction methods are taken in account. However, the above mentioned conditions are similar to those for Canada and, therefore, the available knowledge of ice rinks operation in the Canadian region will be used in this study, when relevant information for Swedish ice rinks is absent.

The limitations used for the experimental results, if any, are further noted in the related chapters.

2. Ice rink's energy system and energy saving potential

2.1. Ice rink classification

There are more than 300 ice arenas in operation in Sweden (Svenska Ishockeyförbundet 2009). They are classified in terms of the design parameters, purpose, audience capacity and others. There are three major groups of ice arenas in Sweden now: Training arenas, Spectator arenas and Event arenas (Svenska Ishockeyförbundet 2009). Each of the above mentioned group consists of three subgroups: A, B and C.

Training arenas are the least advanced arenas used for games in lower series and boys/girls matches. Spectator arenas are the ones, which are built for the different activities up to Championship games. Therefore these ice rinks imply existence of various equipment and service facilities. The example of medium-sized spectator arena is presented on Figure 2.1.

The most advanced ice arenas are Event arenas. The "Eliteserien" games are normally held in Event arenas. However, everything from large music events to exhibitions and motor shows could be held in this type of arenas. Ericsson Globe is a good example of what an Event arena is (see Figure 2.2). Some specific information, characterising the types of arenas is presented in the Table 2.1.

Table 2.1: Ice arenas characteristics, by type (Svenska Ishockeyförbundet 2009)

Arena type	Seats, number	Lighting lux (min)	Eh,	Ceiling height, m	Activities, up to
Training arena C	0	200		5	Boys/girls matches
Training arena B	<200	400		5	Boys/girls matches
Training arena A	>200	400		5	Boys/girls matches
Spectator arena C	500-1000	400		7	Division 2 games
Spectator arena B	>1000	600		7	Division 1 games
Spectator arena A	>2000	1000		7	Championship
Event arena C	>4000	1000		7	Elite series games, variety of different events
Event arena B	>6000	1000		7	Elite series games, variety of different events
Event arena A	>10000	1000		7	Elite series games, variety of different events



Figure 2.1: Medium-sized spectator arena (Svenska Ishockeyförbundet 2009)



Figure 2.2: Ericsson Globe, Event arena B (photo by Fredrik Persson)

2.2. Ice rink energy system

One of the purposes of this study is to perform energy inventory of the Swedish ice rinks' energy system. Therefore the respective energy system and its boundaries should be properly defined and set.

For the sake of this study the ice rink's energy system boundaries are set to be equal to the ice rink building envelope boundaries with outdoor cooling coil and fans, which are usually located outside the building envelope but still a part of the ice rink energy system.

The understanding of the ice rink energy system boundaries is very important as from a holistic perspective. The energy flows across the system boundaries are of the highest importance for the system effectiveness analysis, not the consumption of each of the system's internal elements. In other words, even though some of components could be not very efficient, the whole system can become efficient, if it could only properly deal with residual waste energy flows from different components for its needs. The refrigeration system is a good example for this approach. Considering the refrigeration unit to be a separate component, the dissipated heat from a condenser is a waste heat for the unit. However, this heat can become useful heat which serving as an input for a number of ice rink energy system components, such as ventilation heat, resurfacing water preheat and others.

The conventional ice rink's main energy system is the refrigeration unit (Figure 2.3). The refrigeration unit is usually based on vapour compression refrigeration cycle with ammonia (R717) as the most common refrigerant. R404A and R134a are also to a minor extent used in Swedish ice rinks.

The refrigeration unit's evaporator provides cooling power to the ice sheet and maintains the ice at a specific temperature. There are two dominating methods for the refrigeration units to connect to the ice sheet: indirectly or directly (there also exists another, partly indirect method, which is a combination of both the direct and the indirect methods) (Figure 2.4).

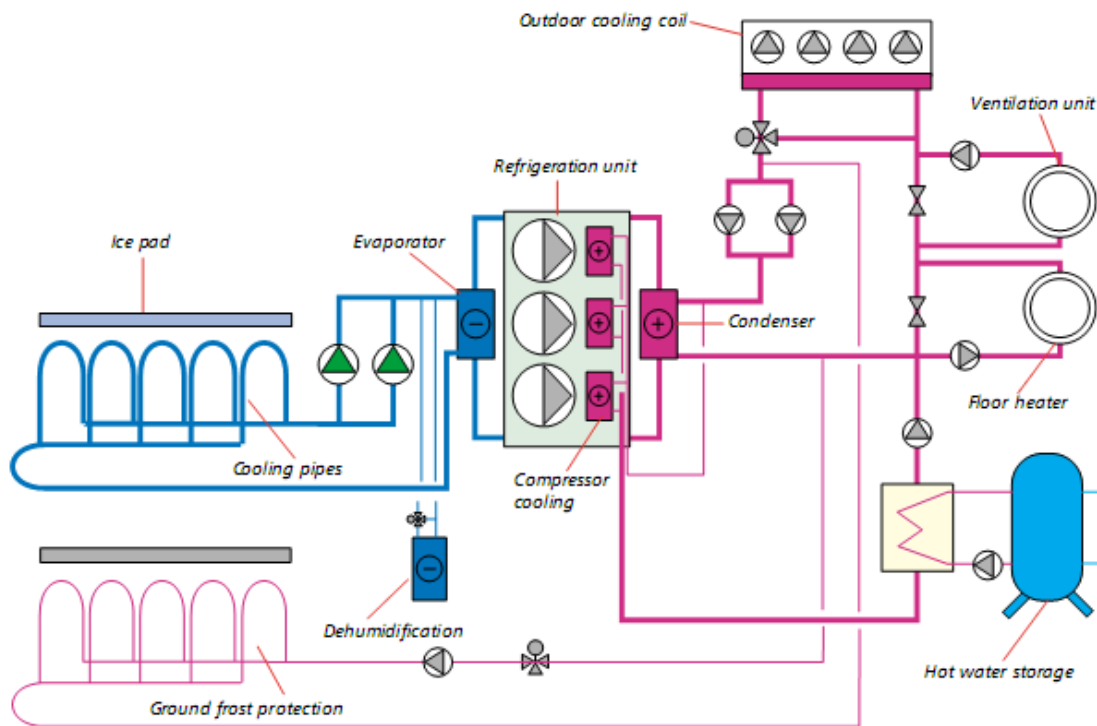


Figure 2.3: Indirect ice rink energy system main components (IIHF 2010)

The indirect method has a number of advantages: a minimum amount of refrigerant required to maintain operation, a reduced refrigeration unit size at same cooling capacity, significantly reduced refrigerant leakage risk, which is of vital importance for closed ice rinks operated especially with ammonia as a refrigerant. The disadvantage of the indirect system is the potential decreased efficiency compared to direct system due to the additional energy required by the pumps and the temperature differences in the extra heat exchangers.

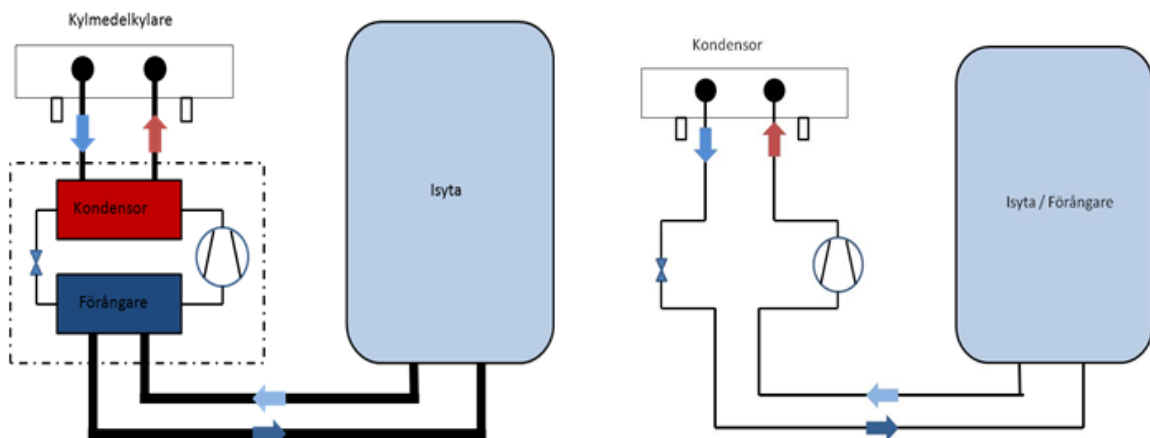


Figure 2.4: Indirect (left) and direct (right) energy system (Månberg 2010)

2.3. Energy saving potential

Ice rinks are huge energy consumers. Proper design and operation of an ice rink require simultaneous cooling and heating activities. The problem is how to maintain different temperature and climate conditions in different parts of ice arena - from -5°C on the ice rink floor to +10°C in the stand and even + 25°C in different service rooms. However, there are often one or more ways to improve this by implementing energy efficiency measures. Some of the Swedish ice rinks have already reduced their energy consumption by 50% (Funktion 2009). It is noticeable that the electricity consumption could be observed to drop already after the implementation of very elementary energy saving measures Figure 2.5:

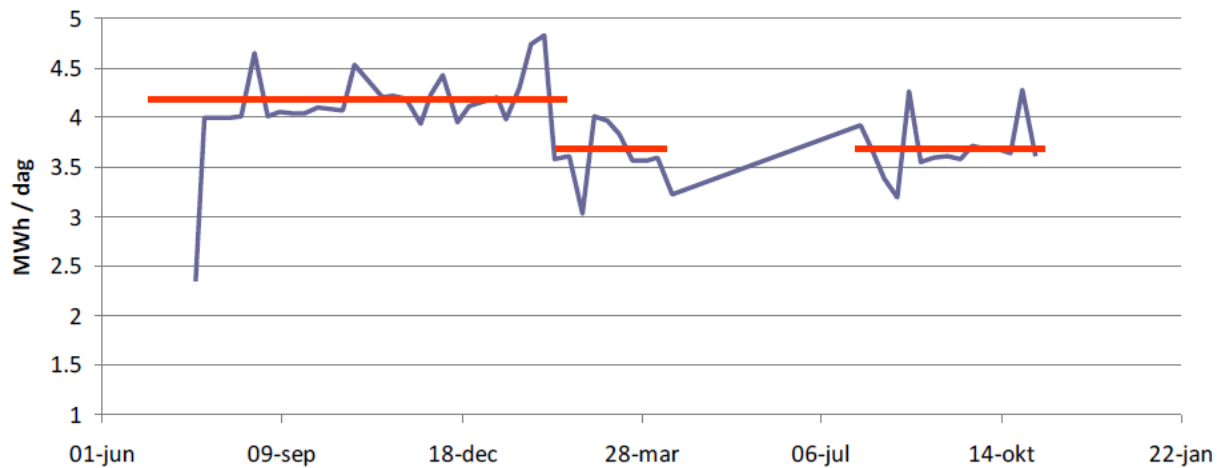


Figure 2.5: Ice rink energy consumption drop, July 2008 – Nov 2009 (J. Rogstam 2010)

This chapter will describe the most useful ways to conserve energy in ice rink arenas and minimizing the operation cost.

2.3.1. Low Emissivity Ceilings

Low emissivity ceiling are considered to be the automatic first choice for energy saving in most ice rinks as they often have a huge energy saving potential (Brendan Lenko 2001). The heat transport from the ceiling to the ice depends on radiation heat transfer, which always occurs between two surfaces of different temperature. The amount of heat transferred from the warm ceiling to the cold ice slab could be estimated based on the Stefan-Boltzmann equation.

$$Q_r = A\varepsilon\sigma \cdot (T_{surf}^4 - T_{ceil}^4) \quad (2.1)$$

where Q_r is radiant energy transfer;

A is surface area;

ε is emissivity;

σ is Stefan-Boltzmann constant;

T is absolute surface or ceiling temperature.

Considering typical ice rink's conditions, the ice temperature is bound within certain limits required for proper arena operation. The ceiling temperature is however depending on outdoor weather conditions, solar radiation, internal heat loads and normal stratification of arena air (Blades 1992). The only factor which is really under control is the ceiling cover material or, which is more important, its emissivity coefficient. The emissivity coefficient for the basic ceiling materials (wood, steel, etc.) lies in the interval from 0.85 to 0.95 (Natural Resources Canada 2003). The following measures are proposed to minimise emissivity coefficient and thus limit heat flux from the ceiling (Natural Resources Canada 2003):

- Install a suspended ceiling of low-emissivity aluminized cloth;
- Cover the ceiling directly with aluminium-based low emissivity (0.05) paint;
- Paint the ceiling with low-emissivity (0.24) paint.

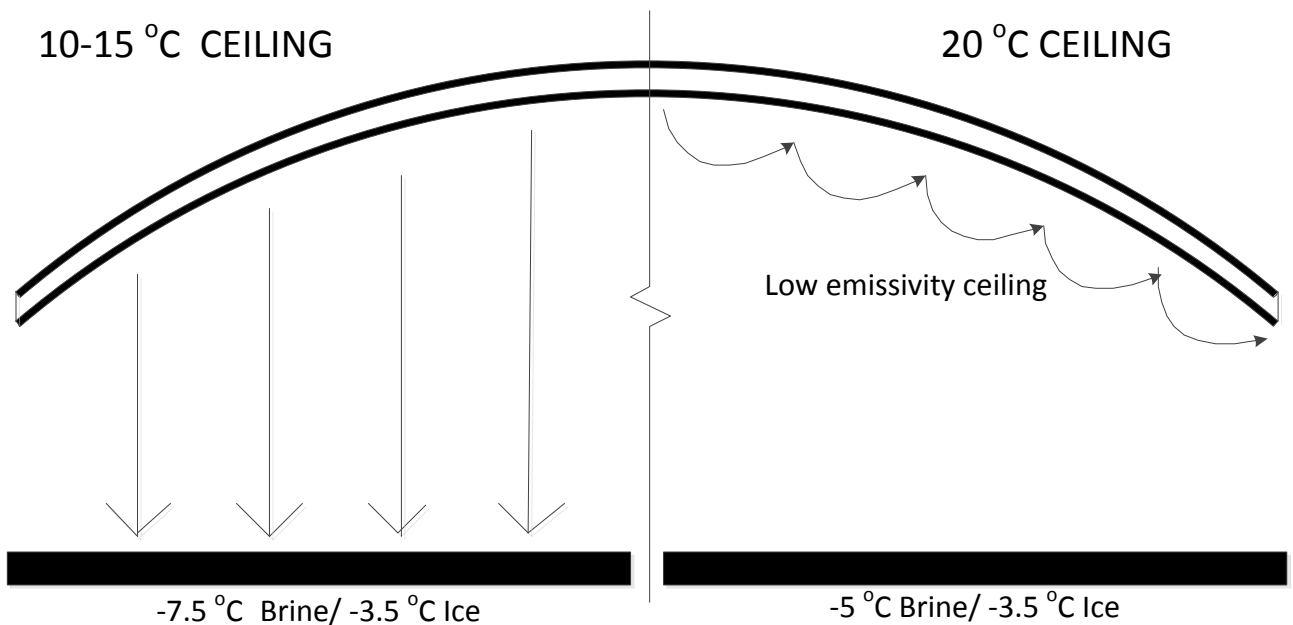


Figure 2.6: Radiant heat transfer mechanism, redrawn from (Manitoba Hydro 1991)

The energy saving effect of a low emissivity ceiling installation is shown to be 15% of the total refrigeration load (Laurier Nichols 2009)

2.3.2. Ice surface temperature controls

The ice rink energy system's main purpose is to maintain the ice surface at a specific temperature level. While it is commonly accepted that the colder the ice surface the better is skating quality, each degree increase in ice temperature could save approximately 6% annually in refrigeration energy costs (Brendan Lenko 2001). Thus it is important to maintain the ice temperature at a level, which is sufficient enough for ice quality but at its

upper limit in order to avoid unnecessary radiation. Just allowing the ice surface temperature to rise 1°C, results in a saving of 40-60 MWh electricity and an additional 70-90 MWh saving of heating per year, when operating the whole year round (IIHF 2010).

In order to keep the ice surface temperature at its optimal level it should be adequately measured. In some of the ice rinks, the surface temperature is controlled sensing the average temperature of the secondary refrigerant or the slab temperature under the ice. It is obvious that such measurements cannot properly maintain the desired temperature of the ice surface and guarantee the desired ice properties. There is usually a large safety margin to keep ice temperature low enough during all operation circumstances. That usually results in significant unnecessary energy consumption.

One of the possible solutions is infrared detectors, installed above the ice slab. These detectors measure the ice surface temperature and, thus, provide a reliable input to the control system and avoid overcooling of the ice. These systems, additionally, could be programmed in the way, which will slightly increase the ice temperature for a certain period of time (e.g. night hours and unoccupied periods) thus resulting in totally 5-15% ice rink operating energy savings (Brendan Lenko 2001).

2.3.3. Capacity controlled brine pumps

In ice rinks the pumps consume significant amounts of energy. Secondary refrigerant pumps (brine pumps) are designed and installed in order to maintain ice surface at designed temperature under extreme conditions. Such conditions include resurfacing, when a certain volume of warm resurfacing water has to get cooled and frozen, and operation during matches, when additional heat flux created from players, spectators and increased lighting tend to heat the ice. However, under normal conditions only a small share of designed pump capacity is needed.

The energy consumed by the secondary refrigerant pumps may be minimized by the use of (Natural Resources Canada 2003):

- Two-speed motors running at full speed during the day and at low speed during unoccupied hours (night),
- Variable-speed motors controlled by the brine temperature differential change;
- Two or more pumps controlled by the brine temperature differential change or with an occupied-unoccupied (day-night) timer.

Variable-speed motors or capacity controlled pumps could lead to 21 MWh/year electricity consumption savings on the average ice rink (J. Rogstam 2010)

Frequency controlled pumps provide a significant energy saving at moderate cost. The payback time of this energy saving measure seldom exceeds 2 years (J. Rogstam 2009). The field measurements taken on one of the Swedish ice rink refrigeration system indicate as much as 55.7% saving potential (see Table 2.2, estimation is based on the assumption that if the pumps had not been controlled, they would have consumed the nominal power).

Table 2.2: Field measurements of frequency controlled brine pumps compared with calculated not controlled ones (J. Rogstam 2009)

Brine pump	Nominal power (kW)	Hours of operation (hrs)	Measured energy (kWh)	None controlled energy (kWh)	Saving (kWh)	Saving (%)
BP1	15	1991	13 227	29 865	16 638	55.7%
BP2	15	5 745	46 580	86 175	39 595	45.9%
BP3	15	10 084	85 400	151 260	65 860	43.5%
BP4	15	6 658	48 800	99 870	51 070	51.1%
Average:			194 007	367 170	173 163	49.1%

The result shows a close to 50% reduction in direct energy by controlling the brine pumps, provided the control strategy used. In this case the pumps are controlled in speed steps given by the number of compressors engaged, which is a simple way to do it. The actual saving is even bigger as also includes the indirect energy which is the energy required to cool the pump energy. Provided a COP of about 3, the direct energy saving should be increased by about 30% (J. Rogstam 2009).

2.3.4. Waste Heat Recovery

Much of the substantial amount heat, which is normally wasted from a refrigeration unit, could be recovered and used to replace different heating requirements in the ice arena. Recovered heat from the condenser could be successfully used as a heat for: service water heating, under-slab heating (freeze protection), space\ventilation heating, under-seat heating, water preheating, snow melting and others (Figure 2.7).

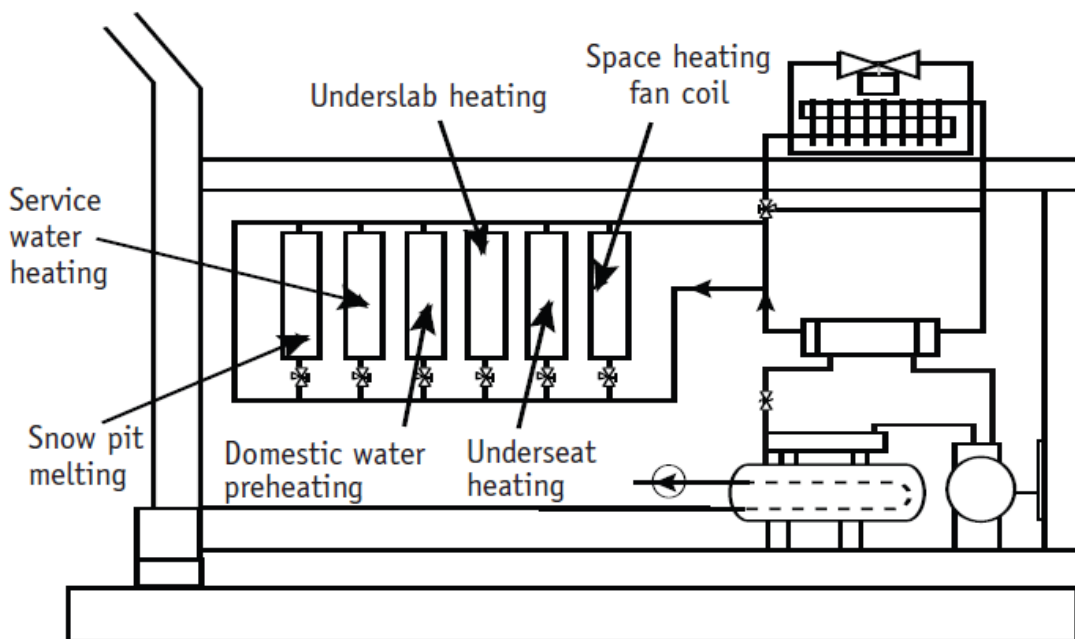


Figure 2.7: Applications for recovered waste heat (CETC 2005)

Although the installed costs of this type of heat recovery vary with the refrigeration system design and building layout, they should always be considered in planning of a new ice rink project. Additionally those rinks that use electricity for water heating should certainly consider this option (Brendan Lenko 2001).

In northern regions, such as in Sweden, also the heat recovery from the air leaving the arena is very important and efficient. It is estimated, that introducing the energy recovery could lead to 250,000 kWh saving annually for typical arena (Laurier Nichols 2009).

2.3.5. Air Handling and dehumidification

The temperature level of the ice rink air has a significant effect on both the electricity consumption of the refrigeration unit and on the heating energy need. Excessive air heating is quite expensive to operate as it is not only requiring energy to heat the air but it also leads to convective heat transfer increase. The most effective way to reduce convective heat load is to keep the ice temperature as high as possible and the air temperature as low as possible (IIHF 2010) (Brendan Lenko 2001).

A, good dehumidification is important for any rink to prevent fog and condensation in the ice rink. If the air is not sufficiently dry - the refrigeration system will have to do extra work to deal with moisture excess. Thus additional energy goes to freeze water vapour instead of water on the ice surface.

2.3.6. CO₂ as a secondary refrigerant

Different CaCl₂ solutions are dominating the Swedish market of secondary refrigerants. Being a cheap and robust choice for indirect refrigeration systems the CaCl₂ solutions have drawbacks due to mainly corrosion problems. Higher pumping power compared to CO₂ is also required to maintain the desired conditions. Recent studies highlight the benefits of CO₂ as a secondary refrigerant (J. Rogstam, Energy usage statistics and saving potential in ice rinks 2009) (Shahzad 2006). The low pumping power required referred to be the most dominant advantage with about 150 000 kWh proven yearly energy saving for a full scale in door ice hockey facility when compared to a conventional calcium chloride brine (Jörgen Rogstam 2005). Another advantage is the even CO₂ temperature, while boiling at a constant pressure, improving the ice quality.



a) CO₂ tank



b) CO₂ pumps

Figure 2.8: CO₂ as a secondary refrigerant at Woodyhallen ice rink, Katrineholm Sweden

However, such a promising energy saving measure cannot be considered as a drop in solution as it requires an adapted piping and refrigeration system.

2.3.7. Water treatment and ice maintenance

Water quality significantly influences the ice quality and thus influences the ice arena energy consumption. In order to minimise the effect of the ice quality on final energy consumption the water should be properly pre-treated. The pre-treatment process includes water purification and degasification leading to improved ice conditions (ASHRAE 2002). The water quality issues and the methods to improve ice quality will be further discussed in Chapter 4 of this paper.

Another issue is the ice thickness. An ice thickness of 20-25 mm is considered to be optimum for energy efficiency. It is noted, that every additional mm of ice will end up with measurable compressor work increase to keep the ice surface temperature at the desired value (Figure 2.9).

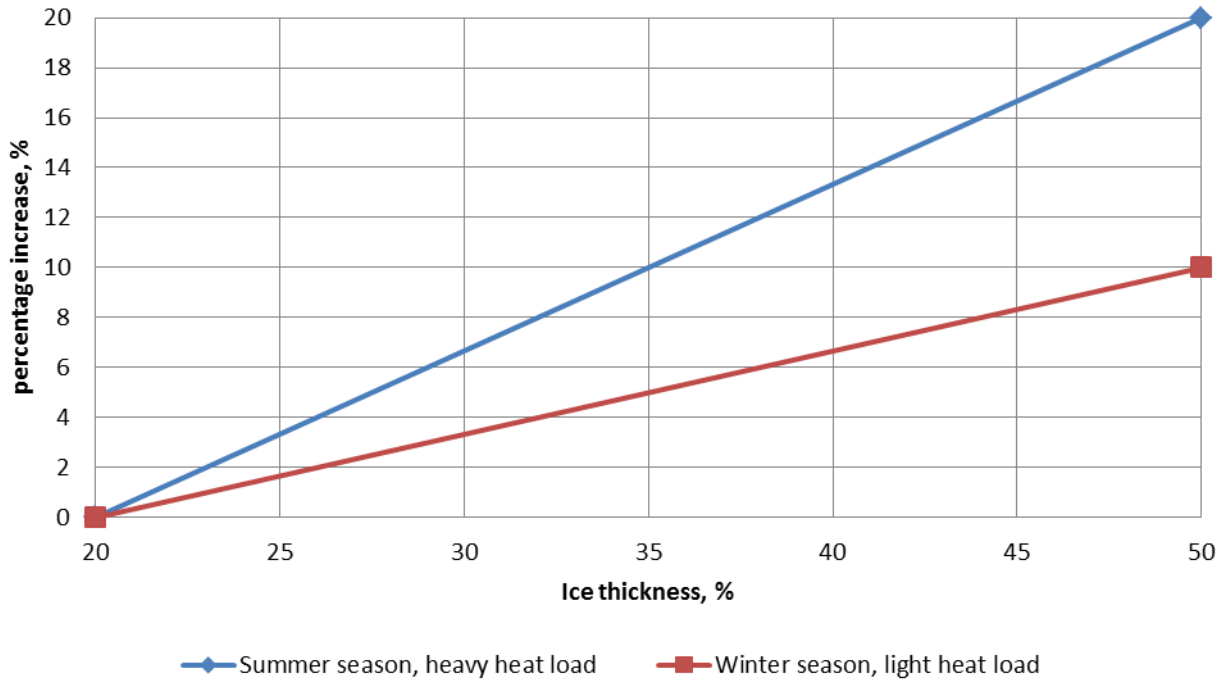


Figure 2.9: Percentage increase in compressor work compared to ice that is 20 mm thick, redrawn from (Manitoba Hydro 1991)

Ice resurfacing is considered to be one of the highest heat loads on the ice after the ceiling radiation and convection. This load, imposed by the resurfacing of ice with flood water in the range of 30 °C to 60 °C and a volume of 0.4 to 0.8 m³ of water per operation, can account for as much as 15 % of the total refrigeration requirements. A lower floodwater volume and temperature should be used to reduce the refrigeration electric energy and the cost of heating the water. (IIHF 2010)

3. Energy saving potential of the Swedish ice rinks: the Stoppsladd study.

While possible potential ice rink's energy saving measures exist everywhere it seems impossible to apply all of them into every ice rink in Sweden due to cost and time it requires to be done. Thus, a data base for decision makers, to help them find relevant energy savings methods for their specific ice rink would be very useful.

This chapter describes the process of collecting, combining and analysing the ice rinks' energy inventory data within the scope of Stoppsladd project.

3.1. Stoppsladd general information

There are 342 recorded indoor ice hockey rinks in Sweden. Today there is a clear trend towards more integrated ice rinks and longer seasons which leads to increased ice rinks' operating time and thus a greater energy use.

According to a number of different studies a typical ice rink's annual energy consumption varies greatly from 600 MWh till 2,000 MWh averaging roughly 1,000 MWh per year splitting up to about 60% for electricity and 40% for heat from various sources (Sutherland 2000) (Energimyndigheten 2009) (SEDAC 2010). This leads roughly to a total energy consumption on the order of 300 000 MWh divided into 180 000 MWh of electricity and 120 000 MWh of heat. These figures are very rough and thus can be refined during statistical analysis, which is a part of the Stoppsladd project.

The Stoppsladd project has been established to focus specifically on hockey arenas as their energy saving potential estimation. One of the objectives of the Stoppsladd project is to create knowledge and statistical base for energy usage in Swedish ice rinks. The energy inventory data have been collected from a hundred ice rinks according to a standardized checklist. The check-lists imply the collection of the information in different areas, such as: site information, general data, building, ice rink floor and Ice, water, heat-/ventilation system, lighting, cooling system (general information, compressors, brine & brine-pumps, coolant & coolant pumps, coolant cooler / condenser), heat recovery and other.

The project "Stoppsladd" has been jointly run by the Swedish Ice Hockey Association (Svenska Ishockeyförbundet) and the Swedish Energy and Refrigeration centre (Sveriges Energi- och Kylcentrum). The activity was financed by the National Energy Agency (Statens Energimyndighet) and participating organizations.

3.2. Main results

The energy statistics gained from the checklists were combined into the single database, providing the throughout access to all the data obtained and valuable comments on different arena operation aspects. The main working screen of the database created is presented in the Figure 3.1. The database consists of different information according to the checklists, providing the user with excellent possibilities to analyse the information. Some of the analysis of the data is presented further in this chapter of the work.

Microsoft Excel - StoppSladd_June_18_v01

File Home Insert Page Layout Formulas Data Review View Add-Ins

F83 Tränning A

Nr	Namn	Allmän information	Distrikt	Ägare	Category	Åskädd arplät ser No	Byggnadsår	Ombyggt / förbättrad	Allmänt: Övergrupp		Köpt energi				Säsong				Säsong m
									01	02	A1	A2	A3	A4	B1	B2	B3	B4	
									År	År	Totalt köpt el, [kWh/år]	Totalt köpt värme, [m3/år]	Kallvatten, [m3/år]	Varmvatten, [m3/år]	Start (v.)	Slut (v.)	Aktivitet (timmar / vecka i snitt)	Isarea (m2)	Byggår
8	E.ON Arena	Medelpad	Conferera AB	Evenemang B	-	1964	2003	Nej	Ja	1,348,890	298,390	900	-	29	16	70	1850	1964	
9	Katrinhallen Ishall	Västergötland	-	Publik B	-	1999	-	-	-	1,264,000	300,000	6,175	-	39	17	-	1800	1999	
14	Ejndals arena	Dalarna	Leksand IF FB	Evenemang B	7650	2005	-	Nej	Nej	2,868,993	996,550	11,397	0	25	18	70	1855	2005	
15	Gärdehov	Medelpad	-	Publik A	-	1965	2009	Ja	Nej	-	-	-	-	31	14	90	1800	1965	
17	Skellefteå Kraft Arena	Västerbottens	-	Evenemang B	6001	2008	-	-	-	2,248,890	1,388,390	-	-	31	17	-	1922	2008	
18	FM Mattsson Arena	Dalarna	Mora IK Fastighet	Evenemang C	-	1967	2004	Nej	Ja	1,100,000	590,000	6,413	-	30	15	90	1820	2004	
23	Linhamns Ishall	Skåne	-	Publik C	-	1970	-	-	-	715,000	142,000	2,698	540	-	-	-	-	1970	
25	Stora Mossan A	Stockholm	-	Publik B	1500	1988	-	-	-	645,512	439,726	5,919	-	30	21	-	1800	1988	
34	Kirsebergs Ishall	Skåne	-	Publik B	-	1970	-	-	-	743,000	0	1,384	415	31	14	-	1730	1970	
38	AXA SportsCenter	Södermanland	SSK Arena AB	Evenemang B	-	1969	2005	Ja	Ja	1,914,809	1,396,217	7,100	-	28	15	80	1800	1969	
40	Bjåsta Ishall	Ängermanland	-	Publik C	1000	1970	-	-	-	975,000	0	1,450	-	36	12	50	1800	1970	
42	Lionshov Ishall	Bohuslän/Dal	-	Tränning A	-	1990	-	-	-	541,000	0	544	272	36	22	-	1800	1990	
49	Fururinken	Norrbottnen	-	Publik C	-	1972	-	-	-	804,000	650,000	4,224	1,267	31	10	-	1800	1972	
48	Ånge Ishall	Medelpad	-	Publik C	-	-	-	-	-	797,000	215,000	-	-	-	-	-	-	-	
50	Behrn Arena	Örebro län	Örebroporten	Publik A	-	1965	2009	Nej	Nej	-	-	6,907	4,122	30	16	100	1800	1964	
58	Slottskogsrinken	Göteborg	-	Tränning A	-	1973	-	-	-	575,000	0	206	82	31	14	-	1800	1973	
59	Asköns Ishall	Göteborg	-	Tränning B	-	1989	-	-	-	1,021,000	0	1,200	420	31	14	-	1800	1989	
65	Vallentuna A-hall	Stockholm	Vallentuna komm	Publik C	-	1974	-	Ja	Nej	1,126,984	0	10,000	-	30	12	100	1800	1974	
67	Grånby Ishall A	Uppland	Uppsala kommun	Publik A	-	1974	2009	Ja	Ja	1,299,889	451,495	6,304	1,229	34	14	-	1800	1974	
70	Lugnets ishäll	Dalarna	Falu kommun, Tr	Tränning A	-	1975	2009	Ja	Ja	1,600,000	0	12,000	-	29	13	50	1845	1975	
82	Vändarparkens Ishall	Stockholm	-	Publik A	3400	1985	-	-	-	-	-	-	-	31	18	60	1800	1985	
85	Himmelstakundshallen	Ostergötland	-	Evenemang C	4200	1977	-	-	-	-	-	-	-	33	11	90	1800	1977	
86	Malungs Ishall	Dalarna	Malung-Sälens kc	Tränning A	-	1983	2003	Nej	Nej	723,913	120,652	1,931	-	37	12	84	1850	1983	
90	Björkängshallen	Stockholm	Huddinge kommu	Publik A	-	1978	2009	Ja	Nej	-	330,000	4,350	2,175	32	15	90	1800	1978	
93	Hipvallen	Ängermanland	Sollefteå kommu	Publik B	700	1977	1999	Nej	Ja	781,761	0	1,800	300	34	12	52	1850	1977	
95	Furudals Hockeycenter	Dalarna	Rättviks Förvaltni	Tränning A	-	1979	1994	Nej	Ja	1,085,000	0	4,675	-	1	52	56	1890	1979	
101	Solnäs (Hagalunds IP)	Stockholm	-	Tränning A	-	1978	-	-	-	717,000	282,000	2,352	588	40	13	-	1800	1978	
102	Nacka Ishall	Stockholm	-	Publik C	1000	1979	-	-	-	1,200,000	0	-	-	29	21	95	1624	1979	
107	Latberghallen	Ängermanland	-	Publik B	-	1970	2009	Nej	Ja	1,063,000	70,000	2,386	-	31	14	59	1850	1970	
118	Björkhalen	Värmland	-	Tränning A	1600	1981	-	-	-	1,210,955	0	-	-	29	14	85	1800	1981	
123	Norvalla Ishall	Värmland	-	Tränning A	-	1985	-	-	-	1,011,000	0	391	156	31	10	-	1800	1985	
125	Köpings Ishall	Västmanland	Köpings Kommun	Tränning A	-	1982	2009	Nej	Nej	1,500,000	0	100	-	36	13	80	1800	1982	
127	Rässhallen	Örebro län	Guldsmedshytte SI	Tränning A	-	1982	2007	Nej	Nej	550,000	31,950	1,500	-	38	9	40	1800	1982	

Figure 3.1: The StoppSladd database main window

The figure below represents the distribution of the analysed arenas by their type according to the Swedish Ice Hockey Association classification.

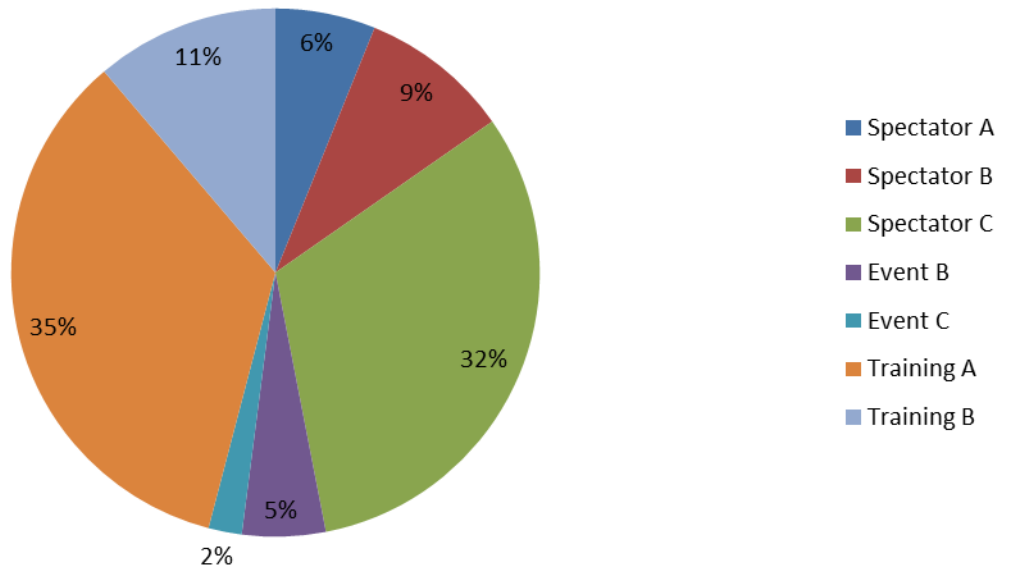


Figure 3.2: The arena type distribution within the analysed data

As one can see the majority of the analysed arenas are of Training A and Spectator C type, accounting to 2/3 of all arenas analysed. Moreover, the Event A and Training C arenas were not included into the analysis due to the statistically insignificant total number of arenas of these types in operation (2 and 8 arenas in Sweden respectively)

The typical Swedish arena was built not earlier than year 1970 (Figure 3.3). However, 6 arenas which were built in the period since 1960 till 1969 are still in operation (5 of 6 after their reconstruction).

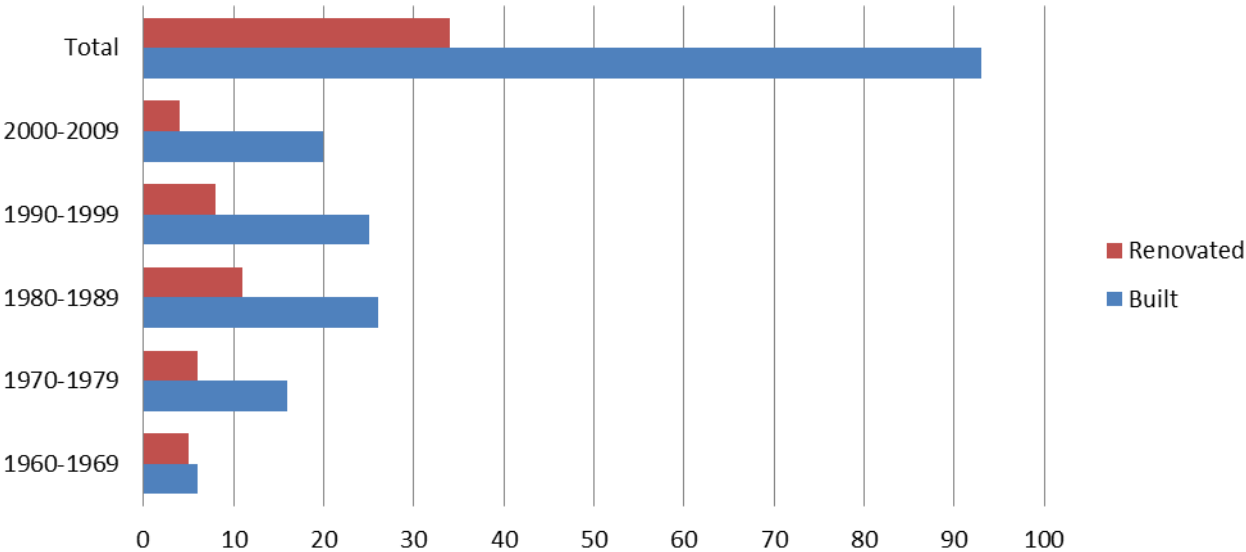


Figure 3.3: Ice rinks by age

Before stating the energy results, it is worth to mention, that during the analysis it was found that 21% of the ice rink data available is lacking the important energy information or that the information provided is doubtful. Thus the data corresponding to these ice rinks was not included in the analysis as it was considered to have too low quality. The remaining data give us the following total amount of energy, both electricity and heat, averaged by arena category (Figure 3.14).

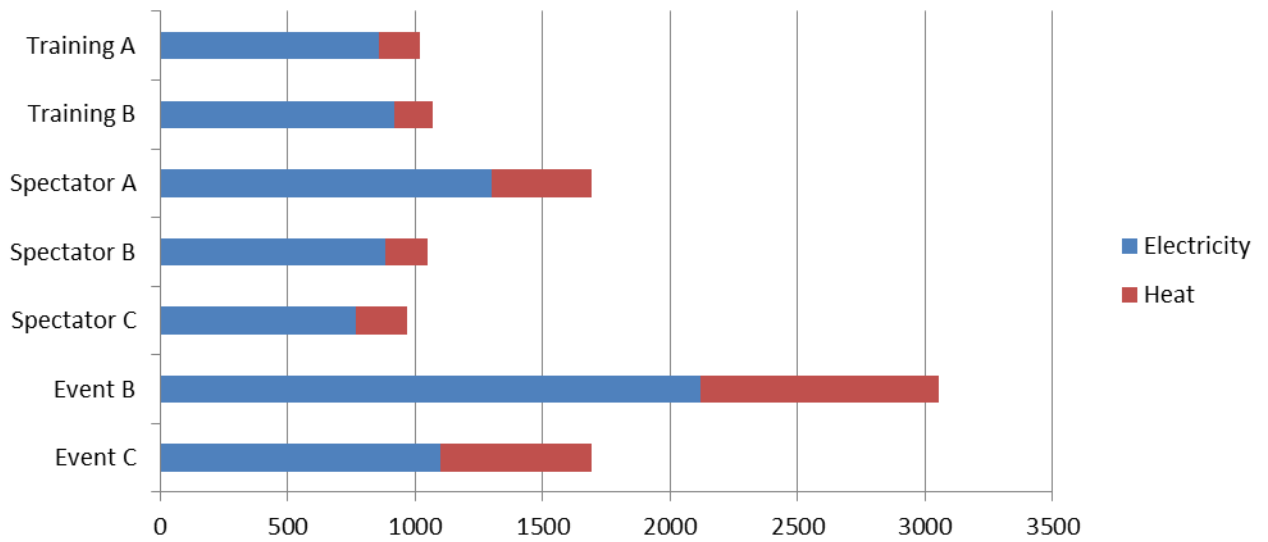


Figure 3.4: Total amount of bought energy, averaged by arena category, MWh/year

From the Figure 3.14 it is clearly seen that the maximum energy consumption within category have Training B, Spectator A and Event B arenas, where Event B arenas the average consumption exceeds 3000 MWh/year.

Another graph shows the total energy consumed by each arena, from maximum to minimum within all arenas in the study (Figure 3.5).

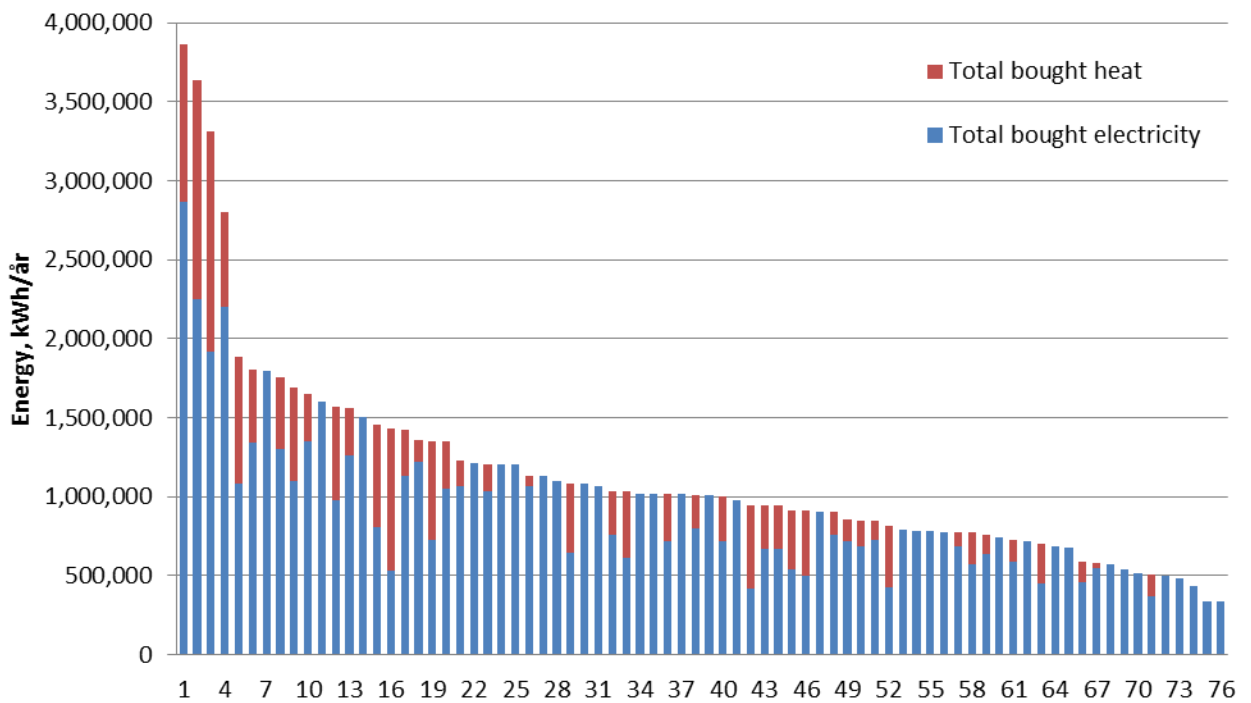


Figure 3.5: Total amount of bought energy by arena, MWh/year

Considering the average value for all arenas bought energy to be 1,137,496 kWh/year, we can see that almost 1/3 of all the arenas bought energy value is above the average. Additionally, four ice rinks have significantly bigger energy consumption than the average. What is worth to mention, even though that the majority of the arenas have a bigger share of bought electricity than bought heat; there are some of arenas which more buy heat energy than electrical energy.

The pump control systems are of vital importance for the energy saving in ice arenas. The Stoppsladd data shows that majority of ice rinks do not use any capacity control in their systems. Thus, 37 of 64 ice rinks have no brine pump capacity control, 32 of 43 – coolant pump capacity control.

Another factor is that not all the ice rinks are air tight. Thus, 12 of 55 ice rinks have leakages in the building envelope allowing uncontrolled air movements. This can lead to significant refrigeration load increase, especially during a season with warm air and high humidity.

Ice rink floors in Swedish ice rinks are made primarily from concrete with plastic tubes embedded in it for the cooling brine. The average Swedish ice rink has an 38 mm thick ice slab and is controlled based on ice temperature. The water quality (measured as electrolytic conductivity), used for in the rink, ranges from 200 till 300 µS/m. When used for resurfacing the water is usually preheated to 33 °C on average (Figure 3.6).

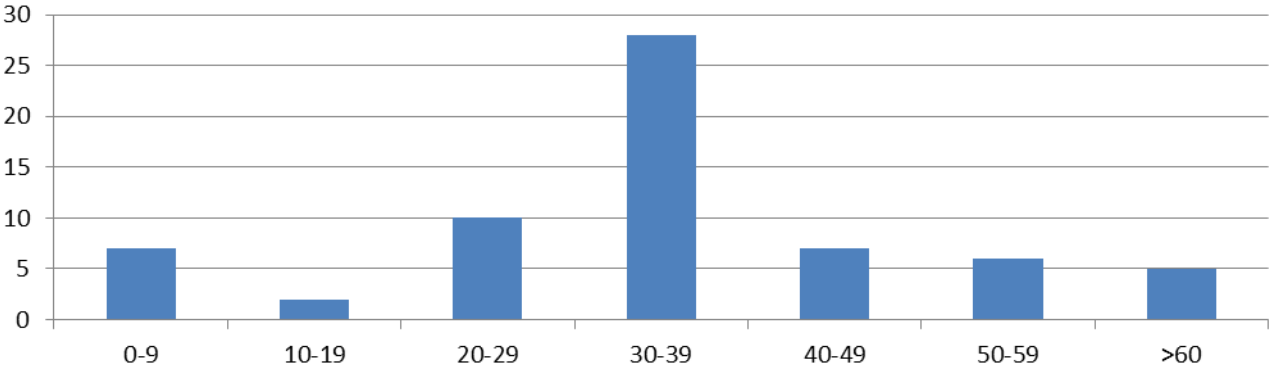
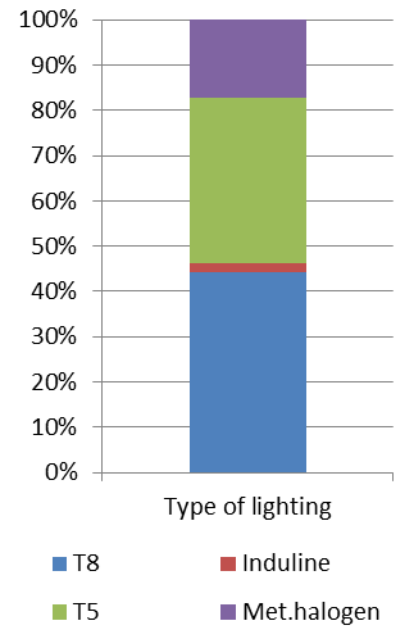
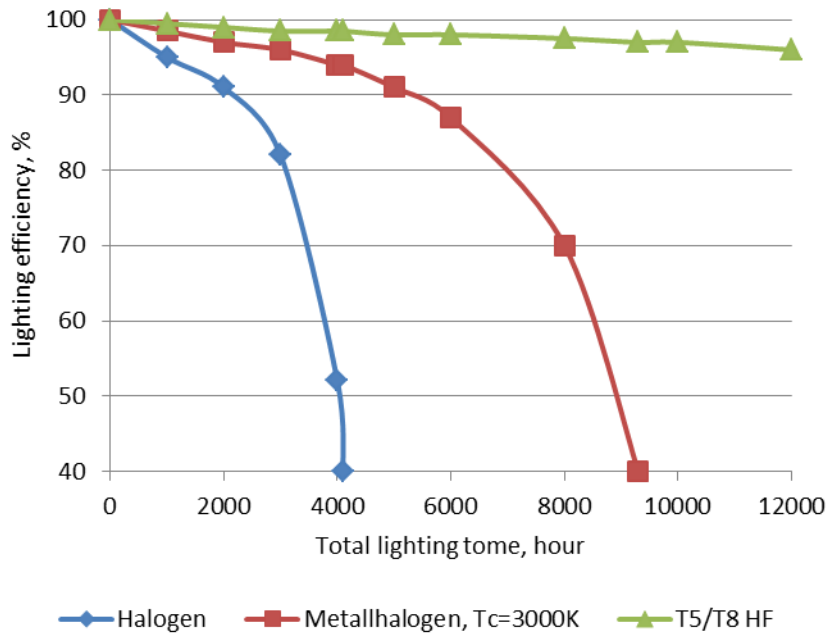


Figure 3.6: Resurfacing water temperature, °C

Different types of lighting equipments are used in ice rinks. Although there is majority of modern T5/T8 HF type lighting installed, almost 20% of ice arenas still use Metal halogen lighting type as a main lighting source. Considering the long operation time of lighting in some arenas and considerable lighting efficiency deterioration from lighting of this type, it is strongly advisable to replace the inefficient lighting with more efficient analogues (Figure 3.7).



a) Lighting efficiency decrease over lighting time, redrawn from (Fagerhult 2009).

b) Lighting, by type

Figure 3.7: Lighting type and lighting time effect on the efficiency

The refrigeration system is a main component of ice rink energy system. In Sweden one can see the following types of refrigeration systems: direct, partly indirect and fully indirect. The majority of systems are of the fully indirect type (68%) and another 29% are of the partly indirect type (Figure 3.8).

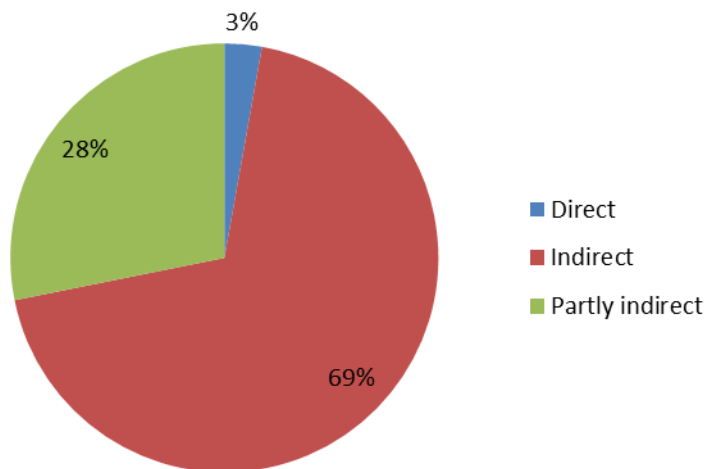


Figure 3.8: Refrigeration system type

The refrigeration systems mostly have between 1 to 3 brine pumps and ammonia is the most commonly used refrigerant (Figure 3.9):

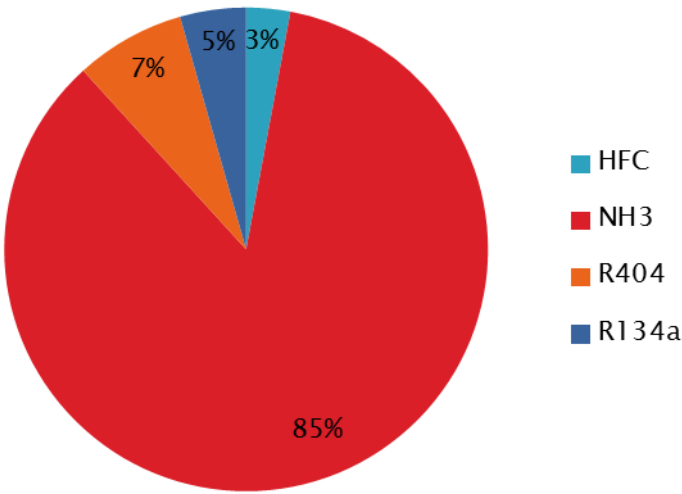


Figure 3.9: Refrigerant type used in Swedish ice rinks refrigeration systems

The cooling is transferred to the ice rink slab by different types of secondary refrigerants (Figure 3.10). The majority of the ice rinks use different calcium chloride solutions as a secondary refrigerant (referred as CaCl₂, Brineguard 25 (29), Swedbrine 25 depending on a manufacturer and CaCl₂ content in the solution). “Brine” and “CaCl₂” entries in the chart below represent the information obtained from the Stoppsladd respondents when the brine properties were not fully known. There are only two rinks among analysed ones in Sweden which utilise carbon dioxide as a secondary refrigerant.

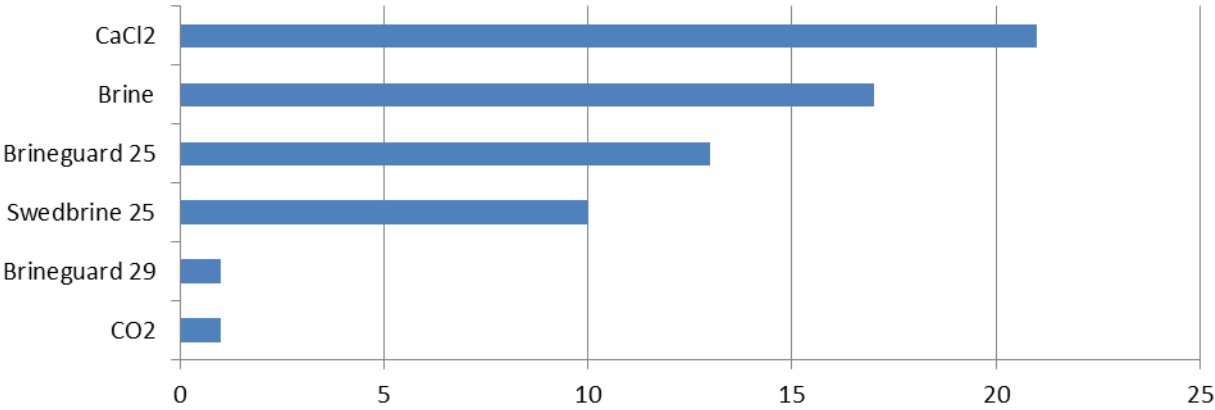


Figure 3.10: Secondary refrigerant types

The refrigeration unit produces a high amount of heat during its operation. This heat is absorbed by a condenser coolant, which is pumped through the condenser using one or two coolant pumps. Different coolants are used for this purpose, with different glycol solutions dominating in the list (Figure 3.11). In the figure below, the entry "Glycol" represents unknown glycol based coolant and could equally correspond to ethylene glycol, propylene glycol or polypropylene glycol.

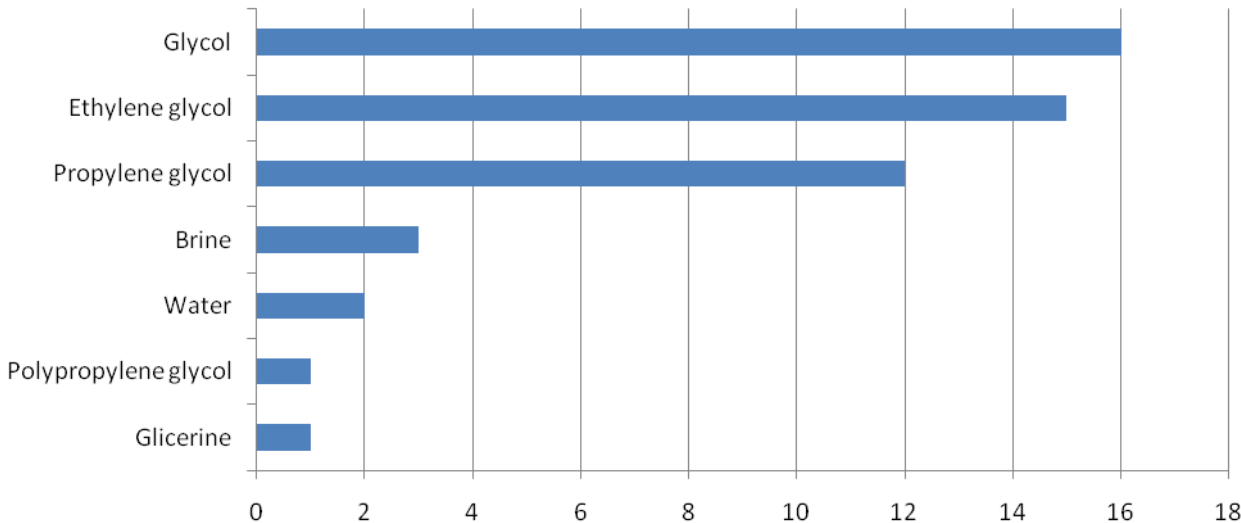


Figure 3.11: Coolant solutions

The heat, recovered from the coolant, can be further used as a heat source for the ventilation system, resurfacing water preheating. Thus, 55% of ice rinks utilise the heat recovery heat for ventilation air heating and thus providing the indoor climate with 7.6 °C temperature and 49% relative humidity on average (Figure 3.12).

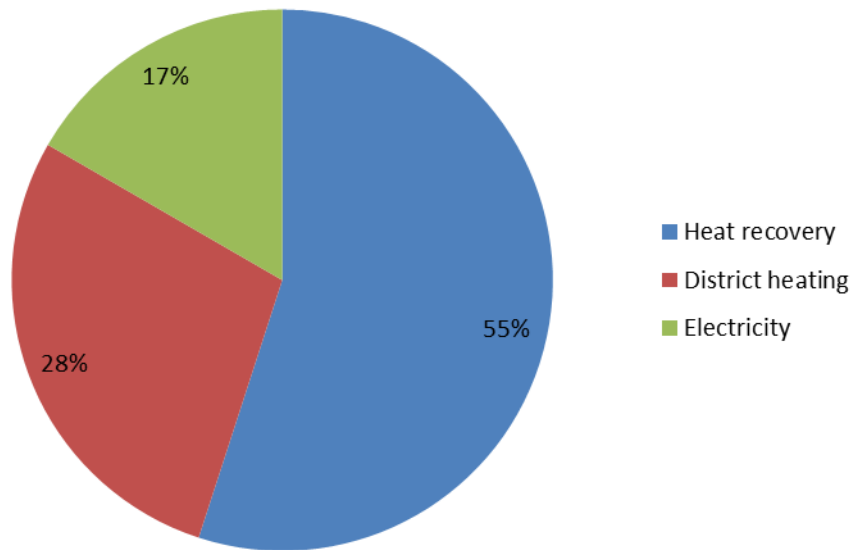


Figure 3.12: Ventilation heat source

The major statistical data is represented above in the current chapter. However, the Stoppsladd database can provide the user with a various energy data according to user's own needs. Some of the data is used for deep studies on water treatment and ice quality and ice rink floor material influence on total cooling performance.

3.3. Statistical prediction of energy load

Significant amount of data have been collected during the ice rink inventories. This allows a statistical approach for a total energy consumption prediction. From a statistical perspective the total energy consumption is a dependent value, which, in turn, is dependent on many different factors and parameters – independent variables. The statistical method, used to help us to understand how the independent values influence the dependent value e.g. the total energy consumption, is called regression analysis.

Denoting Y as ice rink's total energy consumption value and X1, X2 ... Xn as the independent variables affecting total energy consumption, it is expected to estimate the Y as a function of X1..n. Thus, the basic form of the function under the study is:

$$Y = a_0 + a_1 \cdot X_1 + a_2 \cdot X_2 + \dots + a_n \cdot X_n \quad (3.1)$$

The independent values have thus been substituted by numbers. The following 16 independent variables have been chosen for further analysis Table 3.1.

Table 3.1: Regression analysis dentations

Variable	Designation	Yes	No	n.a.
Y	Total energy consumption, kWh/year	-	-	-
X1	Year of construction	-	-	-
X2	Season length, weeks/year	-	-	-
X3	Activity, h/week	-	-	-
X4	Is the ice rink tight (Ijustät), Yes/No	2	1	0
X5	Freeze protection, Yes/No	2	1	0
X6	Normal ice thickness, mm	-	-	-
X7	Ice temperature (training), °C	-	-	-
X8	Resurfacing water temperature, °C	-	-	-
X9	Water quality, (µS/cm)	-	-	-
X10	Ice rink hall temperature, °C	-	-	-
X11	Total lighting rated power, kW	-	-	-
X12	Lighting capacity regulation, Yes/No	2	1	0
X13	Total compressors rated power, kW	-	-	-
X14	Compressor capacity regulation, Yes/No	2	1	0
X15	Secondary refrigerant pump capacity regulation, Yes/No	2	1	0
X16	Secondary refrigerant coolant pump capacity regulation, Yes/No	2	1	0

The quality of the analysis is of course dependent on quality of data in each of the independent variables. Therefore some of the ice rinks were eliminated from the analysis and the regression is based on only 44 of the ice rinks. First a correlation analysis was performed to eliminate any significant correlation between any of the independent variables Table 3.2. This analysis reveals that there is no significant interdependency between the independent variables (criteria: correlation coefficient absolute value < 0.8). Thus it is possible to proceed with further analysis using all the values from the 16 influence factors.

Table 3.2: Correlation analysis of Stoppsladd data

	X1	X2	X3	X4	X5	X6	X7	X8	X9	X10	X11	X12	X13	X14	X15	X16
X1	1															
X2	-0.10	1														
X3	-0.09	0.06	1													
X4	-0.05	0.04	-0.15	1												
X5	0.31	0.13	0.24	0.00	1											
X6	-0.06	0.22	-0.19	0.05	0.08	1										
X7	0.24	0.20	-0.17	-0.56	-0.07	0.10	1									
X8	-0.38	0.21	-0.21	-0.06	-0.07	0.18	0.14	1								
X9	0.10	-0.02	-0.19	0.68	-0.02	0.19	-0.30	-0.23	1							
X10	-0.31	0.17	0.31	0.13	-0.26	0.07	-0.17	-0.02	-0.02	1						

X11	-0.20	-0.05	-0.02	0.16	-0.17	-0.04	-0.08	0.00	-0.18	0.14	1					
X12	0.23	0.08	-0.21	-0.18	0.16	0.07	0.34	0.11	-0.07	-0.41	-0.07	1				
X13	0.13	0.04	-0.21	0.05	-0.11	0.19	0.20	-0.22	0.29	-0.12	-0.04	0.14	1			
X14	0.17	-0.32	-0.11	-0.12	-0.04	-0.07	0.06	0.08	-0.15	-0.21	-0.05	0.06	-0.33	1		
X15	-0.12	0.16	0.05	0.14	-0.03	-0.13	0.02	0.05	0.00	0.31	0.14	-0.03	-0.27	0.17	1	
X16	-0.05	-0.10	0.04	0.17	0.24	-0.40	-0.31	-0.10	0.04	-0.25	0.21	-0.05	-0.14	0.32	-0.01	1

The Microsoft Excel software has been used to perform the regression analysis. The MS Excel's Regression analysis tool performs linear regression analysis by using the "least squares" method to fit a line through a set of observations. The outcome of the analysis tool in terms of function coefficients is presented in Table 3.3.

Table 3.3: Regression function coefficients

a₀	X1	X2	X3	X4	X5	X6	X7	X8
21428477	-10717	10684	-110	-73326	-132958	13450	6538	-1992
	X9	X10	X11	X12	X13	X14	X15	X16
	428	21007	-721	-88061	1083	-142392	66300	200326

In order to increase the quality of the estimation those variables that have a low effect on the total energy consumption value Y, could be eliminated. It is assumed, that the independent values are normally distributed, and thus obeys Student's t-distribution. Under this assumption it can be possible to apply t-statistics in order to justify the degree of influence of each of the 16 factors.

Having a number of 43 observations and setting 90% confidence level the critical t-distribution value is $t_{90,43}=1.303$ (Wikipedia 2010).

By comparing the absolute values of t-statistics for each of the influences factors with the critical t-distribution value it is obvious, that X₃, X₄, X₇, X₈, X₉, X₁₂, X₁₄ and X₁₅ factors should be eliminated from the analysis, as they are statistically insufficient to influence the Y (Table 3.4).

Table 3.4: t-statistics for independent values

Variable	X1	X2	X3	X4	X5	X6	X7	X8
t Stat	-2.54	1.47	-0.08	-0.92	-1.44	3.29	0.30	-0.62
Variable	X9	X10	X11	X12	X13	X14	X15	X16
t Stat	0.93	1.49	-1.34	-0.80	3.12	-0.78	0.64	1.67

Based on the remaining variables two additional regression analyses were performed, in order to reach the sufficient prediction result. The similar to the above described analysis has revealed that factors X₅ and X₁₆ should be eliminated from the final equation in order to

increase prediction quality of the final equation. The resulting equation below thus adequately describes the dependency of total ice rink energy consumption value from a number of affecting variables:

$$Y = 24736426 - 12436 \cdot X_1 + 9757 \cdot X_2 + 9472 \cdot X_6 + 25276 \cdot X_{10} - 583 \cdot X_{11} + 1350 \cdot X_{13} \quad (3.2)$$

where

- Y - Total energy consumption, kWh/year
- X₁ - Year of construction, year; ,decreases 12000 kWh/year
- X₂ - Season length, weeks/year; increases 10000 kWh/week
- X₆ - Normal ice thickness, mm; increases 10000 kWh/mm
- X₁₀ - Ice rink hall temperature, °C; increases 25000 kWh/°C
- X₁₁ - Total lighting rated power, kW; decreases 500 kWh/kW
- X₁₃ - Total compressors rated power, kW; increases 1300 kWh/kW

The quality of the estimation could be characterised by a statistical coefficient of determination, which provides a measure of how well future outcomes are likely to be predicted by the model. For a given estimation the coefficient of determination value $R^2=0.69$ and the standard error is 226203. The R^2 value shows that the analysis model do not perfectly fits the known data, however the mean absolute prediction residual value of 136,686 indicates a sufficient prediction model. The quality of the prediction could also be visualised in a comparison of the predicted data with the measured data, available from the ice rink inventory results (Figure 3.13). The deviation of the data points values from the middle line ($x=y$) reflects the prediction error for every ice rink analysed, each represented by a point on the plot. The data on Figure 3.13 shows that a prediction higher than actual energy consumption up to about 1100 MWh. For larger consumption the opposite is true. The explanation for this observation is that rinks with high energy consumption values have more influencing factors, which are often too complicated to be taken into consideration.

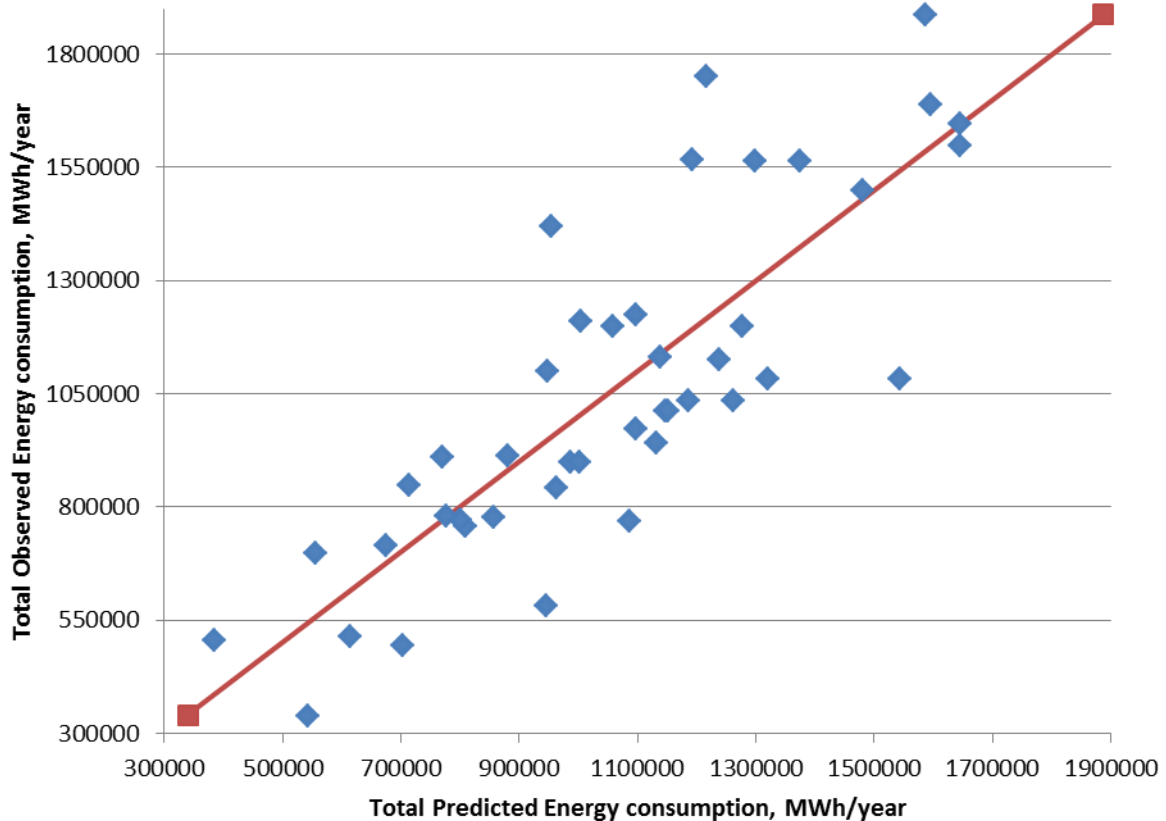


Figure 3.13: Total energy consumption observed over predicted data comparison

Thus, the prediction equation is sufficient enough to allow the model usage for rough total energy consumption estimation and, what is more important, reveal the degree of influence of each of the influencing factors on the final value. It is worth to notice, that the quality of the model could be further increased by increasing a number of significant independent variables, number of observations and using different approximation model for analysis (e.g. exponential).

3.4. Discussion

The study during the Stoppsladd project has resulted in a database comprising the information from the inventory of 100 ice rinks. The database is well structured and utilizes all the MS Excel software functionality in terms of data storing, organizing, filtering and results analysis.

From the data analysis results we can see, that the biggest energy consumers are the Event arenas. Thus, the total energy consumption of Event B arena is more than 3000 MWh/year on average. That is, of course, due to specifics of such arena type: it consumes significant amounts of extra energy for supplement of different facilities, except for the ice rink itself. Training A and B arenas and Spectator B and C have a total energy

consumption around 1000 MWh/year, which expectedly is slightly below the average value for all the arenas.

The Figure 3.5: Total amount of bought energy by arena, MWh/year represents a statistical information which is very interesting for the analysis. Thus, it could be noticed, that 4 out of 76 ice arenas consumes an amount of energy, well above the average value. It could be well worth to study them further.

Additionally, it could be easily seen, that some of the arenas do not consume external heat, others, in turn, consume more heat than electricity. It seems possible, that such a difference could be explained looking at the different degree of heat recovery and waste heat utilisation. Such arenas, especially those belonging to the same class, should be analysed more in detail to detect differences and reveal best available techniques for further energy consumption reduction.

It must be stressed that, even if the average energy consumption is 1,137,496 kWh/year, 2/3 of all arenas consume less energy than this average value.

The major outcome of the Stoppsladd study is that most of ice rinks do not use pump capacity control in their operation. This is a simple and effective measure to improve operation efficiency. Also it is simple to improve the energy efficiency by simply tightening the building envelope. These low cost energy saving measures can lead to a large absolute energy saving.

Another issue is resurfacing water and its quality. While it is doubtful if very hot resurfacing water really improves the resurfacing quality, it is absolutely clear that each additional degree it is warmed causes additional energy consumption, first to heat the water before resurfacing and then the extra energy input to cool it again. The author believe that the resurfacing water effect on ice quality and resurfacing efficiency should be further analysed. The same temperature could then be applied in all the Swedish ice arenas.

It is known, that lighting stands for 10% of the total energy consumption (Månberg 2010). Currently, almost 20% of all ice rinks use Metal halogen lighting as a main lighting source. Considering the tendency of this lighting type to decrease in lighting efficiency, it is suggested to consider the efficiency over operation time factor when changing lighting. The best available option for the installation is T5/T8 lighting, which keep almost 100% of their lighting efficiency over the entire operation time.

The refrigeration system produces a lot of excess heat during ice rink operation. Thus it is very important to address the waste heat utilisation problem properly. The heat excess could be used to preheat ventilation air, to preheat resurfacing water, to maintain freeze protection beneath ice rink floor or for other purposes. However, a number of ice rinks use electrically heated wires for freeze protection, which is very inefficient from an energy perspective. Additionally, only 55% of all the analysed ice rinks use heat recovery as a heat

source for ventilation. At the same time, 17% of the ice rinks use electricity for the same purpose and more than 14% use electricity to heat the resurfacing water. The author believes that the use of electricity in ice rinks for reasons other than lighting and compressor operation should be minimised as much as possible.

Having collected a vast number of different data it is possible to use it for finding statistical interrelations, which can help us to analyse the problem in the study from another perspective. A multifactor linear regression analysis has been done in this study. Sixteen different uncorrelated factors have been chosen for the analysis to estimate their influence on the total energy consumption in the ice rink. The analysis revealed that the least influencing factors are the freeze protection existence and resurfacing water temperature. That could be explained as these factors represent a small share of total energy consumption as consume energy at intermittent basis. The following factors have been found important in the statistical analysis: the year of construction, ice rink air tightness, normal ice thickness and temperature, total lighting rated power and its capacity regulation, compressor capacity regulation and secondary refrigerant capacity regulation. While insignificance of some of the factors could be explained (lighting is not fully on all the time and thus its rated power does not influence total energy consumption a lot), some of the factors elimination is more difficult to explain (ice temperature and compressor capacity regulation).

Equation (3.2) describes the approximation model of the total energy consumption value, which increases with season length, normal ice thickness, ice rink hall temperature and total rated compressor power. The energy consumption decreases with the year of construction and total lighting rated power.

The equation (3.2) represents an interesting relation, as, additionally to the obvious season length and total compressors' rated power, emphasizes importance of proper ice rink hall temperature and reflects building envelope degradation and improved building techniques with time. As can be seen from the equation, each additional degree of the hall's temperature results in 25,274 kWh/year energy consumption excess. Respectively, ten years difference in ice rink year of construction result in 124,360 kWh/year consumption. At some time point it is interesting to build a new one.

Surprisingly, the increase of total lighting rated power decreases total energy consumption. It is difficult to justify this interrelation and, thus, it is assumed to be approximation model error which, probably, could be eliminated in a more detailed study.

4. Water treatment and Ice quality

4.1. Introduction to the problem

Since many years ice surfaces are used for ice skating, and the main reason for that is the unusual slipperiness of ice which makes it a perfect surface for hockey games and other sport activities. Scientists agree on that the lubricating layer on top of the ice that creates the glide. It is depending on at least one of three mechanisms for its formation: friction heating, pressure melting or intrinsic pre-melting (Li and Somorjai 2007). Considering that all of them were proposed long time ago (pressure melting – James Thomson, 1850; frictional heating – Bowden and Hugles – 1939; intrinsic pre-melting – Michael Faraday, 1842), the intrinsic pre-melting mechanism which reflects in quasiliquid water layer on the ice surface seems nowadays the most adequate explanation on why it is easy to skate on the ice (Conde, Vega and Patrykiewicz 2008) (Rosenberg 2005).

Proper ice quality is a vital factor for any activity on the ice. Hockey players distinguish two basic types of ice: so called “hard ice” and “soft ice” (one can find another names but with similar meaning – fast and slow ice, etc.). Those notions imply a set of different ice qualities, which make the possibility to control the game for the players easier or harder. Those properties include friction, density and others. The properties of the ice depend on the water quality, which, in turn, is always different if no water treatment is used. To achieve good ice quality one should consider the following water contaminations (Ontario Recreation Facilities Association Inc. 2007): organic matter, dissolved minerals and air. The mineral content of the water significantly affects ice quality as due to the resurfacing specifics the minerals contents become higher at the ice top, which actually serves as a plying surface.

While the mineral and organic matter could be eliminated from water by a number of existing methods, the air content in the water significantly affects ice quality and should be minimized. That comes from the difference in solubility for air in water and ice, which is normally higher for water, than for ice. That leads to gas bubble nucleation and growth in ice during the freezing process (Inadaa, Hatakeyama and Takemura 2009).

One of the methods to minimize the air content in the water is to rise the water temperature used for ice resurfacing. That comes from the fact that the air (oxygen) absorption ability of water is inversely proportional to the temperature as shown in the Figure 4.1.

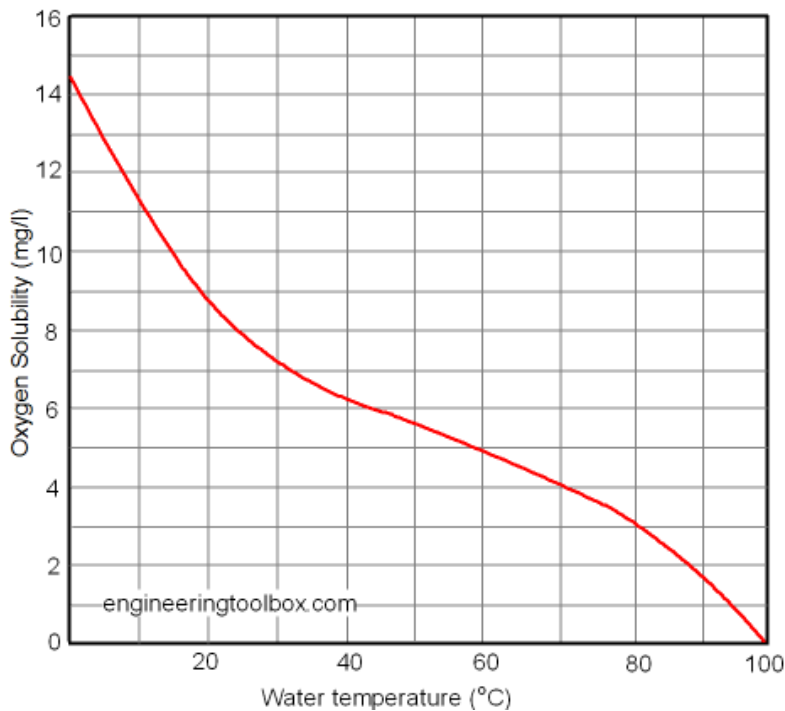


Figure 4.1: Dissolved Oxygen in Fresh Water (at atmospheric pressure) (The engineering toolbox n.d.)

The heating method is not so energy efficient due to the relatively high cooling load required to cool the resurfacing water. Another method which could be utilized is deaeration by means of special device – deaerator, or, more general, degasificator. The degasification process could be based on different techniques: heating, pressure reduction, membrane degasification and others (Wikipedia 2010). One of the products used for ice rink resurfacing water degasification is the Realice (see Figure 4.2 and Figure 4.3).



Figure 4.2: Realice Base product (Watreco 2010)

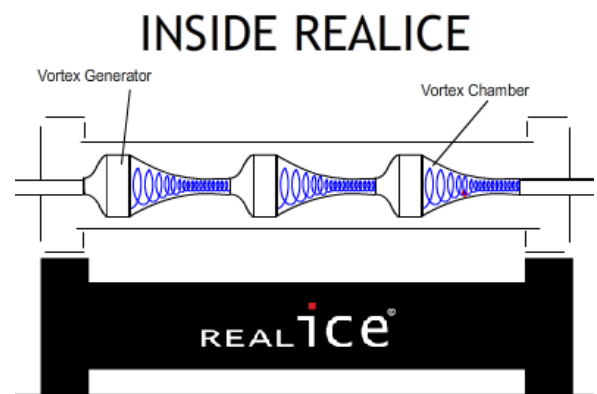


Figure 4.3: Realice system with the 3 vortex generators inside it (Realice System - Improved Ice Quality 2010)

It utilizes a degasification method based on the Vortex generator. The manufacturer claims that “In vortex-treated water, molecules are more structured and thus find it easier to crystallize upon freezing. Furthermore, the viscosity of the water is changed so that it flows out more easily at lower temperatures” (ReallICE 2010), however, no scientific evidence of such a significant effect on water is provided. Additionally, it is stated that the Vortex generator convert the calcite dissolved into aragonite, one of three polymorphs of calcium carbonate (ReallICE 2010); improve the water molecules structure and alter water viscosity (ReallICE 2010).

As there is no scientific evidence supporting these statements provided by the ReallICE manufacturer it is important to investigate the influence of the above mentioned water treatment on the water quality. The influence of water quality on ice quality is easy to show on the ice cube example freezing. During the freezing process the pure water freezes first, pushing the dissolved minerals and gases to the centre of cube. One can see the “cloud” in the centre of the cube then when the freezing is over (Whitman, et al. 2008). Thus the size of the cloud is assumed to be proportional to the water quality.

Additionally the water viscosity test and surface tension test could be performed.

4.2. Water properties tests

Two water samples have been used for a number of measurements. The conventional tap water daily used in one of the Swedish ice arena (Reference water) has been compared with Reallce vortex-treated water (Reallce water) from the same arena.

4.2.1 Electrical conductivity measurement

Electrical conductivity is a measure of a material's ability to conduct an electric current. The HANNA EC/TDS tester have been used to measure the electrical conductivity of both Reference and Reallce water samples (Figure 4.4, a). Two consequent measurements were used to decrease the statistical uncertainty of the measurement. The electrical conductivity values for both samples are following (see appendix A for measurement setup details):

- Reference water $\sigma_{(ref)}=242.5\pm 4.9 \mu\text{S}/\text{sm}$
- Reallce water $\sigma_{(Ri)}=239.5\pm 6.5 \mu\text{S}/\text{sm}$

4.2.2 PH level measurement

pH is a measure of the acidity of a solution. The HANNA pH/ORP/ISE tester has been used to measure the pH level of two water samples: Reference water and Reallce water (Figure 4.4, b). The pH values for both samples are following (see appendix B for measurement setup details):

- Reference water $\text{pH}_{(ref)}=8.1\pm 0.1$
- Reallce water $\text{pH}_{(Ri)}=8.1\pm 0.1$



a) electrical conductivity



b) pH level

Figure 4.4: Water properties measurements

4.2.3 Freeze rate tests

Two different freeze rate tests were performed (see Appendix C). However, both tests utilise the same approach: the 5 ml water samples were applied on the pre-frozen surface to get water frozen (see Figure 4.5). The freezing time that was noted and compared to reveal any difference between two samples under study.

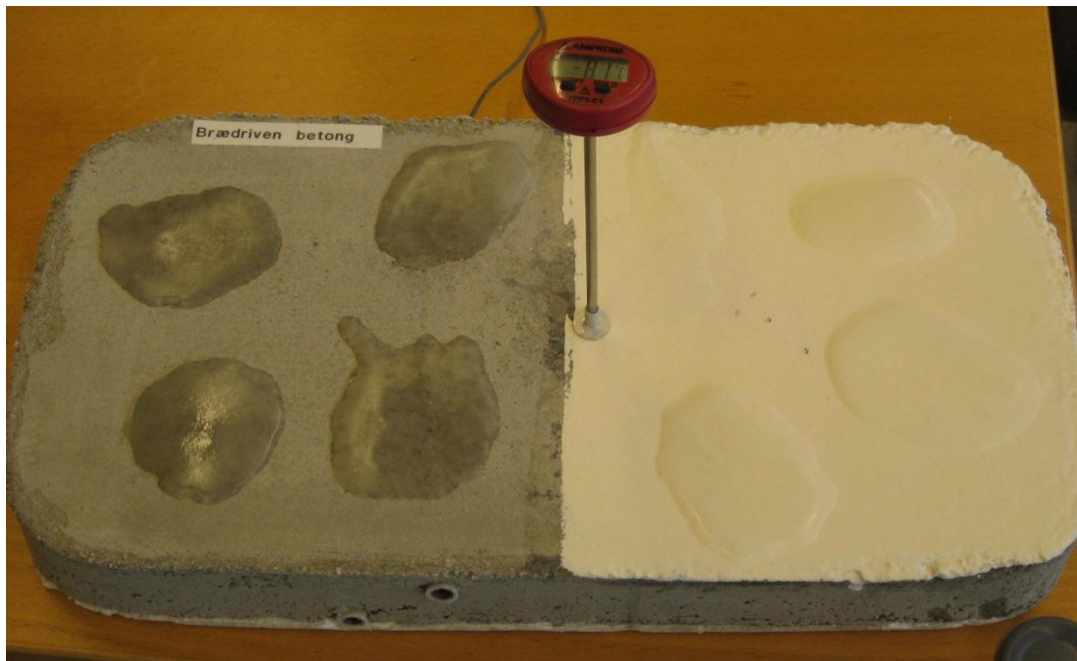


Figure 4.5: Freeze rate test

The test results reveal no significant difference in freeze rate of both water samples. All the samples have been frozen within the following time interval: 457.0-482.5 seconds, thus

leading to the sample standard deviation value of 12 seconds (or only 2.5% of the mean value).

The difference between the samples freeze rate could be explained by the measurement uncertainties effect. It appeared to be difficult to uniformly apply all water samples to the surface. That affected the water surface area and, consequently, heat transfer was uneven between the samples. Under these circumstances the author suggests improving the test conditions to minimise the measurement uncertainties. This could be achieved either by significantly increasing the number of tests or by utilising more precise freezing rate determination method.

In order to increase the scope of the freezing rate test the blind test on ice quality was performed. The, randomly chosen assistant person was asked to determine the “best” ice samples on the concrete slab (Figure 4.5), based on subjective analysis of its properties (clearance, shape, etc.). The person’s choice was randomly distributed among the samples and didn’t reveal any regularity with the two water samples distribution on the ice slab.

4.2.4 Ice visibility test

Ice visibility is known to be dependent on water quality ice made of. The dissolved air and minerals significantly affect ice clearance visible in shape of the “cloud” in which the dissolved air and minerals accumulates during the freezing process. Thus the ice visibility test has been designed and held to study the effect of different deaeration methods. The method used in the test is presented in Appendix D. Three ice samples were examined under the first stage of the test. However, no significant differences were revealed as a result (Figure 4.6).

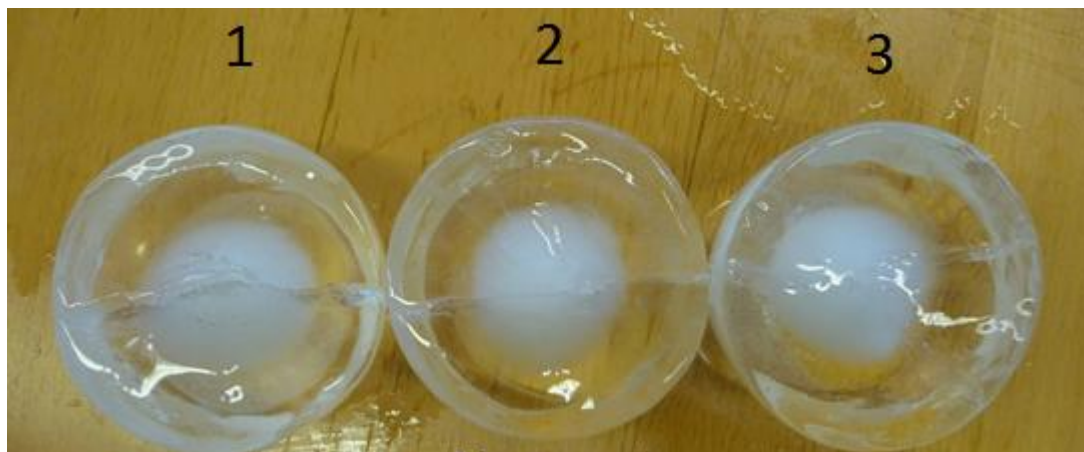


Figure 4.6: Ice visibility test 1 (1 – preheated to boiling temperature; 2 – reference untreated sample; 3 – Realice vortex-treated water)

All the samples indicate quite similar impurities contents: thus indicating that neither vortex treatment nor preheating to the boiling temperature affect water in a way that significantly improves the ice quality.

The ice visibility test results led to another test, in which distilled water sample (thus containing no dissolved minerals) was boiled in order to eliminate dissolved gases and then frozen. The obtained ice sample is shown in Figure 4.7.

As it was observed (and partly seen on the picture below), the ice sample can be characterised by much lower impurities content than prior test results (indicated by the specific “cloud” absence).



Figure 4.7: Ice visibility test 2

Both test results lead us to conclusion that solely deaeration is not sufficient to increase water/ice quality, instead the dissolved minerals content, normally indicated by water electrical conductivity, greatly affect quality of ice and should be taken into consideration.

4.2.5 Viscosity test

In two water samples, the dynamic viscosity have been measured with a falling-ball viscometer. The measurement is based on the velocity determination of a ball, which is falling through the liquid in a tube (Figure 4.8).

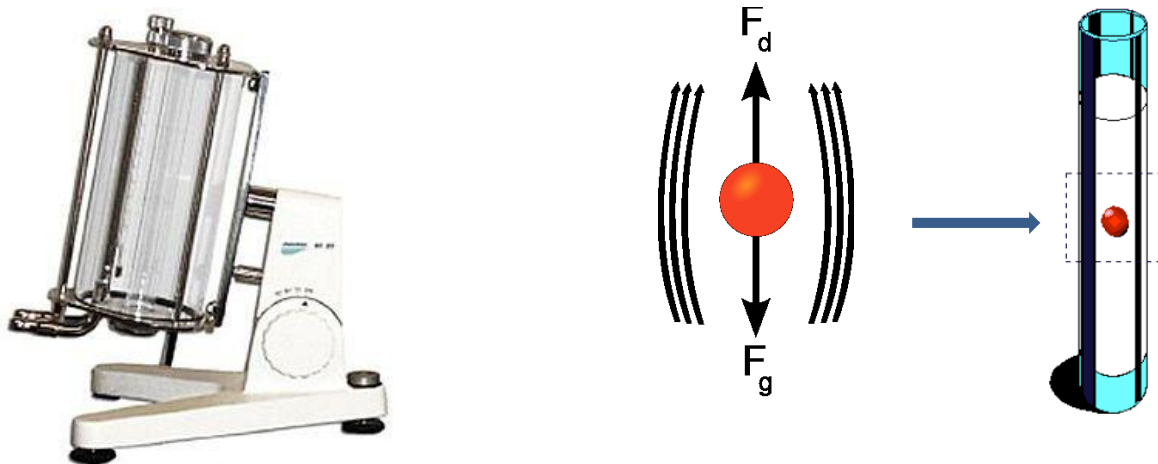


Figure 4.8: Falling ball viscometer (left) and its working principle (right)

The reference water in the measurement results denoted as Sample water II, RealIce vortex treated – as Sample water III. The measurements have been held under different water samples' temperature. The results are generalized in Table 4.1 ($1 \text{ cP} = 1 \times 10^{-3} \text{ N}\cdot\text{s}/\text{m}^2$).

Table 4.1: Dynamic viscosity, measurement result

$T_{\text{water}}, \text{ }^\circ\text{C}$	Reference water, μ (cP)	RealIce treated water, μ (cP)
20	1,002 \pm 0.010	1,002 \pm 0.010
30	0,7996 \pm 0.008	0,8000 \pm 0.008
50	0,5522 \pm 0.006	0,5530 \pm 0.006

The measurement concludes that the difference between the viscosity for both samples and distilled water was smaller than the accuracy of the instrument (Royal institute of technology 2010).

4.3. Discussion

A number of different experiments have been carried out in order to study the effect the vortex generator could have on the water. The interest to this problem was mainly due to the information, available from one of the manufacturer of such equipment. Thus, the following claim was put under the study: "In vortex-treated water, the molecules are more structured and thus find it easier to crystallize upon freezing. Furthermore, the viscosity of the water is changed so that it flows out more easily at lower temperatures. ... As micro and nano-bubbles have been removed from the water, the ice obtains greater clarity so that advertising and lines become more clearly visible through it. (RealICE 2010)"

Electrical conductivity and pH level measurements were done in order to identify a possible variation of these values between two water samples. According to the electrical conductivity measurement results, it is quite difficult to state which sample has the best or worst electrical conductivity. The absolute measured value for the reference water sample is larger than for the RealIce water sample, however the difference is so small that the uncertainty of the measurement makes it impossible to say which sample is the best. The pH level, in turn, appeared to be in limits of 8.1 ± 0.1 .

A more complex freeze rate test has been done to estimate how fast a 5ml water volume can freeze. It appeared to be difficult to maintain constant shape of the ice surface and that led to a degree of uncertainty for the test results. Instead, a blind test was performed to analyse the quality of the ice produced from different water samples under constant conditions. proved to be difficult to determine the difference between the ice surfaces and name any water source. It seemed reasonable for the author to repeat an improved test trying to obtain a more uniform ice surface and thereby increasing the total number of measurements. These improvements could lead to more certain results, creating a better basis for this part of the analysis.

The ice visibility test revealed that the difference in degree of clarity between the ice blocks obtained from different water samples can't be detected by the eye.

Another test, which was designed to clarify the effect of a vortex-generator on water properties, is a viscosity measurement test. The viscosities of two water samples have been measured with a falling ball viscometer. The viscosity, detected for both water samples, appeared to be the same even when measuring at different liquid temperatures. Moreover, it appeared to be very close to the values for the distilled water sample. Thus, it could be concluded that the effect of vortex-generator on water viscosity is so low that it could not be detected by the equipment used for the measurement.

Conclusion: it was not possible to determine the effect of vortex-generator treatment on the water properties or the properties of ice, produced from this water. All the tests resulted in a negligible measured difference between the reference water sample and the Reallce treated water. However, the freeze rate test did not provide enough certainty concerning the ice quality to be absolutely certain. Thus, it seems to be reasonable to carry out more precise measurements in order to increase the quality of the whole analysis.

5. Ice rink floor material influence on system performance (simulation/experiment)

5.1. Introduction to the problem

The ice rink refrigeration system is supposed to maintain the ice slab at a “low temperature”. While research has led to considerable improvements in the refrigeration unit itself, the ice rink slab thermodynamic performance has not been so thoroughly investigated. However, one can conclude that the ice slab is a heat exchanger, aiming for an efficient heat transfer from the ice surface to the brine circulated in the pipes below.

The typical ice rink floor design is presented in Figure 5.1.

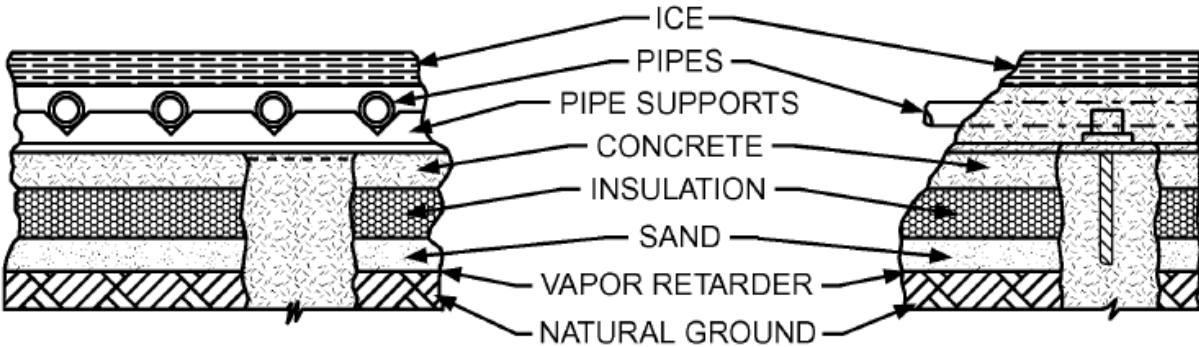


Figure 5.1: Typical ice rink floor design (ASHRAE 2002)

Thus the ice rink floor “heat exchanger” constantly experiences a unnecessary heat gain from heated concrete beneath the insulation, while it should be able to effectively absorb the heat flow from the skating ice surface, above the chilled concrete slab.

Knowledge of the thermal properties of the materials used in the construction of the ice rink slab is very important, as it allows modelling of the behaviour of different components (for instance modelling the temperature distribution in the slab and the heat flow to the refrigerant in the cooling coils).

Additionally, by affecting the thermodynamic properties (such as thermal conductivity, specific heat, density, etc) of the concrete layers beneath and above the brine pipes, it could be possible to simulate the thermodynamic response of the system to a varying heat load from above. That could result in a better maintaining of a constant ice surface temperature with an increased brine temperature. That in turn will lead to energy savings in the whole ice rink operation at a very low investment cost.

While the ice properties are well determined and known (Fukusako and Yamada 1993) the parameters of the concrete below can be varied. Different studies estimate thermal conductivity of dry concrete to be within the range of 0.62-2.77 W/(m·K) (Khan 2002) (Kook-Han Kima 2003). Thus, it is clear that using different techniques when producing it could significantly vary the thermal conductivity of concrete. Moreover, it could be possible to predict the conductivity by using, for example, Campbell-Allen and Thorne's model (Thorne 1963). However, this implies that the investigator has knowledge of all the components constituting the concrete and that all their thermodynamic characteristics are known. It is obvious, that such information is not always available. For the sake of simplicity in this study we do not try to predict the thermal conductivity, but instead we measure it using relevant equipment.

5.2. Thermal conductivity measurements of a number of samples

5.2.1 Principle

Thermal conductivity is defined from the following equation, which is an interpretation of the Fourier equation:

$$k = \frac{Q/A}{\Delta T/\Delta L} \quad (5.1)$$

, where Q - amount of heat passing through a cross section A and causing a temperature difference ΔT over a distance of ΔL . In other words, the thermal conductivity is measured through heat flux and temperature difference measurements (Holman 2001).

There are two common groups of measurements which are used: steady-state and transient methods. The Transient Plane Source (TPS) method is used to measure thermal properties on various sample types such as liquids, pastes, solids and powders regardless of if they are electrically conducting or not. Thermal conductivity, thermal diffusivity and specific heat capacity of a material can be measured using the TPS method.

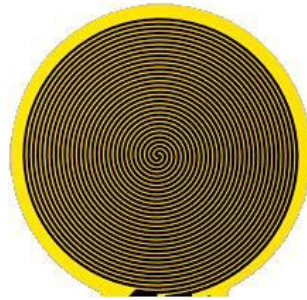
The TPS probe comprises a sensor (Figure 5.2) acting both as heat source for increasing the temperature of the sample, and a resistance thermometer for recording the time depending temperature increase of the sensor. The TPS sensor element is made of a 10 μm thick electrically conducting Nickel foil in the shape of a double spiral. The Nickel foil is sandwiched between two layers of (0.013 - 0.025 mm) polyimide (Kapton) in order to

keep its physical shape, increase mechanical strength and supply electrical insulation (Bitaraf H. 2010).

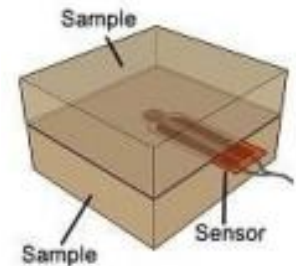
The measuring sensor (Figure 5.2, a and b) is placed in between of two pieces of the sample in contact with the surfaces (Figure 5.2, c).



(a) Hot Disk sensor 5501



(b) tip of the Hot Disk sensor 7281



(c) Measurements for solids

Figure 5.2: A typical TPS sensor (Bitaraf H. 2010)

The measurement is based on the temperature increase, which is created by passing a current through the Nickel foil. The time and power output are adjusted manually, depending on the characteristics of different materials. The generated heat is dissipated on both sides of the sensor and the selected rate are dependent of the thermal transport characteristics of the sample (Bitaraf H. 2010).

TPS is an absolute method, which provides fast and convenient measurements. Additionally, there is no requirement to calibrate the sensor against a known thermal transport property material. The specifications for TPS 2500 is shown in the table below:.

Table 5.1: specifications for TPS 2500 (Bitaraf H. 2010)

Thermal Conductivity (TC):	0.005 to 500 W/(m•K)
Thermal Diffusivity:	0.1 to 100 mm ² /s
Specific Heat Capacity:	Up to 5 MJ/m ³ K
Measurement Time:	1 to 1280 seconds
Reproducibility for TC:	Typically better than 1%
Accuracy for TC:	Better than 5%
Temperature Range:	Standard; Ambient (Room Temp. only) With Circulator; -50°C to 150°C

5.2.2 Results

The measurements have been done in two tests sessions. Four different concrete samples have been studied in the first test. Those four concrete samples have been manufactured using different techniques to get the desired thermodynamic properties (most importantly to increase the thermal conductivity of the concrete sample). The samples were further tested according to the principle described above. The samples and the assembling procedure are presented in Figure 5.3.



a) Different concrete samples



b) Assembling the sensor in the room-temperature - the solid sample holder

Figure 5.3: The samples and the assembling procedure

The measurement results from the first thermal conductivity measurement session were used to adjust the concrete sample production technique and, thus, two more concrete samples were created and tested for the second test session. The first test measurement session procedure is described in detail in the “Measurement report for TPS 2500 thermal conductivity” (see Appendix G). The second test session has been held according to the same procedure and the combined results from both sessions are shown in Table 5.2.

Table 5.2: Results (Bitaraf H. 2010)

Sample	Temp	Avg of 5 Meas. Polished surface		
		Th.Cond. (W/(m•K))	Th.Diff. (mm ² /s)	Spec.Heat (MJ/m ³ K)
Con 01	Room	1,769	0,989	1,789
Con 02	Room	1,662	0,834	1,993
Con 03	Room	1,866	0,888	2,105
Con 04	Room	2,119	0,828	2,560
Con 05	Room	2,806	1,144	2,452
Con 06	Room	2,647	1,099	2,409

As we can see from fig 5.4 the result measured on the same sample has a spread. That can be partly explained by to the non-uniformity of the material and partly by the surface shape which is completely fully flat.

The thermal conductivity measurements were complemented with density measurements for each sample. The density values were obtained using the samples' volume and weight. The combined conductivity and density results are presented in Figure 5.4.

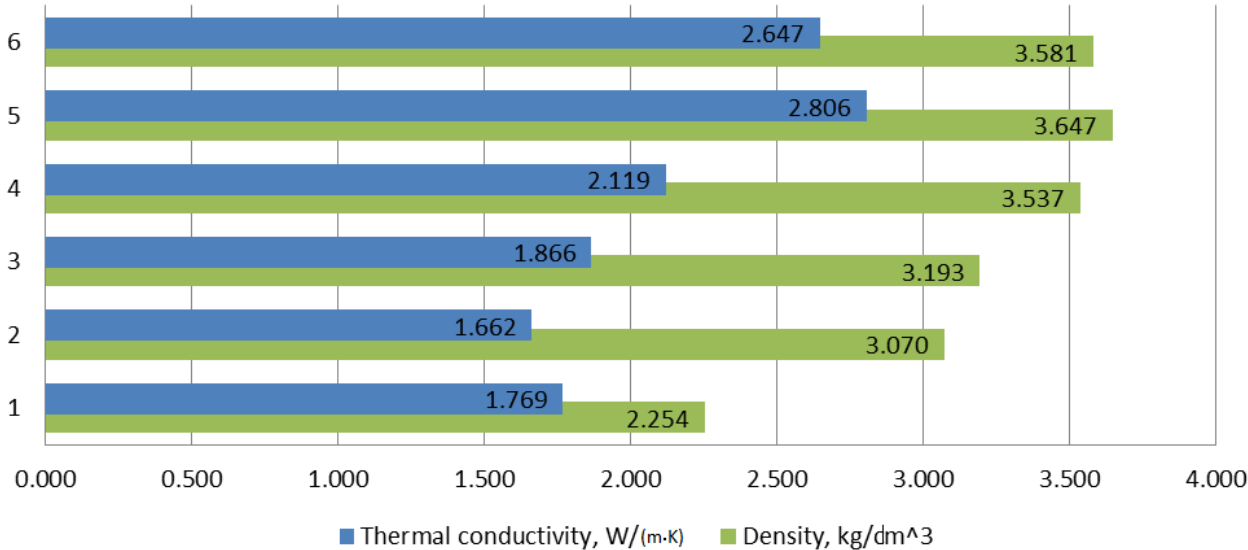


Figure 5.4: Concrete samples properties.

5.3. Static simulation of temperature distribution within the ice rink slab with different concrete samples.

The purpose of static simulation is to investigate the effect of increased thermal conductivity of concrete on temperature distribution in ice slab as well as the possible energy saving potential of improved concrete in ice slab construction.

The COMSOL Multiphysics simulation software has been chosen for simulation process as it provides a variety of modelling options and sufficient working environment.

The model design chosen for simulation presented on Figure 5.5. The model consists of tubes carrying the secondary refrigerant imbedded into the concrete slab covered with ice. The tubes are chosen to be 25x2.5 mm PEM tubes with the following thermodynamic properties: thermal conductivity $k=0.33$ W/(m·K); Density $\rho=940$ kg/m³ and specific heat $c_p=1.916$ kJ/kg.K (Bruce Bersted 2010) (Wikipedia 2010) and the ice is assumed to have the following characteristics: $k=2.25$ W/(m·K), $\rho=917.5$ kg/m³ and $c_p=2.027$ kJ/kgK (The Engineering Toolbox 2005). Additionally there is a 100 mm Rockwool thermal insulation at the bottom of the ice which maintains 5 °C at the ground surface thus preventing it from

freezing. The thermodynamic properties used in the simulation are: $k=0.037 \text{ W/mK}$, $\rho=80 \text{ kg/m}^3$, $c_p=0.4 \text{ kJ/kgK}$ (Paroc 2002). There are two layers of concrete within the slab.

Two cases are modelled: one represents the conventional case when the conventional concrete is used in both of the layers. Another one investigates the effect of more conductive concrete used for the upper concrete layer. The ice surface temperature is fixed to be $-3 \text{ }^\circ\text{C}$ and the temperature of the bottom layer of insulation is fixed to the value of $5 \text{ }^\circ\text{C}$ in both cases. The refrigeration load is fixed and assumed to be 100 W/m^2 .

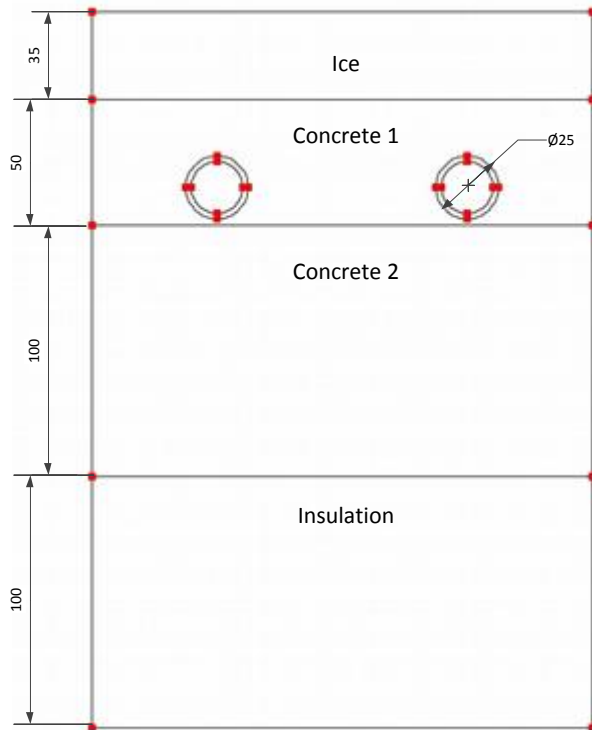


Figure 5.5: The simulation model design

For the first simulation concrete sample Con_02 has been chosen with the following thermodynamic properties: $k= 1.66 \text{ W/(m}\cdot\text{K)}$, $\rho= 3070 \text{ kg/m}^3$, $c_p=0.649 \text{ kJ/kg.K}$. The simulation was held in two stages.

During the first stage the temperature profile have been determined. According to the results a temperature of at least $-8.0 \text{ }^\circ\text{C}$ is required to keep the ice surface temperature at maximum -3°C during steady heat flux towards the ice surface (Figure 5.6).

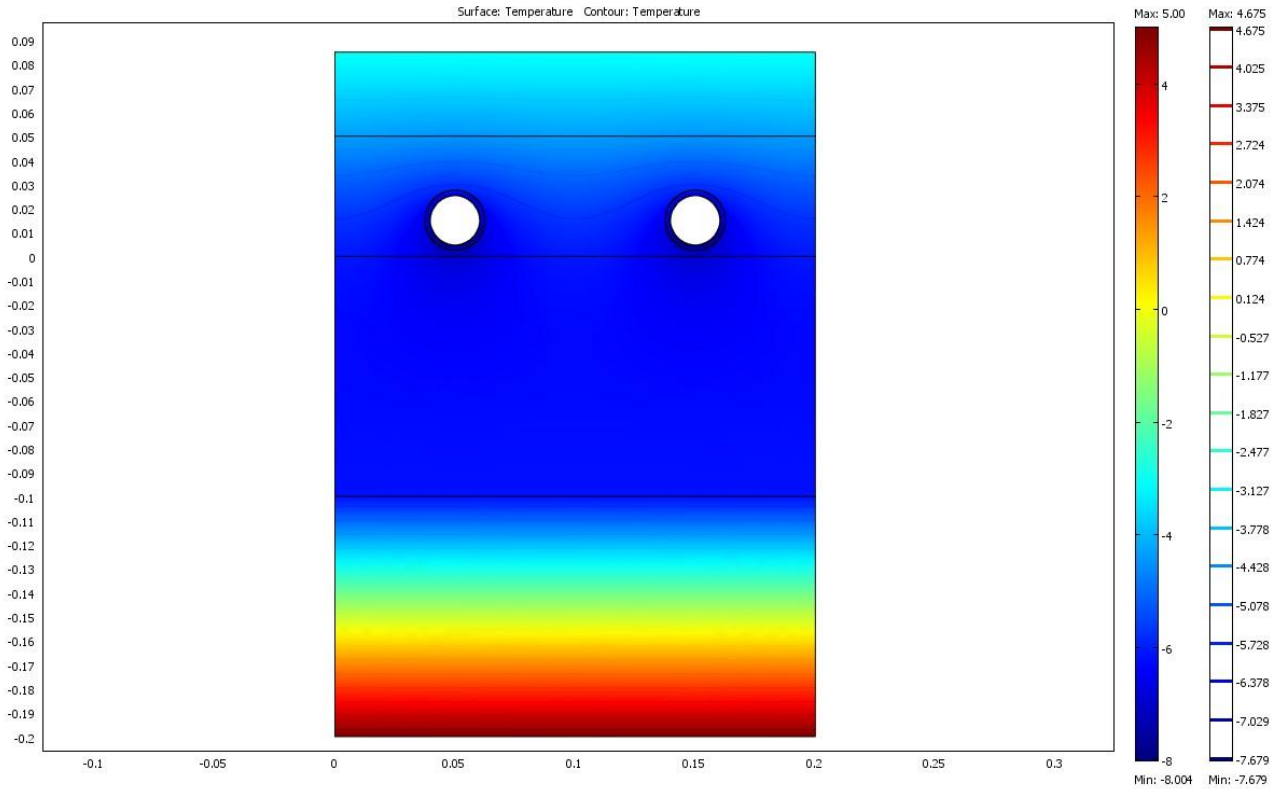


Figure 5.6: COMSOL model of ice slab: constant Ice temperature simulation

However, the results don't imply the limitation on the temperature distribution on the inner tube diameter. It is most probably to achieve the uniform temperature distribution on the inner tube surface due to turbulent secondary refrigerant flow inside the pipe. Thus, keeping the inner pipe's surface at constant temperature $-8.004\text{ }^{\circ}\text{C}$ we can more adequately simulate temperature distribution in the ice slab. The Figure 5.7 shows the temperature distribution in ice slab with heat flux applied to the ice surface and constant ground temperature. There are coloured isotherms and heat flux arrows for better process perception on the graph also.

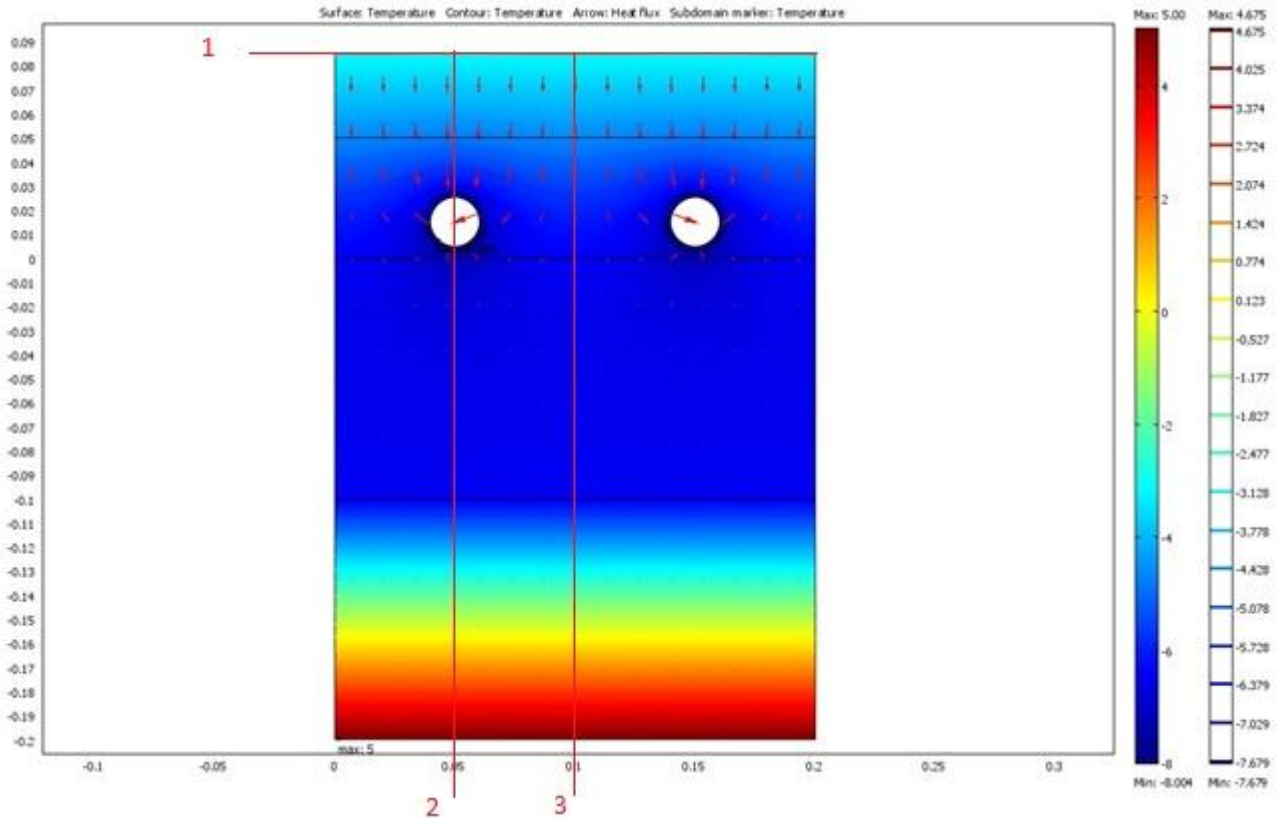


Figure 5.7: COMSOL model of ice slab: constant inner tube temperature simulation

Figure 5.8 represents the plot showing temperature distribution on the ice surface (line 1 on the Figure 5.7). The minimal ice temperature is right above the pipes' centres and maximum close to maximum allowable value of $-3\text{ }^{\circ}\text{C}$ achieved between the pipes. The difference between the maximum and minimum temperatures on the ice surface is approximately $0.04\text{ }^{\circ}\text{C}$ and thus negligible. Thus the chosen pipe pitch and ice slab design is sufficient for proper ice rink operation and creates ice of uniform temperature.

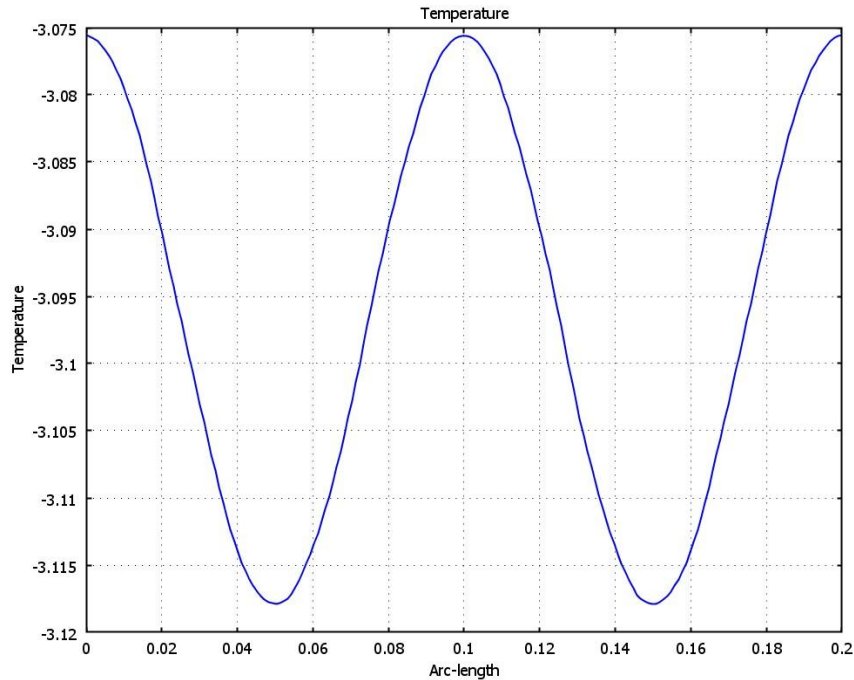
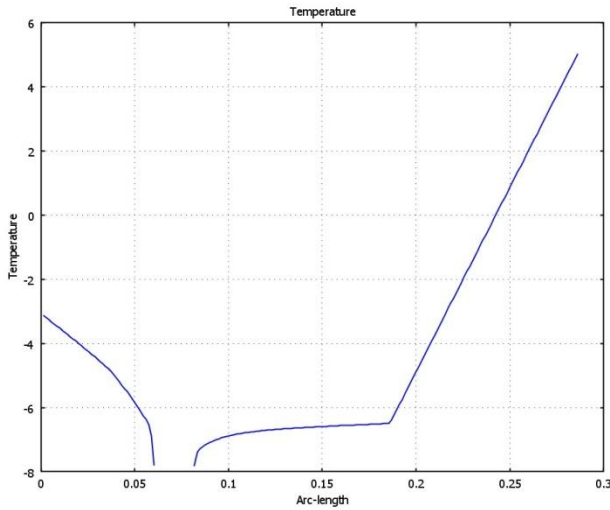


Figure 5.8: Horizontal cross section for temperature distribution at ice surface, line 1 in Figure 5.7

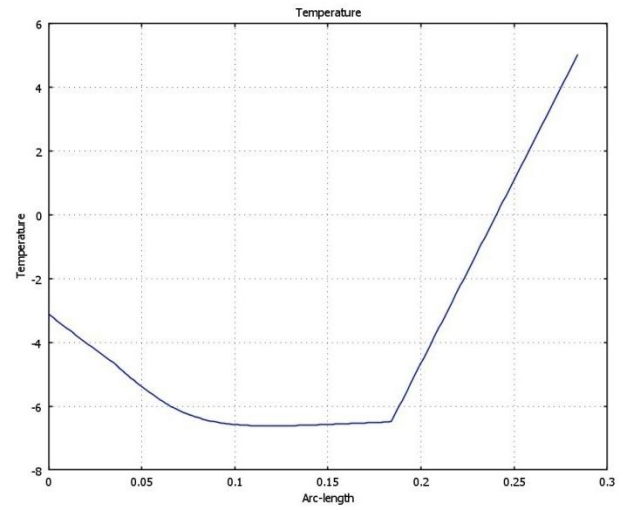
The vertical cross sections on Figure 5.9 (a and b) represent the temperature distribution through the slab. We can see from the plots that the temperature above the tube is parabolically decreasing from $-3\text{ }^{\circ}\text{C}$ at the surface to $-8.004\text{ }^{\circ}\text{C}$ at the inner tube surface. The temperature drop across the plastic tube is up to $1.3\text{ }^{\circ}\text{C}$ at the tube's part facing the heat flux. This drop is rather significant and due to the low thermal conductivity of tube's material. That is not the case when copper is used as material for tubes, where the temperature drop could be as low as $0.001\text{ }^{\circ}\text{C}$ (Shahzad 2006).

The 100mm thermal insulation significantly eliminates the heat gain from the ground, which is kept at the constant temperature $5\text{ }^{\circ}\text{C}$ to prevent freezing. Thus, the bottom concrete layer is in contact with the insulation surface at a temperature close to $-6.5\text{ }^{\circ}\text{C}$ and consequently the temperature slightly increases from $-7.35\text{ }^{\circ}\text{C}$ on the pipe's bottom surface.

The vertical cross section through the centre of the pipes' pitch (Figure 5.9,b) indicates the major temperature change in the area between the ice surface and the tubes level. The concrete temperature below the tubes level is almost constant.



a) Line 2



b) Line 3

Figure 5.9: Vertical cross section for temperature distribution in COMSOL model, lines 2 and 3 in Figure 5.7

In order to investigate the potential of concrete with high thermal conductivity, another simulation was made. The Concrete 1 layer properties were changed to those which correspond to Con_05 concrete sample: $k = 2.80 \text{ W}/(\text{m}\cdot\text{K})$, $\rho = 3637 \text{ kg}/\text{m}^3$, $c_p = 0.674 \text{ kJ}/\text{kg}\cdot\text{K}$. The simulation was done following the same methodology: during the first stage the maximum required temperature on the tube's inner surface was determined to be $-7.03 \text{ }^\circ\text{C}$; during the second stage the temperature distribution was obtained (Figure 5.10).

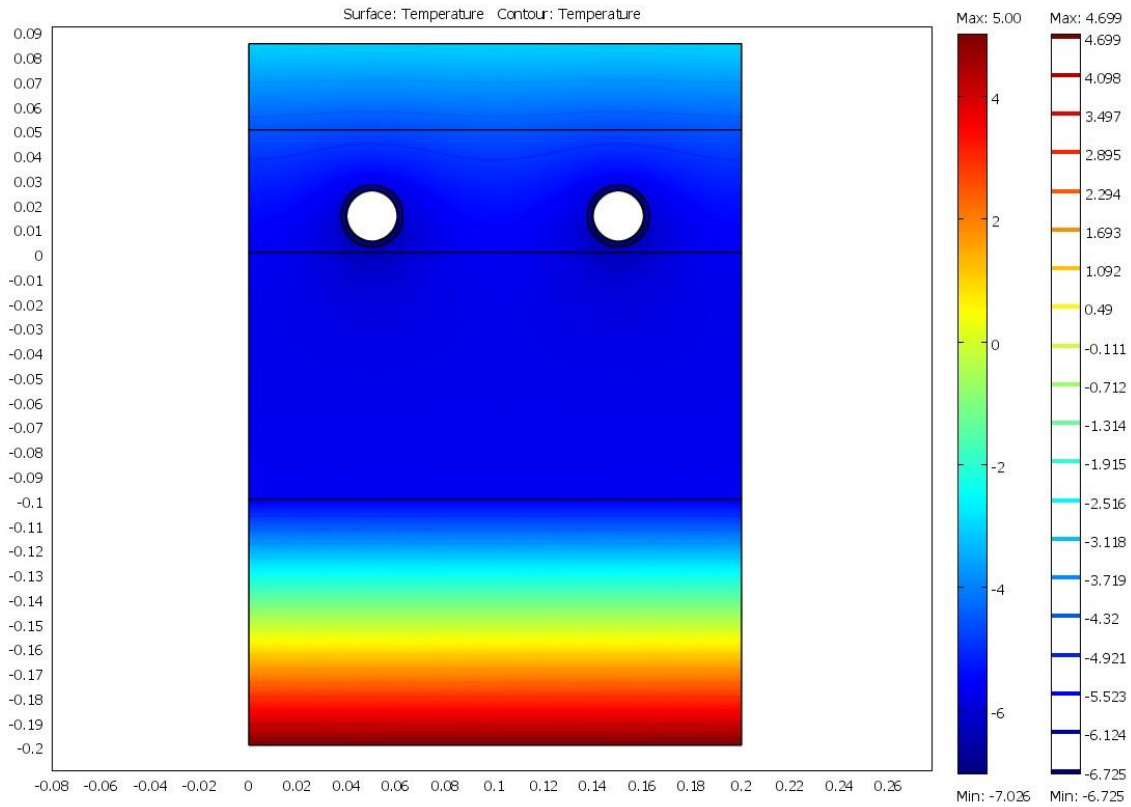


Figure 5.10: COMSOL model of the ice slab

It is important to notice, that the temperature distribution is more rapid if compared with the Model1 results. The improved thermodynamic properties of Concrete_1 layer and thus improved concrete slab allow using the secondary refrigerant at almost 1 °C higher temperature. The possible effect of this change will be further discussed later in this report.

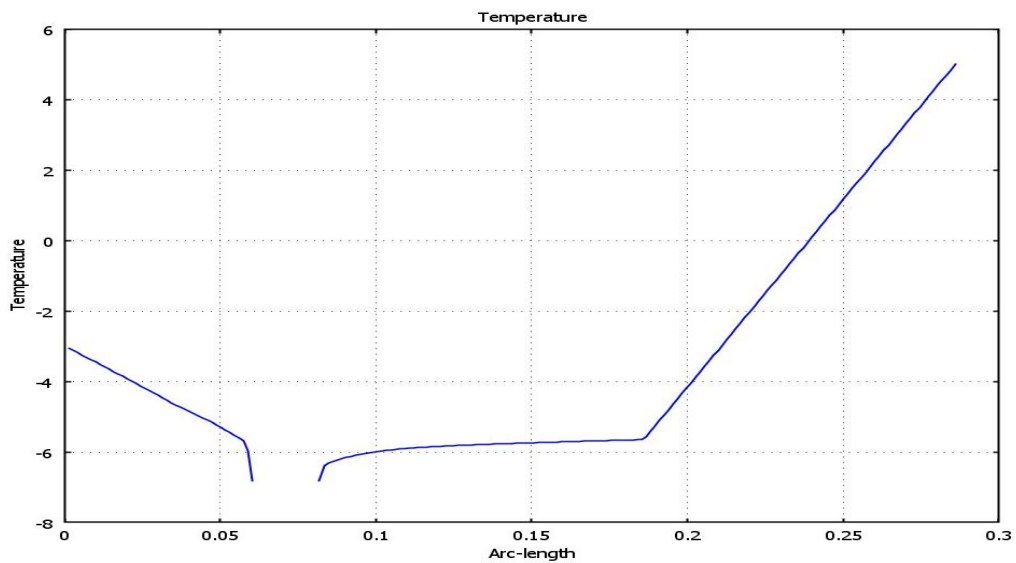


Figure 5.11: Vertical cross section for temperature distribution in COMSOL model

The simulation results indicate that the improved slab (with high conductivity concrete layer 1) lead to an increase of the secondary refrigerant temperature, required to maintain the desired ice slab properties. The temperature increased from -8.00, as for the Model1 case, till -7.03 for the Model2.

The possible economic benefit of such concrete slab design will come from the energy saved during ice rink operation. The above described solution is even more advisable, as available at almost no extra cost when designing and building new concrete slab.

5.4. Energy saving potential estimation

In order to roughly estimate the possible saving potential a number of assumptions have to be made. Considering the basic ice rink with ice surface area $A=1800 \text{ m}^2$ and assuming the normal heat flux of $q=100 \text{ W/m}^2$ we come to the conclusion that the secondary refrigerant should be able to transfer as much as $Q_{sr}=A*q=1800*100 \text{ W} = 180 \text{ kW}$ cooling capacity to absorb all the heat coming to the ice. This cooling power provided by the refrigeration unit evaporator through the heat exchanger and delivered by a number of pumps. Considering the total evaporator-to-cooling medium efficiency to be 95% we can conclude that the evaporator should be able to provide $180/0.95=189.47 \text{ kW}$ cooling power.

In order to estimate the COP_2 increase between Model1 and Model2 cycles, both models were simulated with the CoolPack software. Considering a one stage ammonia cycle, flooded evaporator with $x=0.8$ quality, fixed condenser temperature $T_1=35 \text{ }^\circ\text{C}$ one can observe the COP_2 3.1% increase (from $3.494@T_2=-8.004$ till $3.601@T_2=-7.026$) while varying evaporator temperature T_1 (see Figure 5.12). The analytical estimation of the COP_2 increase is presented in the Appendix F to this study and reveals similar result of 3.5% increase (the difference between the two approaches comes from a more rough estimation in analytical approach).

include the complex air movement, heat and mass transfer between the ice surface and the air, radiation exchanges and effect from water dispersion (Ahmed Daoud 2006).

There are a number of methods to predict heat flow in ice arena proposed by different authors.

There are two main operation conditions in ice rink operation: pre-cooling load and operating cooling load (Caliskana and Hepbaslib 2010). The response of the ice slab under normal operating load is studied in this report, thus the energy analysis during ice rink operation will be modelled.

We can calculate the operating cooling load (\dot{Q}_{cool}) as a sum of the loads due to convection (\dot{Q}_{cv}), radiation (\dot{Q}_r), heat transfer from the ground (\dot{Q}_{gr}) and load due to resurfacing of ice (\dot{Q}_{res}):

$$\dot{Q}_{cool} = \dot{Q}_{cv} + \dot{Q}_r + \dot{Q}_{gr} + \dot{Q}_{res} \quad (5.3)$$

The convective heat load, assuming there is no mass transfer from water vapour in the air to the ice, could be estimated by following relation:

$$\dot{Q}_{cv} = h(T_{air} - T_{ice})A_{rink} \quad (5.4)$$

where T_{air} is the air temperature ($^{\circ}\text{C}$), T_{ice} is the ice temperature ($^{\circ}\text{C}$), A_{rink} is the ice rink area (m^2) and h is the convective heat transfer coefficient ($\text{W}/\text{m}^2\text{C}$), which is dependent on air velocity v (m/s) over the ice surface:

$$h = 3.41 + 3.55 \cdot v \quad (5.5)$$

The radiant heat flow to the ice surface is a sum of radiant heat flow from the warm ceiling over the cold ice and radiant heat component of the lighting. The Stefan-Boltzman equation provides an estimation of infrared heat gain component from the ceiling and building structure:

$$\dot{q}_r = A_{ceiling} f_{ceiling,ice} \frac{\sigma(T_{ceiling}^4 - T_{ice}^4)}{1000} \quad (5.6)$$

where \dot{q}_r is the radiant heat load from ceiling (W), $A_{ceiling}$ is the ceiling area (m^2), σ is the Stefan-Boltzmann constant to be $(5.67)10^{-8} \text{ W}/\text{m}^2 \text{ K}^4$, $T_{ceiling}$ and T_{ice} are the ceiling/ice temperatures (K), and $f_{ceiling,ice}$ is the grey body configuration factor, which is obtained by:

$$f_{ceiling,ice} = \left[\frac{1}{\alpha_{ceiling,ice}} + \left(\frac{1}{\varepsilon_{ceiling,ice}} - 1 \right) + \frac{A_{ceiling}}{A_{ice}} \left(\frac{1}{\varepsilon_{ice}} - 1 \right) \right]^{-1} \quad (5.7)$$

In this equation $\epsilon_{\text{ceiling}}$ is the emissivity of ceiling, ϵ_{ice} is the emissivity of ice, A_{ceiling} and A_{ice} are ceiling/ice area (m^2), and $\alpha_{\text{ceiling,ice}}$ is the angle factor, ceiling to ice interface. The angle factor could be estimated by knowing the composition of the ceiling over the ice surface, however for the sake of this study it is assumed to be 0.65 (Caliskana and Hepbaslib 2010).

Another radiant heat source for the ice rink is lighting. It could be assumed that as much as 60% of the luminaries' power reaches the ice surface as a radiant heat:

$$\dot{Q}_{\text{light}} = 0.6\dot{Q}_{\text{lum}} \quad (5.8)$$

The equation above is, of course, a rough estimation. The actual radiant heat flux from the lighting is dependent on type of lighting, its applied style and configuration.

Additionally the heat gain from the ground could be considered. It could be calculated as:

$$\dot{Q}_{\text{gr}} = \frac{A_c k \Delta T}{1000} \quad (5.9)$$

where A_c is the concrete area (m^2), ΔT is the temperature difference between the ambient and ice temperatures, and k is the heat transfer coefficient ($\text{W}/\text{m}^2 \text{K}$).

These is one more major cooling load component to be considered in cooling load estimation – ice resurfacing cooling load \dot{Q}_f . During ice resurfacing procedure flood water volume V_f (m^3) of temperature T_f ($^{\circ}\text{C}$) is applied on the ice surface with temperature T_{ice} ($^{\circ}\text{C}$). By knowing the time, required for resurfacing, the respective cooling load could be estimated from the following equation:

$$\dot{Q}_{\text{res}} = \frac{1000 \cdot V_f [4.2(T_f - 0) + r + 2(0 - T_{\text{ice}})]}{t_f} \quad (5.10)$$

The described model is built under the number of assumptions which include: the heat gain from spectators and players is not considered; heat gain from the secondary refrigerant pump is neglected; heat flux over the ice surface assumed to be uniform; there is no heat transfer over the building envelope; vapour diffusion and condensation is neglected. Although the assumptions increase uncertainty in the modelling results, we can easily admit them for the sake of the modelling as the main trends in transient cooling load distribution are well modelled and thus will allow us to investigate the parameters under interest: influence of ice slab concrete layer on the ice slab response to the varying heat load.

The Contigahallen arena located in Norrtälje was chosen for the heat load distribution modelling over the time. The 24-hour operation schedule as for the May 18, 2010 was used to base the heat load profile on. Based on the existing data on lighting and resurfacing

period, weather profile, and using the above mentioned methodology, the following heat flux profile was estimated (see Appendix 2 for estimation procedure description):

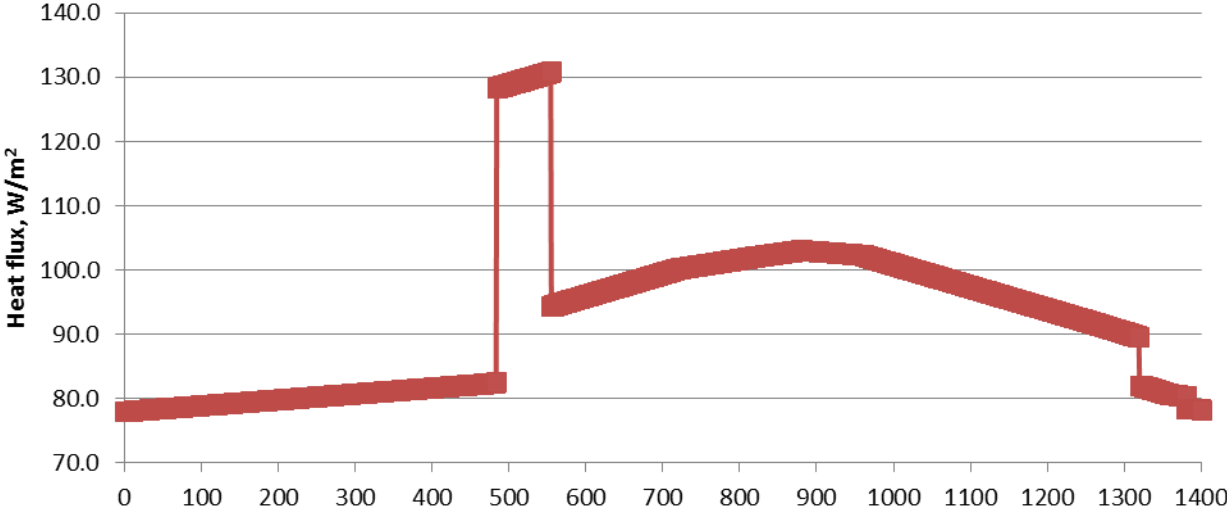


Figure 5.13: Predicted heat flux to the ice surface

On the figure above one can see the heat flux distribution over the ice surface, as predicted for a 24-hour operation period (May 18, 2010). The heat flux distribution is slightly increased till the time $t=1000$ min (approximately 5 p.m.) due to the heat gained from lighting and radiation from the ceiling (the ceiling temperature assumed to follow the ambient temperature, which is slightly increased from morning to the day). The significant heat flux increase within 490 and 550 minutes is due to the resurfacing procedure. The resurfacing time thus maintains the ice before the arena is open to the visitors.

Additionally, the cooling capacity maintained by the refrigeration equipment installed in the Contigahallen arena was logged with the 1 minute time step by the logger, as it is presented in the Figure 5.14: The ClimaCheck Performance Analyser product, which is complete product with hardware and software for troubleshooting and optimizing of refrigeration system, heat pumps and air conditioning, has been used for data logging

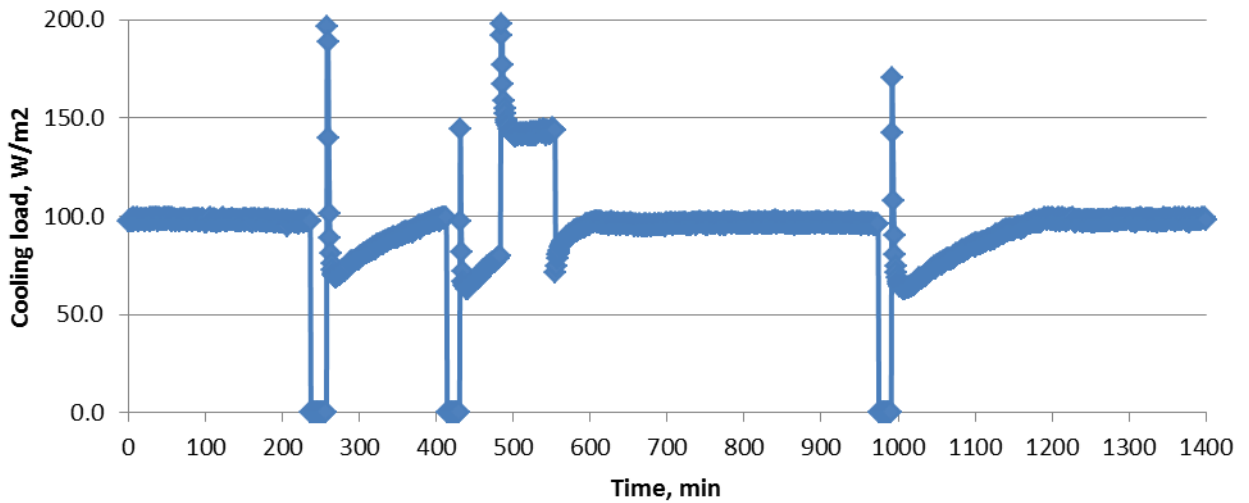


Figure 5.14: The measured cooling capacity maintained by refrigeration equipment. (1 day , 1400 min)

Figure 5.14 shows the variation of cooling load during a conventional weekday (May 18, 2010). The peak load located close to the 500 minute time point represents the resurfacing on the ice. There are some peaks that could be seen, which follows the cooling load decrease below the average value. Those peaks are always located after refrigeration machine stops and, thus, could be explained with the specifics of the machine operation: it starts at full load and then adjusts to the current operational conditions.

Figure 5.15 compares the measured data with the data predicted.

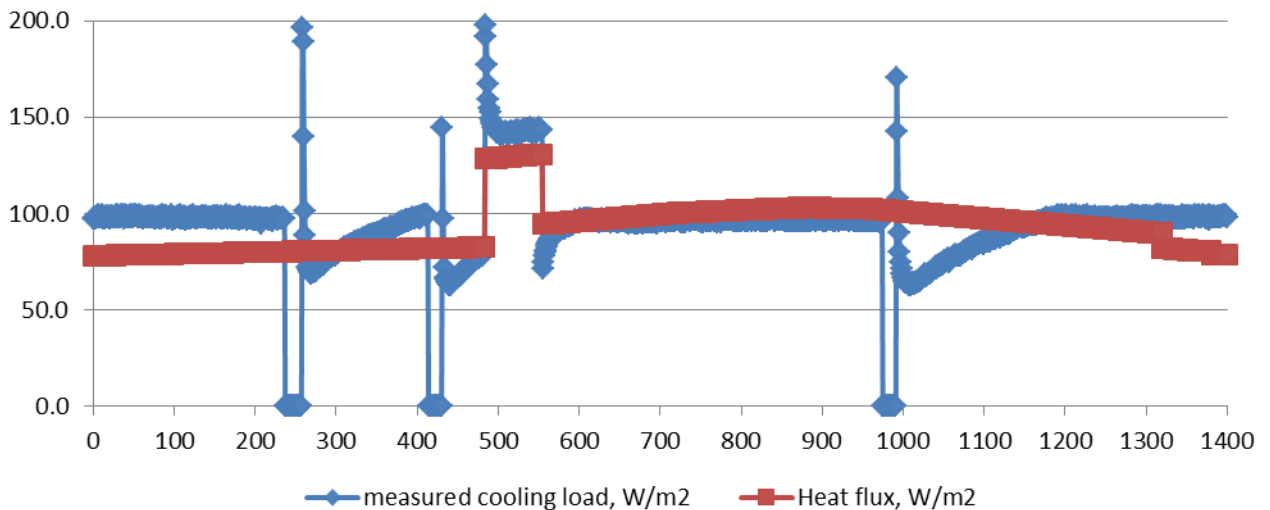


Figure 5.15: Predicted heat flux and respective measured cooling load

The cooling load does not perfectly match the predicted heat flux due to the specifics in the refrigeration system operation and due to the slow response of the ice slab to the changing conditions.

Although the 24-hour operation is not enough to validate the heat flux model, the result obtained is sufficient for the objective of the model. Therefore, the presented heat flux profile is used to simulate ice slab transient temperature response.

Model 1 and Model 2 will be used for the dynamic simulations to investigate which effect the thermal conductivity of the concrete could have on the system behaviour under varying conditions. The similar approach was used for the dynamic simulation as was successfully used to simulate the heat transfer under static conditions.

The aim of the dynamic simulation is to investigate what will be the response of the system at varying heat loads on the ice slab. The response could be indirectly estimated by modelling the required secondary refrigerant temperature.

The input of the predicted heat flux was made by creating the piecewise function cool(t) in COMSOL. The created function sufficiently well represents the heat flux distribution over the time ($R^2=0,92$).

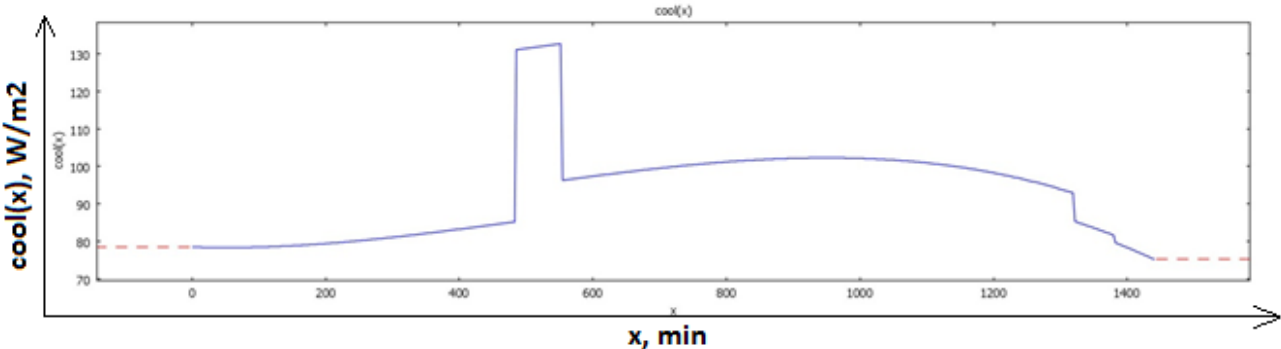


Figure 5.16: Function cool(t) plot, 24 hours operation period

On Figure 5.16 we can see the heat flux distribution over the time (minutes) as it is modelled in the COMSOL software.

Two transient simulations have been done. The first simulation starts at 12 pm at $-3\text{ }^{\circ}\text{C}$ as an initial temperature for all the ice rink floor layers. The ice rink responds to a certain applied heat flux and is then simulated over 5 days period with heat flux identical to indicated on Figure 5.16 every day.

The minimum required secondary refrigerant temperature over the 5 days period is indicated in Figure 5.17, where the bottom blue curve shows the simulation results for Model1 (ice rink with conventional concrete layers); upper curve – for Model2 (ice rink with high conductive upper concrete layer).

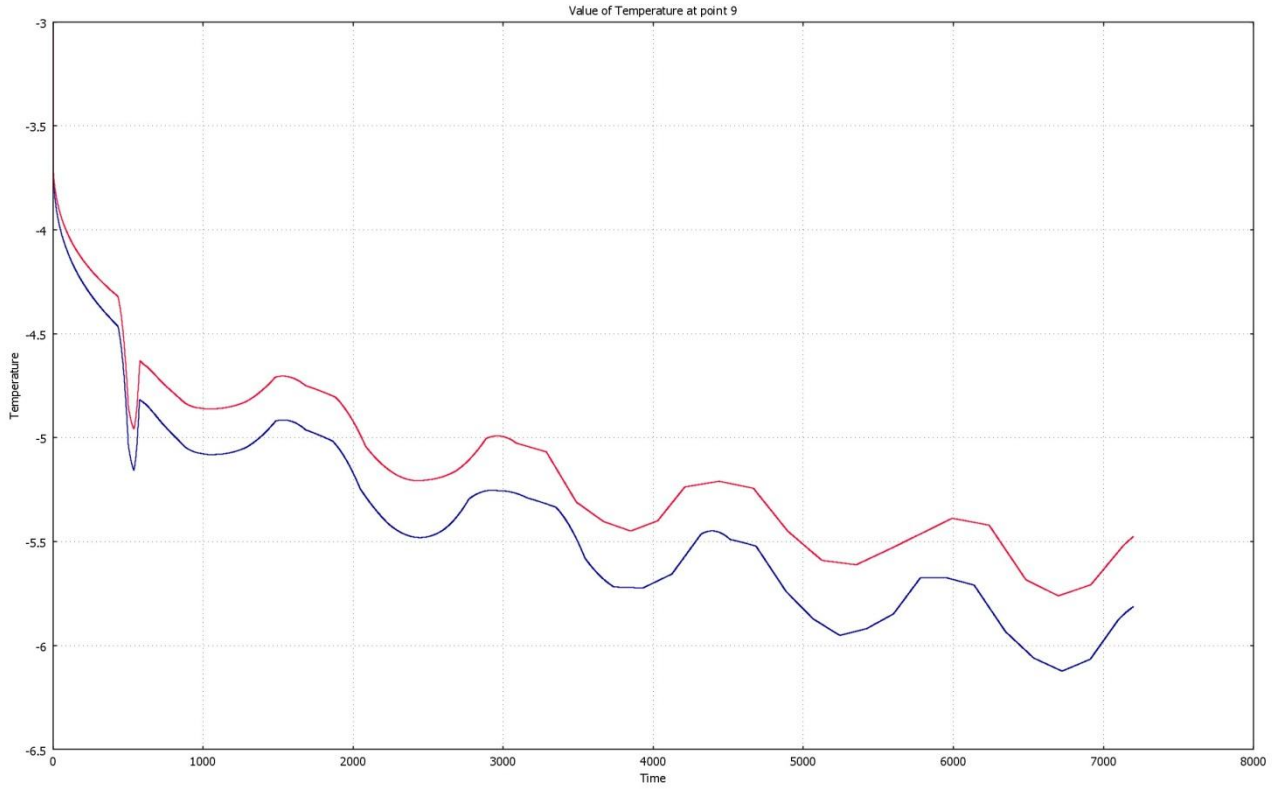


Figure 5.17: The required second refrigerant temperature distribution over the time, Model1 (conventional concrete, blue line) and Model2 (improved concrete, red line). Simulation 1: 5 days operation.

As one can notice from the plot above, stationary conditions are not reached after 5 days operation under new conditions. In order to detect the effect under steady state conditions another simulation has been made. The plot in Figure 5.18 represents the required second refrigerant temperature distribution over the 24 hours period, when steady state is reached in the ice rink floor.

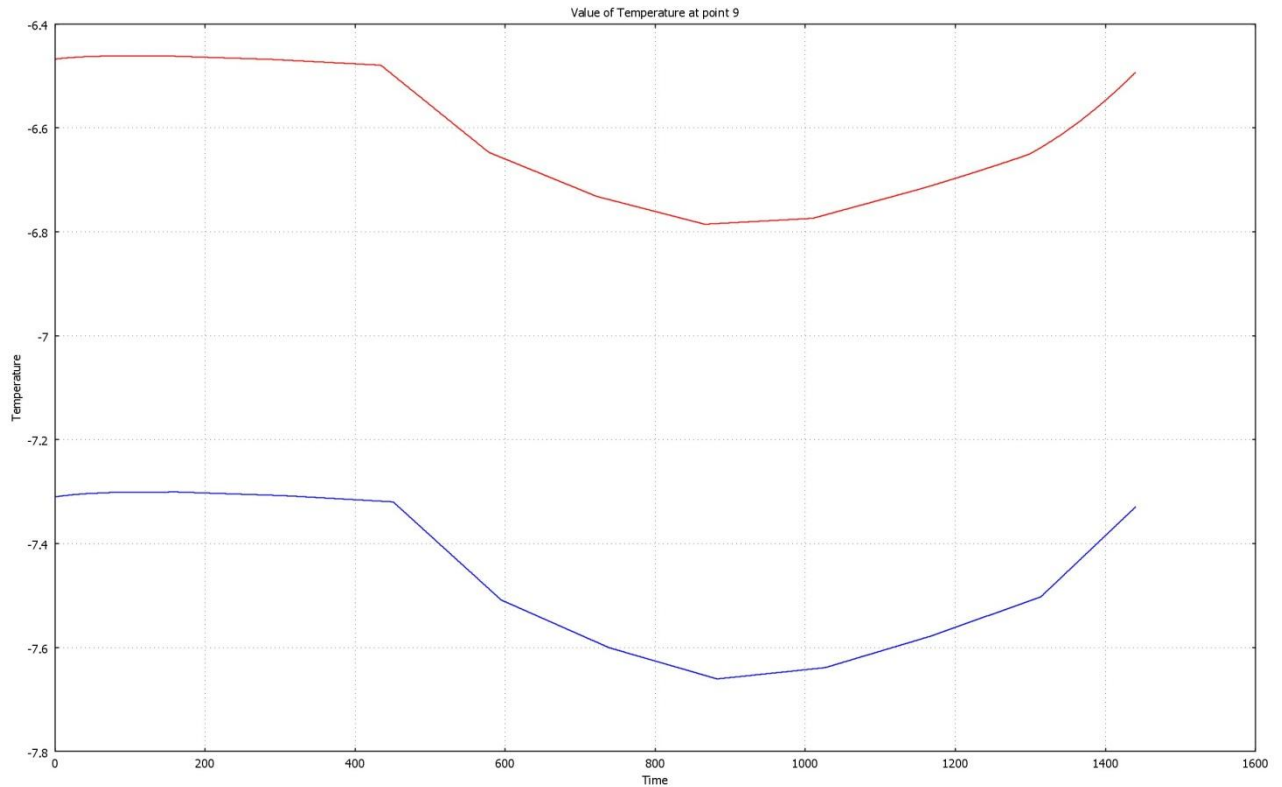


Figure 5.18: The required secondary refrigerant temperature distribution over time period, Simulation 2: 24 h operation, steady conditions.

5.6. Discussion

The results presented above reveal an obvious possibility to vary the thermodynamic behaviour of a concrete floor. A high thermal conductivity value has been achieved by using different components for concrete production. The concrete sample with $k=2.80 \text{ W}/(\text{m}\cdot\text{K})$ thermal conductivity value has been used for the simulations, which is slightly bigger than maximum value noted in different literature sources. Thus, it seems to be possible also to minimise thermal conductivity of concrete down to $k = 0.65 \text{ W}/(\text{m}\cdot\text{K})$. However, no concrete samples have been produced with such conductivity value as it is beyond of the scope of the current project.

Two static models has been simulated and studied in the current study. The Model1 is used as a reference model to investigate the temperature distribution in a conventional ice rink floor where it is entirely made of conventional concrete with thermal conductivity $k=1.662 \text{ W}/(\text{m}\cdot\text{K})$. The Model1 results have been further compared with the Model2 results, where Model2 stands for the model, which has upper concrete layer with thermal conductivity value increased to $k=2.80 \text{ W}/(\text{m}\cdot\text{K})$. The simulation reveals, that using the thermodynamically improved concrete, it is possible to achieve a 1 degree increase in brine temperature ,which results in a 3.5% refrigeration system COP_2 increase.

Even though obtained COP_2 increase is relatively small, it is worth to notice that concrete floor improvement is a one-time investment and, if applied during ice rink construction process, could be considered to be no-cost energy saving improvement.

The author expects additional effect of bottom concrete layer thermal conductivity decrease could have on total thermodynamic performance of the ice rink floor. Although this effect is not evaluated in the current study, it should be further studied in the future.

The dynamic simulation was based on a heat flux prediction model, created based on heat loads, affecting the ice surface, and tested over the real measurement data from Contigahallen arena located in Norrtälje. The comparison indicated sufficient prediction accuracy of the model and thus was used for dynamic simulation of the concrete floor response to varying heat flux.

Two different approaches have been used in the dynamic modelling: one evaluates the ice floor response to varying heat flux, starting from specific initial temperature; another indicates the response rate, when operating at steady conditions. Both approaches reveals, that modified ice rink floor (Model2) require smaller temperature different between the ice surface and the secondary refrigerant, and provides faster response to a varying heat flux applied to the ice surface. Consequently, ice rink floor design with high thermal conductivity upper concrete layer provides better control over the ice temperature, can respond to a heat flux change more rapidly. This will result in a reduced ice rink operational cost and a better ice temperature control.

6. Conclusion

The technology and energy inventory data of more than hundred different ice rinks has been combined and generalised into a computer database, which can provide the user with versatile data access and analysis methods.

The inventory data analysis indicates that the average Swedish ice rink energy consumption is 1,137,496 kWh/year; almost 1/3 of all inventoried ice rinks are operated above average energy consumption. A significant number of ice rinks are not operated efficiently: pump capacity control is missing in majority of ice rinks; water conductivity is high; inefficient metal halogen lighting is still used in 20% of arenas in the study. Moreover, the building envelope of some arenas has appeared to have leakages, which significantly increases refrigeration load and results in a higher electricity bill.

The analytical inventory data analysis was supported by statistical multi factor linear regression analysis. The analysis resulted in an empiric relation between total energy consumption and it affecting factors. The analysis show season lengths, activity length, water quality, ice rink hall temperature, total compressors rated power and secondary refrigerant pump capacity regulation as the factors which affect total energy consumption mostly.

Water treatment and its effect on ice quality have been studied as one of deep studies. Two water samples – a reference water as a first water sample and the reference water treated by a Reallce vortex generator, as the second one – have been studied by different methods in order to evaluate the influence of a vortex generator water treatment on the ice quality. No significant influence has been detected.

The effect on improved thermodynamic properties of concrete has been studied. The results show a possibility to vary the thermodynamic properties of concrete. The concrete sample with a thermal conductivity value of $k=2.80 \text{ W}/(\text{m}\cdot\text{K})$ can be used in ice rink floor design in order to increase its thermodynamic performance. A 3.5% COP_2 increase is proven to be possible to achieve.

The static simulations results have been complemented with a dynamic simulation. The cooling load prediction model has been developed and compared to the real measurements from ice rink in central Sweden. Dynamic simulation indicated that improved ice rink design with upper concrete layer made from high thermally conductive concrete lead to better control over the ice surface temperature, faster response to varying heat flux change and lower ice rink operational cost.

7 Suggestion for further work

The author emphasise that some of the studies, described in the report, require additional work. Thus, the Stoppsladd study results could be fulfilled with even more inventory data from other Swedish ice rinks in order to create more detailed statistical data with even larger analysis potential. The study could be also complemented with more detailed analysis of each separate refrigeration system part influence on total system's performance and respective energy saving potential. Additional effort should be made in order to increase quality of the obtained results: in a number of cases the information obtained from the questionably was either not complete or doubtful.

Some of the water/ice quality measurements have appeared uncertain enough: their uncertainty could be further minimised by utilising more certain measurement methods and increase the number of measurements values.

The concrete floor thermodynamic response static simulation could be repeated having different initial conditions, improved lower concrete layer properties, different secondary refrigerant tubes location. The dynamic simulation is worth to be repeated under different time periods, heat flux distribution and different concrete thermodynamic properties.

The analysis of energy efficiency for arenas should consider the building as a whole with all its mechanical systems and architectural systems. A refrigeration load to the ice rink coexists along with other needs for heating. Taking this into consideration it is vital to utilise heat, rejected from refrigeration system in specially designed heat recovery process, thus making refrigeration system to act as a heat pump to supplement the heating requirements. For many arenas, proper heat recovery could lead to a 50% annual energy savings.

References

- Ahmed Daoud, Nicolas Galaris. *Calculation of the Thermal Loads of an Ice Rink using a Zonal Model and Building Energy Simulation Software*. Vol. 112, in *ASHRAE Transactions*, by Refrigerating and Air-Conditioning Engineers American Society of Heating. 2006.
- AK-konsult Indoor Air AB. "Isolerförmåga relaterat till vatteninnehåll." Spånga, 2009.
- ASHRAE. *Refrigeration handbook. Chapter 35: Ice rinks*. ASHRAE, 2002.
- Bitaraf H., Ehsan. "Measurement Report for TPS 2500 thermal conductivity." Department of Energy Technology, The Royal Institute of Technology, Stockholm, 2010.
- Blades, Russel W. "Modernizing and retrofitting ice skating rinks." *ASHRAE Journal*, April 1992.
- Brendan Lenko, P.E. "Ice Rink Energy Conservation." 8 2001.
- Bruce Bersted, Steven A. Cohen. "Polyolefin resins." <http://www.accessscience.com>. AccessScience@McGraw-Hill. 2010.
<http://www.accessscience.com.focus.lib.kth.se/content.aspx?searchStr=polyethylene&id=535900#535900s001> (accessed May 25, 2010).
- Caliskana, Hakan, and Arif Hepbaslib. "Energy and exergy analyses of ice rink buildings at varying reference temperatures." *Energy and Buildings*, 2010.
- CETC. "The energy management manual for arena and rink operators." *Heat recovery and financial assistance*. Canada: Canadian Energy Technology Center, 2005.
- Conde, M. M., C. Vega, and A. Patrykiejew. "The thickness of a liquid layer on the free surface of ice as obtained from computer simulation." *The journal of chemical physics*, no. 129 (July 2008).
- Conservation, Ice Rink Energy. n.d.
- Energimyndigheten. *Energianvändning idrottsanläggningar*. . Förbättrad statistik för lokaler, STIL2, Eskilstuna: Statens energimyndighet, 2009.
- Eric Granryd, Ingvar Ekroth, Per Lundqvist, Björn Palm. *Refrigerating engineering*. Stockholm: Royal Institut of Technology, KTH, 2005.
- Fagerhult. *Mats Wernberg presentation, Arenadagarna*. Stockholm, 2009.
- Fukusako, Schoichiro, and Masahiko Yamada. "Recent advances in research on water-freezing and ice-melting problems." *Experimental Thermal and Fluid Science* (Elsevier Science Publishing Co., Inc.,) 6 (1993): 90-105.
- Funktion. "Prima is för halva kostnaden i Umeå Arena." *Funktion: Sporthallarnas dolda kapital*, Juni 2009: 5-7.
- Holman, J.P. *Experimental methods for engineers*. NewYork: McGraw-Hill series in mechanical engineering, 2001.

- IIHF. "IIHF Arena Manual: Technical guidelines of an ice rink (Chapter 3)." *International Ice Hockey Federation*. 2010. <http://www.iihf.com/iihf-home/sport/arena-manual.html> (accessed September 03, 2010).
- Inadaa, Takaaki, Tomohiko Hatakeyama, and Fumio Takemura. "Gas-storage ice grown from water containing microbubbles." *International journal of refrigeration*, no. 32 (2009): 462-471.
- Jörgen Rogstam, Samer Sawalha, Per-Olof Nilsson. *Ice Rink Refrigeration System with CO2 as Secondary Fluid*. Katrineholm, August 2005.
- Khan, M. I. "Factors affecting the thermal properties of concrete and applicability of its prediction models." *Building and Environment* 37, no. 6 (June 2002): 607-614.
- Kook-Han Kim, Sang-Eun Jeon, Jin-Keun Kim and Sungchul Yang. "An experimental study on thermal conductivity of concrete." *Cement and Concrete Research* 33, no. 3 (March 2003): 363-371.
- Laurier Nichols, P.E.. "Improving efficiency in ice hockey arenas." *ASHRAE Journal* (American Society of Heating, Refrigerating and Air-Conditioning Engineers, Inc.), June 2009: 18.
- Li, Yimin, and Gabor A. Somorjai. "Surface Premelting of Ice." *The journal of physical chemistry* (American Chemical Society), June 2007.
- Månberg, Jakob. *Energianvändning i Sveriges ishallar*. Stockholm: Institutionen för Energiteknik, Kungliga Tekniska Högskolan (KTH), 2010.
- Manitoba Hydro. *Energy Efficiency Guide for Ice Arenas and Curling Rinks*. Winnipeg, 1991.
- Natural Resources Canada. *Technical fact sheets on the impacts of new energy efficiency technologies and measures in Ice rinks*. Varennes (Quebec): CANMET Energy Technology Centre - Varennes, 2003.
- Ontario Recreation Facilities Association Inc. *Hockey and Curling Ice on the Same Sheet*. Ontario, 2007.
- Paroc. *Byggboken: produktinformation*. August 2002.
- RealICE. *Ice quality*. 2010. http://www.realice.se/eng_kvalite.php (accessed May 16, 2010).
- . "Products." *RealICE*. 2010. water molecules are more structured (accessed May 17, 2010).
- . *Reduced limescale*. 2010. http://www.realice.se/eng_frysprov.php (accessed May 16, 2010).
- "Realice System - Improved Ice Quality." *Watreco AB*. 2010. http://www.watreco.com/eng_produkter_is.php (accessed May 17, 2010).
- Rogstam, J. *En teknik-och energiinventering av svenska isarenor*. Sveriges Energi- & Kylcentrum. Katrineholm, 17 March 2010.
- Rogstam, Jörgen. *Energihandledning ishallar. En guide till effektivare energianvändning i svenska ishallar*. Sveriges Energi & Kylcentrum. Katrineholm, 06 May 2010.

- Rogstam, Jörgen. *Energy usage statistics and saving potential in ice rinks*. Katrineholm: Sveriges Energi och Kylcentrum, 2009.
- Rosenberg, Robert. "Why is ice slippery?" *Physics Today* (American institute of physics), December 2005.
- Royal institute of technology. "Measurement results for two water samples by Höppler viscometer." Department of energy technology, Royal institute of technology, Stockholm, 2010, 8.
- SEDAC. *Energy Smart Tips for Ice Arenas*. Champaign, IL, November 2010.
- Shahzad, Kruham. *An Ice Rink Refrigeration System based on CO₂ as Secondary Fluid in Copper Tubes*. Stockholm: Royal Institut of Technology, 2006.
- Sutherland, Art. "Energy efficiency in the ice rink." *The Air Conditioning, Heating & Refrigeration News*. 03 August 2000. <http://goo.gl/H4tGo> (accessed Nov 2010).
- Svenska Ishockeyförbundet. *Bygga Ishall, en faktabok för byggnation av ishallar*. 2009.
- . *Om Svenska Ishockeyförbundet*. 18 May 2009. <http://www.swehockey.se/Om-forbundet/Historikstatistik/> (accessed May 12, 2010).
- The engineering toolbox. *Air solubility in water*. n.d. http://www.engineeringtoolbox.com/air-solubility-water-d_639.html (accessed May 14, 2010).
- The Engineering Toolbox. "Ice - Thermal Properties." 2005. http://www.engineeringtoolbox.com/ice-thermal-properties-d_576.html (accessed May 25, 2010).
- Thorne, D. Campbell-Allen and C.P. "The thermal conductivity of concrete." *Magazine of Concrete Research*, 1963: 39-48.
- Watreco. "Downloads." *RealICE*. 2010. http://www.realice.se/eng_vortex_down.php (accessed May 17, 2010).
- Whitman, Bill, John Tomczyk, Bill Johnson, and Eugene Silberstein. *Refrigeration and Air Conditioning Technology*. Cengage Learning, 2008.
- Wikipedia. *Degasification*. 2010. <http://en.wikipedia.org/wiki/Degasification> (accessed May 16, 2010).
- . "Medium density polyethylene." *Wikipedia, the free encyclopedia*. 18 May 2010. http://en.wikipedia.org/wiki/Medium_density_polyethylene (accessed May 25, 2010).
- . "Student's t-distribution." *Wikipedia, the free encyclopedia*. 03 September 2010. http://en.wikipedia.org/wiki/Student's_t-distribution (accessed September 5, 2010).

Appendix A: Water electrical conductivity test

Purpose:

to determine electrical conductivity values for two water samples

Method:

The measurements done with the specific equipment; two consequent measurements for each water sample are done to increase the precision of the measurement result

Basic Principle:

When an electrical potential difference is placed across a conductor, its movable charges flow, giving rise to an electric current. The conductivity σ is defined as the ratio of the current density J to the electric field strength E : $J = \sigma E$

Measuring equipment:

HANNA HI 98311 Waterproof EC/TDS/Temperature Tester with automatic thermal compensation. The tester has the following specifications for electrical conductivity measurement:

Range	EC	0 to 3999 $\mu\text{S}/\text{cm}$
Resolution	EC	1 $\mu\text{S}/\text{cm}$
Accuracy	EC	$\pm 2\%$
Calibration		automatic, 1 point
Environment		0 to 50°C (32 to 122°F); RH max 100%

Experimental procedure:

1. two water samples prepared and placed under the identical conditions;
2. the probe submerged in the liquid to be tested;
3. the measurements taken when the stability symbol disappeared (see Figure below).



Figure A.1: Water electrical conductivity measurement

Measurements:

Table A.1: Electrical conductivity measurement results

Measurement, #	Reference water, $\mu\text{S}/\text{sm}$	Realce water, $\mu\text{S}/\text{sm}$
1	242	237
2	243	242
Sample mean	242,5	239,5

Uncertainty analysis:

Reference water

Type A uncertainty (standard deviation of the mean):

$$s_{\sigma} = \left(\frac{1}{n(n-1)} \sum_{k=1}^n (x_{i,k} - \bar{x}_i)^2 \right)^{1/2} = 0.18 \mu\text{S}/\text{sm} \quad (\text{A.1})$$

Type B uncertainty:

$$w_{\sigma} = 2\% = 0.02 * 242.5 = 4.85 \mu\text{S}/\text{sm} \quad (\text{A.2})$$

Total uncertainty of the measurement:

$$u_{\sigma} = \sqrt{w_{\sigma}^2 + s_{\sigma}^2} = \sqrt{0.18^2 + 4.85^2} = 4.85 \mu\text{S}/\text{sm} \quad (\text{A.3})$$

Realce water

Type A:

$$s_{\sigma} = \left(\frac{1}{n(n-1)} \sum_{k=1}^n (x_{i,k} - \bar{x}_i)^2 \right)^{1/2} = 4.42 \mu\text{S}/\text{sm}$$

Type B uncertainty:

$$w_{\sigma} = 2\% = 0.02 * 239.5 = 4.79 \mu\text{S}/\text{sm}$$

Total uncertainty of the measurement:

$$u_{\sigma} = \sqrt{w_{\sigma}^2 + s_{\sigma}^2} = \sqrt{4.42^2 + 4.79^2} = 6.52 \mu\text{S}/\text{sm}$$

Electrical conductivity measurement results:

Reference water $\sigma(\text{ref})=242.5\pm 4.85 \mu\text{S}/\text{sm}$

Realice water $\sigma(\text{Ri})=239.5\pm 6.52 \mu\text{S}/\text{sm}$

Appendix B: pH level test

Purpose:

to determine pH level of two water samples

Method:

The measurements done with the specific equipment; the samples are measured under constant ambient conditions to eliminate any possible influence from the environment

Measuring equipment:

HANNA HI 98311 Waterproof EC/TDS/Temperature Tester with automatic thermal compensation. The tester has the following specifications for electrical conductivity measurement:

Range	pH	-2.0 to 16.0 pH
Resolution	pH	0.1 pH
Accuracy	pH	±0.1 pH
pH Calibration		automatic, at 1 or 2 points with 2 sets of memorized buffers (pH 4.01 / 7.01 / 10.01 or pH 4.01 / 6.86 / 9.18)
Temp. Compensation		Automatic

Experimental procedure:

1. submerge the electrode in the solution to be tested while stirring it gently.
2. take the measurements when the stability symbol on the top left of the LCD disappears.
3. read the automatically compensated for temperature pH value (see Figure below).



Figure B.1: Water pH measurement

Measurements:

Table B.1: pH measurement results

Measurement, #	Reference water, pH	Reallce water, pH
1	8.1	8.1

Uncertainty analysis:

Reference water, Reallce water

Type A uncertainty (standard deviation of the mean): No

Type B uncertainty: $w_{pH} = 0.1pH$

Total uncertainty of the measurement: $u_{pH} = 0.1 pH$

pH measurement results:

Reference water $pH_{(ref)}=8.1\pm 0.1 pH$

Reallce water $pH_{(Ri)}= 8.1\pm 0.1 pH$

Appendix C: Water freeze rate test

Purpose:

to determine the water samples' freeze rate

Method:

Two water samples of identical volume applied on pre-frozen concrete slab. The freezing time measured with stopwatch.

Measuring equipment:

Conventional digital stopwatch used. The time watch has the following specifications for time measurement:

Range	0 to 60 min
Resolution	1 s
Accuracy	± 0.5 s

Experimental procedure:

1. Freeze the concrete slab before the experiment start;
2. Apply evenly 5 ml of first water sample, note the time;
3. Apply evenly 5 ml of second water sample, note the time;
4. Observe visually the freezing process;
5. Note the freezing end time for both water samples;
6. Repeat the procedure for different slab surfaces.

Test 1 measurement:



Figure C.1: Water freeze rate test 1

Table C.1: Water freeze rate test results

Time, s	Observation
0	Realice water sample applied on the surface
25	Reference water sample applied on the surface
460	Realice water get frozen
505	Reference water get frozen

Uncertainty analysis:

Reference water, Realice water

Type A uncertainty (standard deviation of the mean): No

Type B uncertainty: $w_t = w_{t1} + w_{t2} = 2 * (\pm 0.5 s) = \pm 1 s$

Total uncertainty of the measurement: $u_t = \pm 1 s$

Freeze rate test 1 measurement results:

Reference water $t_{(ref)} = 480 \pm 1 s$

Realice water $t_{(Ri)} = 460 \pm 1s$

Test 2 measurements:



Figure C.2: Water freeze rate test 2

Table C.1: Water freeze rate test results

Sample	Type	Time (start), s	Time (end), s	Time (total), s	Mean, s
Unpainted					
1	RI	374	914	540	
2	RI	279	704	425	482.5
3	RF	344	944	600	
4	RF	339	704	365	482.5
Painted					
1	RI	164	434	270	
2	RI	0	644	644	457
3	RF	104	644	540	
4	RF	44	434	390	465

Uncertainty analysis:

Reference water, RealIce water

Type A uncertainty (standard deviation of the mean): the measurements are rather uncertain due to a significant deviation of measured values from their mean values.

Type B uncertainty: $w_t = w_{t1} + w_{t2} = 2 * (\pm 0.5 \text{ s}) = \pm 1 \text{ s}$

Freeze rate test 2 measurement results:

See Table C.1. for the results.

Appendix D: Ice visibility test

Purpose:

to determine the influence of vortex-treatment and conventional deaeration methods on the ice visibility

Method:

The water sample is subdivided in a number of smaller samples. Different treatment methods are applied to different samples in order to influence the water quality in the sample. All the samples are visually examined after they got completely frozen.

Measuring equipment:

No specific equipment was used for the visibility level determination. The visibility estimated with naked eye.

Experimental procedure:

1. Prepare three water samples: first sample – reference water without treatment; second sample – vortex-treated reference water; third sample – reference water pre-deaerated by bringing to the boiling point;
2. Freeze three samples under uniform cooling condition;
3. Evaluate ice samples visibility.

Measurement results:

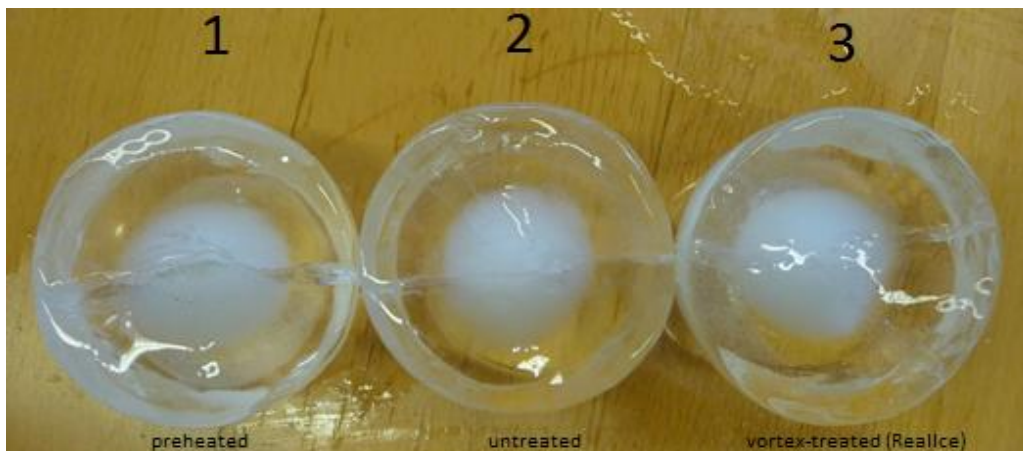


Figure D.1: ice visibility test 1 (1 – preheated to boiling temp; 2 – reference untreated sample; 3 – RealIce vortex-treated water)

Results:

No visible difference observed

Appendix E: Viscosity test (measurement report summary)

Measurement Results for two water samples by Höppler viscometer

Doc. No: 2010-06-16-001



Department of Energy
Technology

1. Purpose

Measurement of viscosity in two different water samples.

2. Scope

The falling-ball viscometer enables the precise measurement of the dynamic viscosity of clear liquids or gases.

Different test balls will be used for samples of low viscosity in the chemical industry, pharmaceutical industry, food industry or crude oil industry

3. Principle

The sliding and rolling movement of ball in studied liquid are determined a time through a cylindrical tube .The viscosity of the sample liquid is related to the time takes the ball pass a distance between upper and lower lines. Turning the measurement tube results in returning of ball and it is possible to re-measure the time in previous distance. The result is dynamic viscosity with the standard dimension (mPa.s).

3.1. Basic principle

Viscosity of liquids changes the velocity of ball which is falling through the liquid in the tube. When the ball moves through the liquid, it is affected by the gravity, buoyancy and frictional forces: Gravity as downward force, buoyancy and friction as the upward forces.

$$W=mg=V\rho_s g=4/3\pi r^3\rho_s g \quad (1)$$

ρ_s :density of ball

g :gravitational acceleration

V : volume of ball

r :radius of ball.

Buoyant force, F_1 , acts upward and it is weight of liquid which is displaced by the ball.

$$F_1=V\rho_L g=4/3\pi r^3\rho_L g \quad (2)$$

ρ_L =density of liquid

Liquid which has a dynamic viscosity produces a resistance against the ball movement. This frictional force is derived from the Stokes's law:

$$F_2=6\pi\eta r u \quad (3)$$

u:velocity of the ball

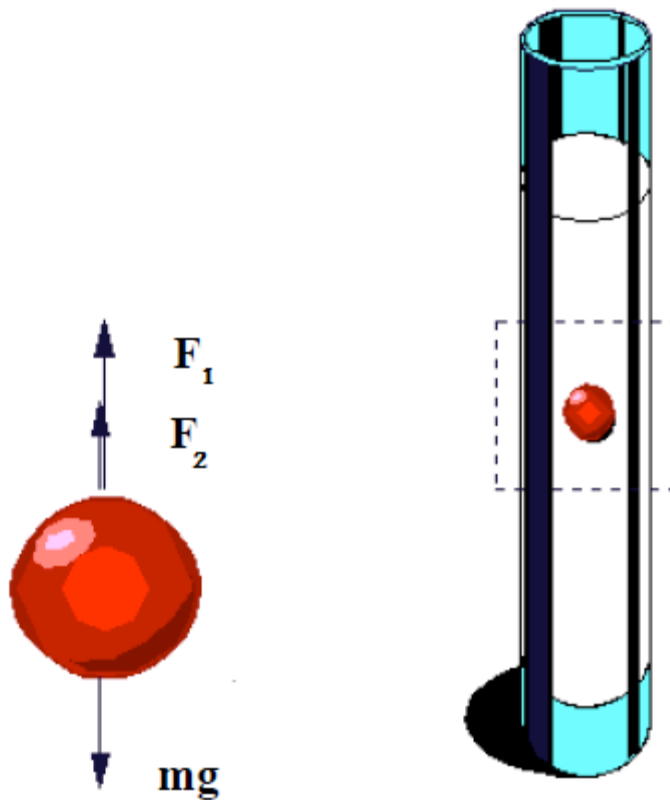


Figure [1].Body diagram of a ball in a fluid

Whilst gravity and buoyant force are static and independent from the velocity, the frictional force rises with the velocity. Therefore, the velocity of the falling ball rises till the net forces is zero.

$$W-F_1-F_2=0 \quad (4)$$

Combination of these equations would result in:

$$u=2/9 r^2 g (\rho_s-\rho_L)/\eta \quad (5)$$

Equation 5 shows that the viscosity of liquid, η , can be gained from the velocity of ball which is going down through this liquid.

The studied liquid is in a glass tube which has two marks by distance L. In the experiment, the time takes for liquid to pass through these two marks is measured. Modification of equation (5) yields:

$$\frac{L}{t} = \frac{2}{9} r^2 g \frac{\rho_s - \rho_L}{\eta} \quad (6)$$

In which the dynamic viscosity, η , is:

$$\eta = \frac{2}{9} r^2 g (\rho_s - \rho_L) t \quad (7)$$

Generally for simplification the constant coefficients are changed into a single coefficient:

$$K = \frac{2}{9} r^2 g \quad (8)$$

$$\eta = K(\rho_s - \rho_L) t \quad (9)$$

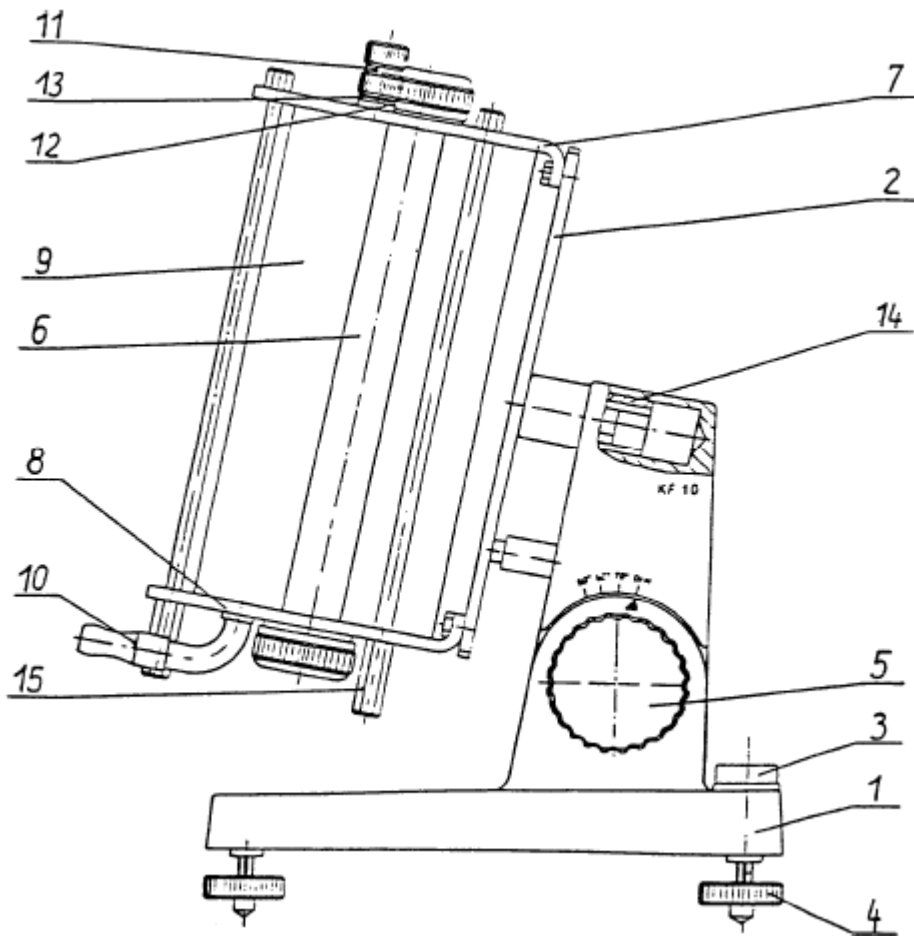
K is viscometer constant and can be determined by using distilled water as it has well-known viscosity [3].

4. Technical data [1]:

Measuring range:	0.6-80000 mPa.s according to DIN 53015
Limit:	30-300 s
Inaccuracy of measurement:	05-2 % according to the diameter of ball.
Temperature range:	-60...+150 °C
Measuring distance:	100mm (50mm between upper and middle lines in both directions)

5. Equipment

In measuring viscosity by Höppler viscometer the following things are used: studied solutions, distilled water, stop watch and thermometer, water bath in order to have homogenous bath temperature.



Figure[2].Falling ball viscometer[2].

- | | |
|-------------------------------------|--------------------------------|
| 1. Stand | 12. Screw neck |
| 2. Viscometer | 13 .Sealing washer |
| 3. Spirit level | 14 .Bearing |
| 4. Adjusting screw | 15 .Nuts |
| 5. Adjustment screw | 16 .Upper locking plug |
| 6. Falling tube | 17 .Lower locking plug |
| 7 .Upper plate | 18 .Cap |
| 8. Lower plate | 19 .Sealing |
| 9. Water bath jacket | 20 .Lid |
| 10 .Olive shaped tubes | 21 .Falling tube screw fitting |
| 11. Fastening screw for thermometer | |

Experimental procedure

1. Fill the falling tube with studied liquid and put in the ball cautiously. Add more liquid till no air bubbles can't be seen. Then close the falling tube with cap.

2. Turn the falling tube 180° and when the ball reaches to the first marks, start stop watch and measure the time between these two marks. For better and more accurate results it is recommended to repeat it 5 times at each temperature.
3. After changing the bath temperature, it's highly recommended to rest the sample at least 20 minutes in the falling tube to ensure the sample has reached to the desired temperature.
4. Before starting the measurement, it is better to turn the falling tube up and down in order to enhance temperature uniformity along the tube.
5. At the end of the experiment, empty the falling tube and be careful about the ball exiting the tube. Clean the tube with suitable solvent or a brush.
6. Write down the density of liquid and ball, ρ_L and ρ_s respectively. Calculate the average t for each temperature and by means of equation (9).

Calibration:

For calculating the viscometer constant, do all the above steps with a liquid which has a known viscosity such as distilled water but use the dynamic viscosity of distilled water in equation (9) and calculate the viscometer constant, K [2].

Notes:

- The liquid in the falling tube should be free of bubbles.
- Generally the measurement for calibration is done at ambient temperature.
- Measuring of the time starts when the lower edge of the ball touches the upper mark and ends when crosses the lower mark [2].

Ball selection:

Choice of ball is made on basis of the assumed viscosity of studied liquid and the specification which is given in following table:

Table[1].Balls characteristics [1].

Ball No.	Material	Density ρ (gr/cm ³)	Ball weight (gr)	Ball constant (mPa. cm ³ /gr)	Measuring range (mPa.s)
1	glass	2.228	4.599	0.00891	0.6-10
2	glass	2.228	4.816	0.0715	7-130

3	glass	2.411	4.454	0.07755	30-700
4	alloy	8.144	16.055	0.1239	200-4800
5	alloy	7.909	14.536	0.6523	800-10000
6	alloy	7.907	11.073	0	6000-75000

Temperature control

Falling ball viscometers allow an accurate temperature control of studied liquid through the bath. The following is recommended thermostatic fluids [1]:

+1...+95 °C distilled water

+80...+150 °C glycerine mixed (pure or in appropriate ratio with water)

-60...+30 °C methyl alcohol or ethyl alcohol (pure or mixed in appropriate ratio with water)

Cleaning

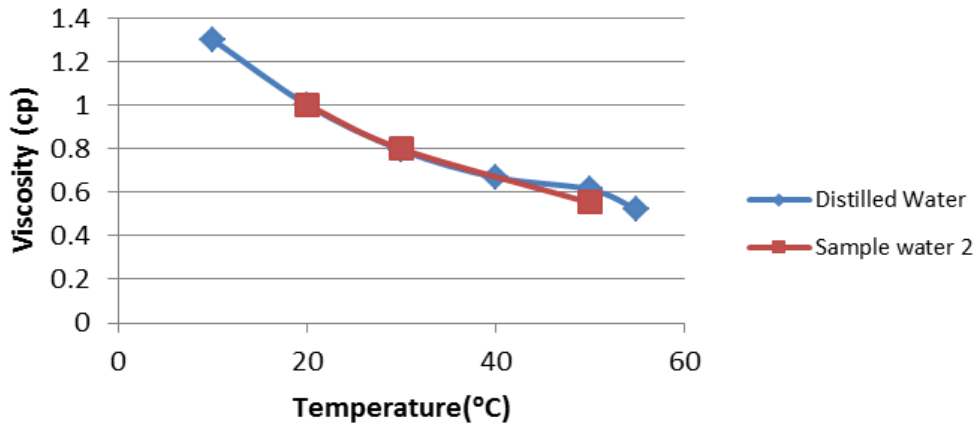
It is so crucial not to be remained any residues in tube and the ball. The equipment should be cleaned and dried completely. Rinse the tube and ball with suitable solvent or a brush [2].

Results

Sample water II

T(°C)	t _{avg} (s)	ρ _{ball} (g/m ³)	ρ _{water} (g/m ³)	μ _{ref} (cp)	K(m.pa.cm ³ /g)	μ _{cal} (cp)
20	44,368	2,228	0,9982071	1,002	0,018364	1,002
30	35,333	2,228	0,9956502	0,7975	0,018315	0,799614
50	24,25	2,228	0,9880393	0,5468	0,018185	0,552186

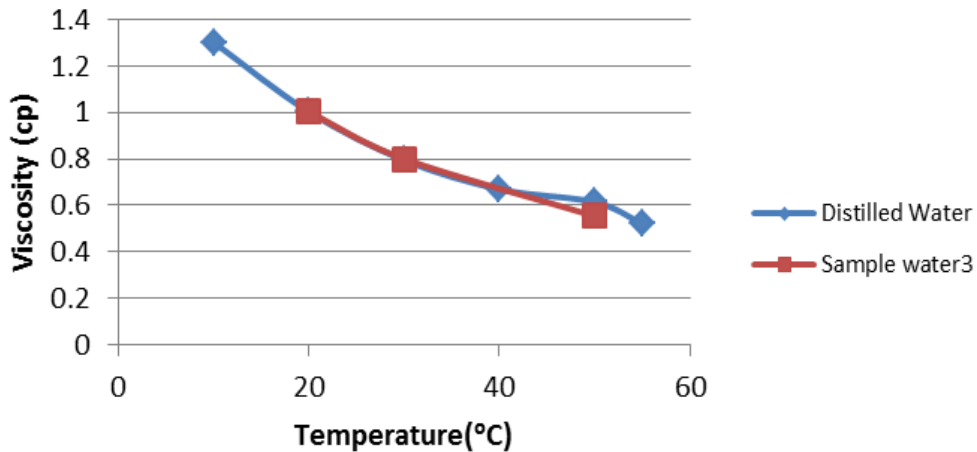
Sample water II



Sample water III

T(°C)	t _{avg} (s)	ρ _{ball} (g/m ³)	ρ _{water} (g/m ³)	μ _{ref} (cp)	K(m.pa.cm ³ /g)	μ _{cal} (cp)
20	44,463	2,228	0,9982071	1,002	0,018324704	1,002
30	35,425	2,228	0,9956502	0,7975	0,018267825	0,799983
50	24,337	2,228	0,9880393	0,5468	0,018119806	0,552983

Sample water III



Conclusion

The difference between the viscosity for both samples and distilled water was smaller than the accuracy of the instrument.

References:

1. Anleitung G., *Hoppler – Viskosimeter*, D.R.P.Nr.644312.
2. Rheo Tec Messtechnik GmbH, *Operating manual, Falling Ball Viscometer KF10*, Germany.
Available at www.rheotec.de
3. DocStoc, 2008, *Using a falling-ball viscosimeter to determine the viscosity*, version 1.1,
Available at <http://www.docstoc.com/docs/28564042/Using-a-falling-ball-viscosimeter-to-determine-the-viscosity-of/>

Appendix F: The COP₂ increase estimation, analytical approach.

The energy saving potential from the improved concrete usage comes from more efficient refrigerant unit operation, which is most commonly indicated by the coefficient of performance:

$$COP_2 = Q_2 / E, \quad (F.1)$$

Where Q_2 stands for the refrigeration effect and E is the operating energy

Thus the operating energy could be calculated from (F.1) as:

$$E = Q_2 / COP_2$$

Coefficient of performance for real processes obeys following relation:

$$COP_2 = \eta_{ct} \frac{T_2}{T_1 - T_2}, \quad (F.2)$$

where T_2 and T_1 are the respective temperatures of the evaporator and condenser;

η_{ct} - total Carnot efficiency of vapour compression cycle. This efficiency is very much dependent on the cycle and, considering the condenser temperature to be $t_1=35^\circ\text{C}$, could be estimated from the diagram on Figure F.1: Approximate values for the Carnot efficiency of practical vapour compression systems (Eric Granryd 2005)..

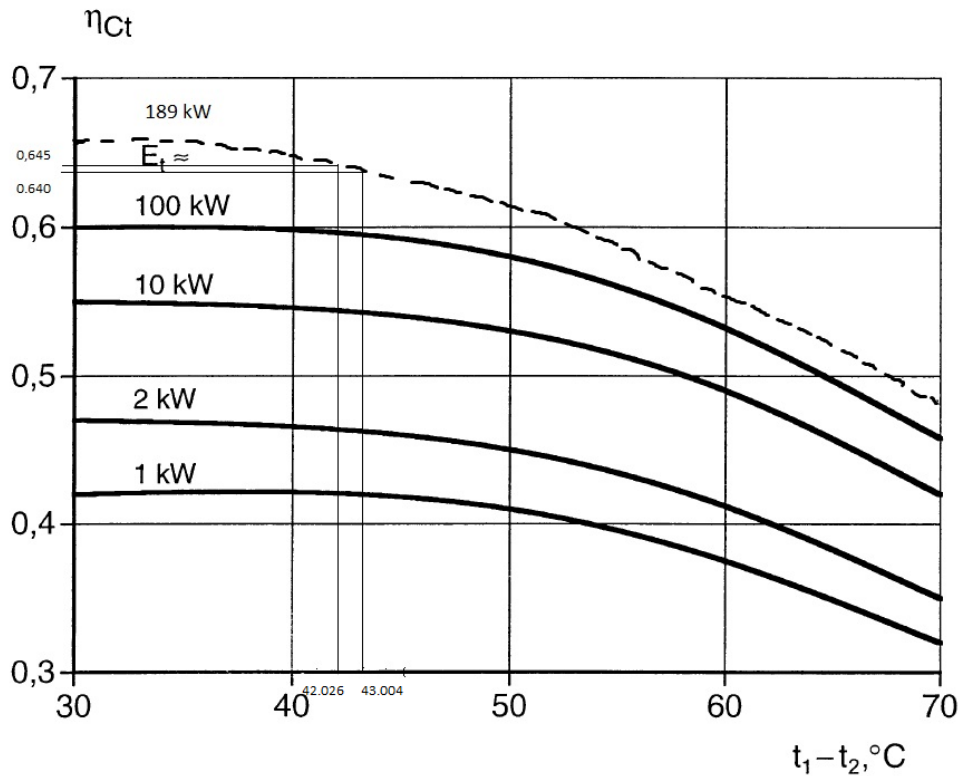


Figure F.1: Approximate values for the Carnot efficiency of practical vapour compression systems (Eric Granryd 2005).

Assuming that there is no temperature drop between evaporating refrigerant and secondary refrigerant in evaporator heat exchanger, we can determine Carnot efficiency for both cases.

Case 1: $T_2 = -7.026$ °C; $T_1 - T_2 = 35 - (-7.026) = 42.026$ °C, thus $\eta_{Ct} = 0.645$

Case 2: $T_2 = -8.004$ °C; $T_1 - T_2 = 35 - (-8.004) = 43.004$ °C, thus $\eta_{Ct} = 0.640$

Consequently, respective coefficient of performance for both cases are:

Case 1: $T_2 = -7.026$ °C; $COP_2 = 0.645 * 35 / (35 - (-7.026)) = 4.084$

Case 2: $T_2 = -8.004$ °C; $COP_2 = 0.640 * 35 / (35 - (-8.004)) = 3.946$

Thus, we can observe the 3.5% COP2 increase with improved concrete slab usage comparing with the conventional technology.

Appendix G: thermal conductivity measurement

Measurement Report for TPS 2500 thermal conductivity

Doc. No: 2010-04-08-001



Measure thermal conductivity in different concrete samples

1. Purpose

1.1. Measure thermal conductivity in four different concrete samples.

2. Principle

Transient Plane Source (TPS) method is used to measure thermal conductivity and thermal diffusivity on various sample types such as liquids, pastes, solids and powders disregarding they are electrically conducting or not. However the sensors to accommodate all of this variety in samples are different in sizes and formats. The TPS probe comprises a sensor (figure 1) acting both as heat source for increasing the temperature of the sample and a resistance thermometer for recording the time dependent temperature increase of the sensor. The TPS sensor element is made of a 10 μm thick electrically conducting Nickel foil in the shape of a double spiral. The Nickel foil is sandwiched between two layers of (0.013 - 0.025 mm) polyimide (Kapton) in order to keep physical shape, increase mechanical strength and supply electrical insulation.

For measurement the sensor is placed between two pieces of the sample in contact with the surfaces. Figure 2 shows the position of the sensor relative to the samples of which the thermal conductivity is being measured. For liquids a special stainless steel liquid holder and for solids a room-temperature solid sample holder both designed by Hot Disk AB are used.



(a) Hot Disk sensor 5501



(b) tip of the Hot Disk sensor 7281

Figure 1 - A typical TPS sensor

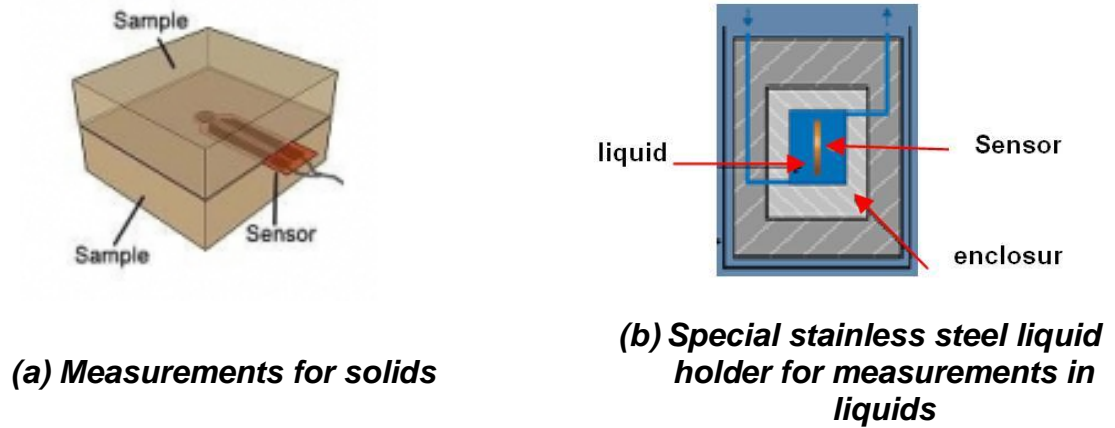


Figure 2 - A typical TPS sensor

An increase in temperature is created by passing a current through the Nickel foil during the measurement. The time and output of power are adjusted manually depending on characteristics of different materials. The generated heat is dissipated on both sides of the sensor and the selected rate is dependent on the thermal transport characteristics of the sample. The thermal characteristics are calculated from the recording of the temperature increase versus time response in the sensor (figure 3). The graph (b) in figure 3 results from 200 resistance recordings taken during the pre-set time and at the pre-set output power in the sensor.

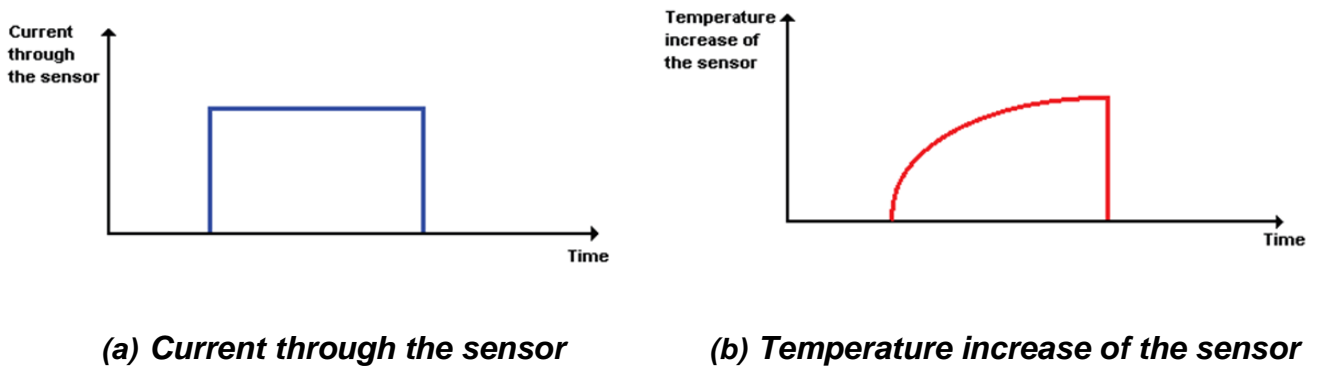


Figure 3 - Measurement basis in TPS method

TPS is a fast, convenient and absolute method. The latter means that there is no requirement to calibrate the sensor against a known thermal transport property material. Table 1 shows the specifications for TPS 2500.

Table 1 - specifications for TPS 2500

Thermal Conductivity (TC):	0.005 to 500 W/(m•K)
Thermal Diffusivity:	0.1 to 100 mm ² /s
Specific Heat Capacity:	Up to 5 MJ/m ³ K
Measurement Time:	1 to 1280 seconds
Reproducibility for TC:	Typically better than 1%
Accuracy for TC:	Better than 5%
Temperature Range:	Standard; Ambient (Room Temp. only) With Circulator; -50°C to 150°C

3. Samples

Four delivered different concrete samples to Energy Department of KTH in order to measure their thermal conductivity are shown in figure 4.



Figure 4 - Different concrete samples

4. Procedure

4.1. Sensor 5501 with radius 6.4mm appropriate for measurement in solids is selected, and assembled in the room-temperature solid sample holder (figure 5).

- 4.2. Appropriate values of power and time (0,20 W and 40 s) are selected based on some preliminary tests and thermal conductivity in every concrete sample is measured based on the instruction in the manual with the instrument.
- 4.3. Each measurement is repeated at least five times with 25 minutes time span using the same settings of power and time.
- 4.4. A single measurement on non-worn down surfaces for each sample is implemented. Non-worn down surfaces seems to be more flat and the effect is interesting to be investigated.
- 4.5. The sensor from the room-temperature solid sample holder is disassembled and stored in a safe place.

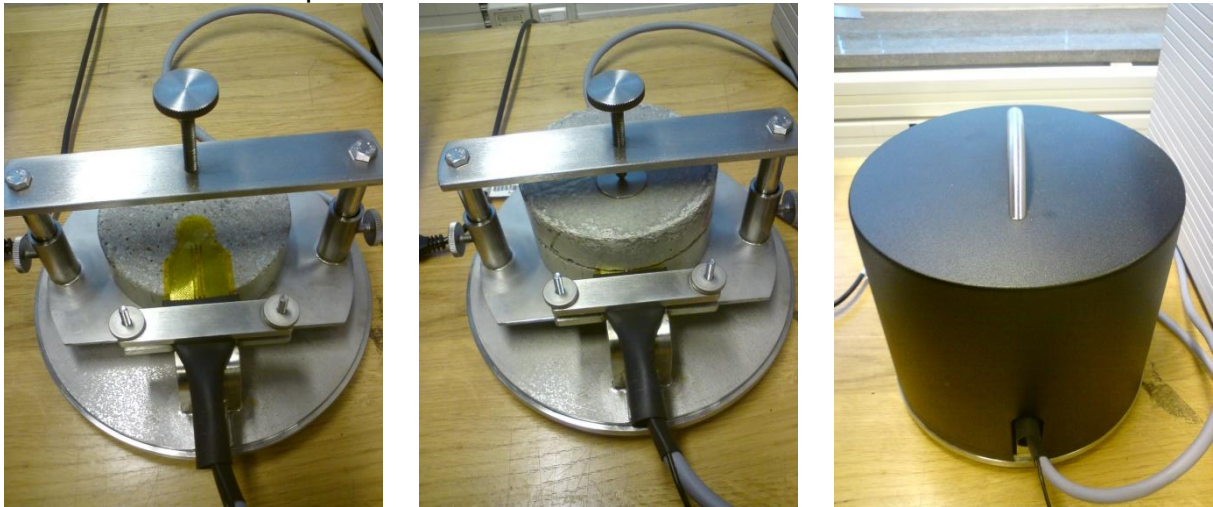


Figure 5 - Assembling sensor in the room-temperature solid sample holder

5. Results

Table 2 and figure 6 shows the results.

Table 2 - Results

Sample	Temp	Avg of 5 Meas. Worn down surface			Std Div		
		Th.Cond. (W/(m•K))	Th.Diff. (mm ² /s)	Spec.Heat (MJ/m ³ K)	Th.Cond. (W/(m•K))	Th.Diff. (mm ² /s)	Spec.Heat (MJ/m ³ K)
Con 01	Room	1,769	0,989	1,789	0,003	0,001	0,005
Con 02	Room	1,662	0,834	1,993	0,002	0,008	3.8. 0,018
Con 03	Room	1. 1,866	12. 0,888	3.13. 2,105	14. 0,026	15. 0,049	3.16. 0,121
Con 04	Room	9. 2,119	20. 0,828	3.21. 2,560	22. 0,004	23. 0,008	3.24. 0,021
		Single Meas. Non worn down surface					
Con 01	Room	1,914	1,028	1,862			
Con 02	Room	1,843	0,745	2,475			
Con 03	Room	1,958	0,807	2,426			
Con 04	Room	2,217	0,823	2,693			

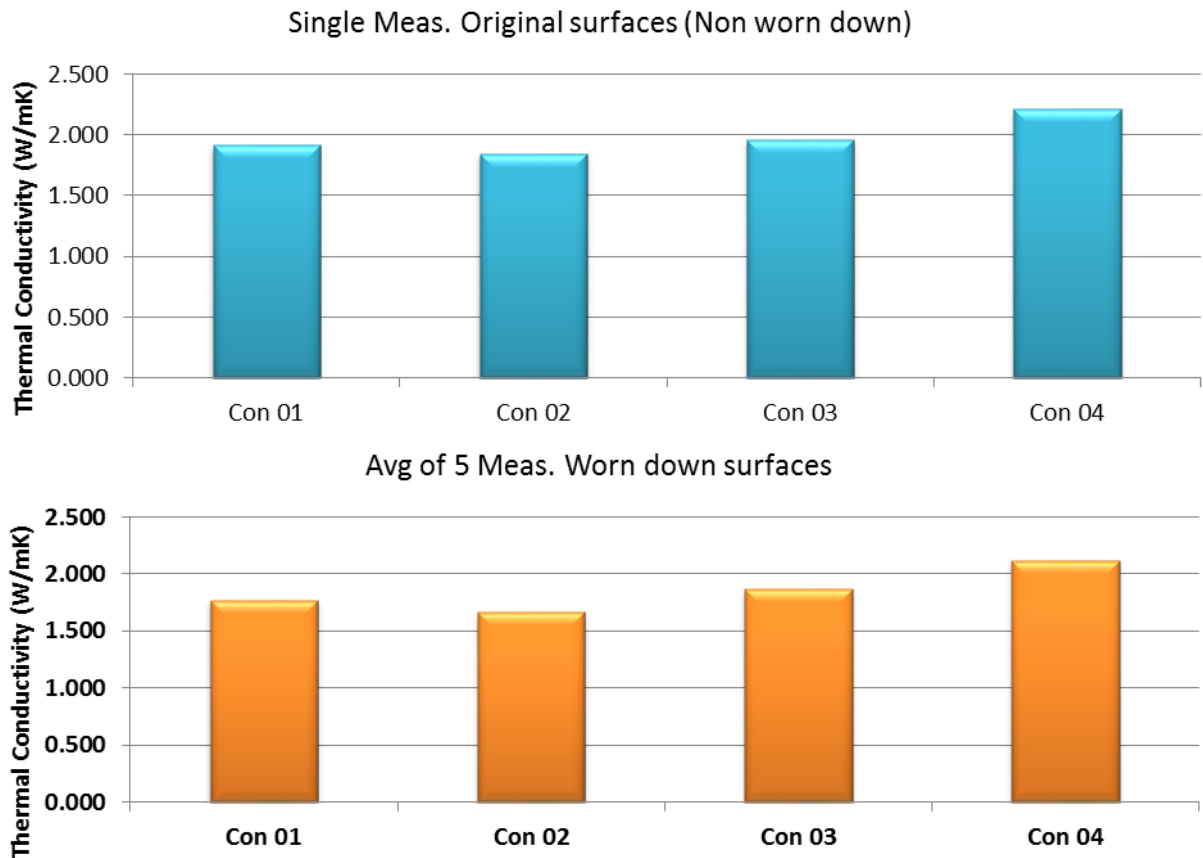


Figure 6 - Results, graphically

6. Risks

- 6.1. Non-fully flat worn down surfaces may cause the source of air gap between the surfaces and the sensor and wrong measurements as a result. (figure 7)
- 6.2. Non-homogeneity in the samples may cause different measured values depends on where the sensor is located.



Figure 7- the surface of the samples wasn't fully flat